Diffusion pathway across stratum corneum via the corneocytes and quantification of free amino acids and urea in the isolated corneocytes

Dissertation

zur Erlangung des
Doktorgrades der Naturwissenschaften (Dr. rer. nat.)

der Naturwissenschaftlichen Fakultät I
Biowissenschaften

der Martin-Luther-Universität Halle-Wittenberg,

vorgelegt

von Frau Hina Hussain
geboren am 06.09.1984 in Lahore, Pakistan

Gutachter:

1. Prof. Dr. Dr. h.c. Reinhard Neubert
2. Prof. Dr. Johannes Wohlrab
3. Prof. Dr. Christel Müller-Goymann

Halle (Saale), 26.04.2019

Dedicated to my beloved parents

Table of Contents

Abbreviations

1D	One dimensional
2D	Two dimensional
3D	Three dimensional
AAA	Amino acid analyzer
Aas	Amino Acids
ACC	Acceptor compartment
AD	Atopic dermatitis
Ala/A	Alanine
Arg/R	Arginine
Asn/N	Asparagine
Asp/D	Aspartic acid
Avg	Average
BH4	Tetrahydrobiopterin
C/M	Chloroform/methanol
CERs	Ceramides
Conc.	Concentration
Cit	Citrulline
Cr	Chromium
DAD	Diod array detector
DDW	Double distilled water
DON	Donator compartment
DW	Distilled water
EASI	Eczema area and severity index
EtOH	Ethanol
FAAs	Free amino acids
FMOC-Cl	9-Fluorenylmethoxycarbonyl chloride
Gln/Q	Glutamine
Glu/E	Glutamic acid
Gly/G	Glycine
His	Histidine
HO	Healthy old
HY	Healthy young
Ileu/I	Iso leucine
IS	Internal standard
KCl	Potassium chloride
LC	Liquid chromatography
LC-ESI-MS/MS	Liquid chromatography- electron spray ionization-mass spectrometry/mass spectrometry

Leu/L	Leucine
LiCl	Lithium chloride
LOD	Limit of detection
LOQ	Limit of quantification
Lys/K	Lysine
MeOH	Methanol
Met/M	Methionine
MRM	Multiple reaction monitoring
MS	Mass spectrometry
mTOR	Mammalian target of rapamycin
NADP	Nicotinamide adenine dinucleotide phosphate
NMDA	N-methyl-D-aspartate
NMFs	Natural moisturizing factors
NV	Norvaline
OPA	o-Phthalaldehyde
Orn	Ornithine
PASI	PS area and severity index
PBS	Phosphate buffered saline
PCA	Pyrrolidone carboxylic acid
Phe/F	Phenyalanine
Pro/P	Proline
Psoriasis	PS
RC	Regenerated cellulose
SC	Stratum corneum
SCB	Sodium cocadylate buffer
SDS-EB	Sodium dodecyl sulphate- extraction buffer
Sec.	Section
SEM	Scanning electron microscopy
Ser/S	Serine
Soln.	Solution
SPE	Solid phase extraction
Tau	Taurine
TEM	Transmission electron microscopy
TEWL	Transepidermal water loss
Thr/T	Threonine
Trp/W	Tryptophane
Tyr/Y	Tyrosine
V/P	Volunteer/patient
Val/V	Valine

Chapter 1. Introduction

1.1. Skin

Skin is the largest organ of the human body and about 15 % of the total adult weight. For an average adult human, the skin has a surface area of between 1.5-2.0 meter square (Kanitakis, 2002; Proksch *et al.,* 2008). It plays a vital role of immunity hence, protecting the body from pathogens as well as dehydration during dried environmental conditions (Madison, 2003). The thickness and the type of the skin varies significantly over all parts of the body and from individual to individual. For example, skin of the forearm is thinner than the skin of the palms while the facial skin is more water resistant than the other body areas. Skin is composed of three primary layers: the epidermis, the dermis and the subcutaneous (Wysocki, 1999).

Epidermis is the outermost layer of the skin so performing the main function of protection against different physical, chemical and microbiological aggressions.

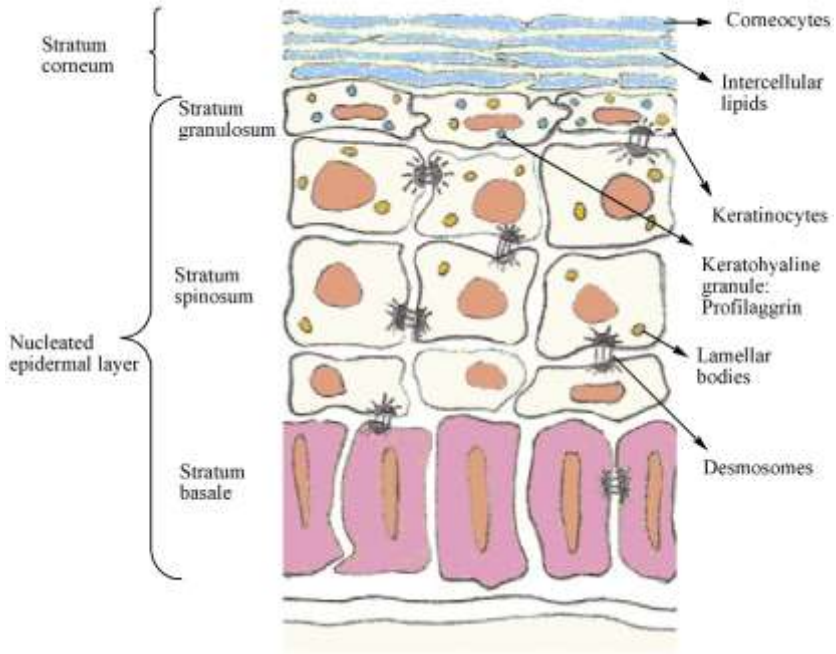

Figure 1. Epidermal differentiation. Lipids are synthesized in the keratinocytes, stored in the lamellar bodies, and released into the SC, where they form intercellular layers, arises from profilaggrin (contained in keratohyaline granules), contributes to the formation of the barrier, and its degradation products, involved in hydration of the SC (Baroni *et al.,* 2012).

Epidermis further comprised of i) stratum basale ii) stratum spinosum iii) stratum granulosum iv) stratum corneum (SC). Stratum basale is the deeper most layer of mitotically active cells called keratinocytes undergoing continuous movement towards upper layers. 10 % of the basale keratinocytes are stem cells, which produce daughter cells, destined to differentiate further while moving upwards however, the stem cell remains in the basale layer. The process of differentiation of these cells to reach to the SC takes about 14 days and is called desquamation (Zeeuwen, 2004). During this phase, keratinocytes become polyhedral, flattened and filled with new organelles and relatively higher amount of keratin. These keratinocytes together called stratum spinosum and contain abundance of focal junctions called desmosomes in between the cells (Simon *et al.,* 2001). Going farther from the stratum spinosum is another layer of the cells called stratum granulosum. The cells of this layer, recognized by the presence of characteristic basophilic keratohyaline granule filled with keratin and intermediate filaments of profilaggrin. Profilaggrin mRNA is synthesized in the granular cells and code for a high molecular mass of > 400 kDa. These histidine-rich polyphospholrylated proteins are made up of tandem repeats of peptide monomers called filaggrin. Profilaggrin converted to filaggrin during the transition period of keratinocytes into the corneocytes of the SC and this process is called cornification. In the granular layer the continued expression of suprabasal keratin K1, K2 and K10 results in the strengthening of cytoskeleton and post transitional modification. These cells called the corneocytes, together with intercellular lipids, the layer called SC.

During transitional phase or cornification, there are other changes that occur within the cells for example, formation of cornified envelope around the cells and assimilation of dead cells into supracellular interconnected structure. At microscopic level cornification is associated with complete disintegration of subcellular compartments i.e., organelles such as nucleus, mitochondria, endoplasmic reticulum and lysosomes. About 85 % of the proteins of the corneocytes consist of keratin. SC consists of 15-20 layers of the corneocytes and a two-compartment structure when observed under light microscope, which refers to as `brick and morter´ model, with the corneocytes embedded in the lipid matrix. Corneocyte acts as brick while the intercellular lipids, which are produced from the lamellar bodies during transitional phase, are considered as mortar (Albery and Hadgraft, 1979; Heisig *et al.,* 1996; Smeden *et al.,* 2013; Tojo, 1987). Going deeper into

structural details of the SC, the corneocytes 20-40 µM diameter (Menon, 2002) are surrounded by a protenaceous covering called cornified envelope. Which is formed by highly crosslinked insoluble protein molecules mainly involucrin, locricrin and trichohyalin and covantly bound lipids. These covalent bonds of the lipids are the ester linkages between the glutamic residue of involucrin and hydroxyl group of the ceramide lipids Together this the whole envelope functions to provide physical resistance and acting as water barrier for the cells (Candi *et al.,* 2005; Kalinin *et al.,* 2002; López *et al.,* 2007; Michel *et al.,* 1988) Involucrin contains glutamic acid (20 %) and glutamine (25 %) of cornified envelope. Involucrin is present in small amount while loricrin constitutes about 70 % of the cornified envelope proteins(Kalinin *et al.,* 2001; López *et al.,* 2007).

Lipids present in between these stacks of the cells consist mainly of ceramides (CERs), free fatty acids (FFAs) and cholesterol which are reported to be present in 16 molar % and 32 molar % respectively, in addition to small amounts of triglycerides, glycosphingolipids and cholesterol sulphate. While, CERs accounts for 37 % of total lipid content of the free intercellular lipids and are very important for the lipid organization and barrier function of the SC (Norlén, 2001; Norlén *et al.,* 1999). The corneocytes are filled with two types of keratin, type I, (K9- K20) that are acidic in nature and type II basic (K1– K8) keratin. Which are expressed in pairs. K1 and K10 are the first keratin that are expressed in the corneocytes during cornification. Both of these keratin molecules are synthesized from the pre-existing K5, K14 keratin intermediate filaments.

All keratins exhibit a similar secondary structure, consisting of head and tail non-helical sequence and a central rod domain comprised of four α- helices (Chan *et al.,* 1994; Kalinin *et al.,* 2002). Keratin K5 and K14 are expressed in the basal layer of the epidermis and K1, K2e and K10 are produced in suprabasal layers, and thus exhibiting 80 % of the total mass of the corneocytes (Eckert *et al.,* 1997; Fuchs, 1994). At the thickened sites of the skin such as palms and soles the corneocytes contain K9 and K2e type of keratin (Candi *et al.,* 2005). Keratin is utmost important for the barrier properties of the skin. **Dermis** the second main layer of the skin mainly consists of collagen, elastin salts and water. All of these proteins provide density to dermis. Hair follicles sweat glands, sebaceous glands, apocrine glands and blood vessels are partially present in this layer and exits through dermis. This protects the body from mechanical injury, retains water and helps in thermal

regulation. The blood vessels found in this region play a significant role in temperature regulation.

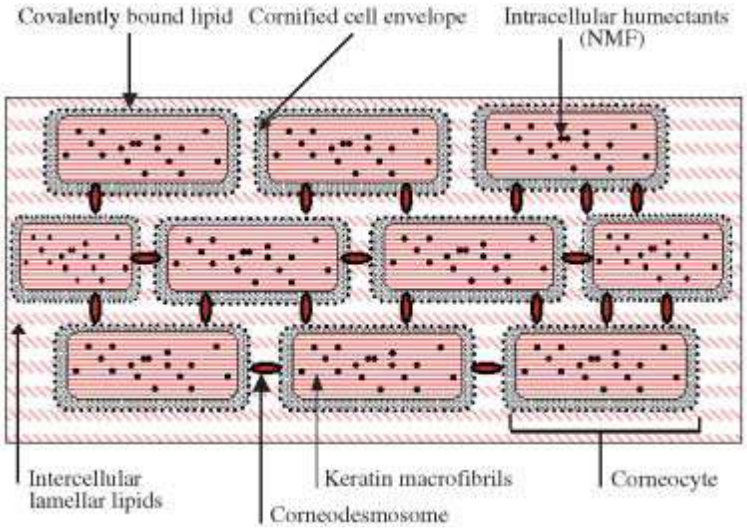

Figure 2. Schematic diagram presenting SC the corneocytes with intercellular lipids in between. The corneocytes are filled with humectants or NMFs and surrounded by cornified cell envelope and covalently cound lipids. The corneocytes are connected with each other with the help of corneodesmosomes (Harding, 2004).

Underneath the dermis and epidermis found subcutaneous and, the lower most layer of the skin. It refers to as vascularized loose areolar connective tissues which functions to insulate body from cold and works as shock absorbance.

1.2. Hydration of skin

As discussed earlier, during the process of desquamation, old cells of the SC worn out and are replaced with new cells originated from the deeper layers. In a healthy skin, it takes about thirty days for the cells to produce in the basal layers move to the surface and shed. The rate of travel to the surface, partially controlled by the rate at which the surface cells are lost. When the surface cells are lost at faster speed, as in case of sunburn or external injuries, they are replaced quickly. Thus, a healthy SC plays a vital role in helping to hold moisture within the rest of the skin layers and regulating the natural moisture, travelling from the deeper layers to the skin surface and to be lost via evaporation, this movement of water is called **transepidermal water loss (TEWL).** Under normal conditions SC hold about 15 % of the moisture which is not only important for flexibility but also regulates

the enzymatic activities responsible for maturation and desquamation process of SC. There are three types of water present in the SC. I) Free surface water ii) bound water, which is about five times the dry tissue weight in completely hydrated SC and iii). Strongly bound water with polar group of keratin side chains of the corneocytes. In which one type of specie is lost upon dry condition faced by skin while the other type of water is lost after extremely heat treatment (Anderson *et al.,* 1973). In a healthy skin water is > 10 % of total weight of SC. When this water content falls below critical level, the natural function of the skin is lost and the skin becomes dry (Verdier-Sévrain and Bonté, 2007).

Intercellular lipids surrounding the corneocytes are believed to play a vital role in preventing the excessive loss of water from the skin (Mizutani *et al.,* 2009; Ponec *et al.,* 2003) in dry environmental conditions or low humidity by forming an impermeable hydrophobic layer. Which is quite evident by the loss of lipids due to the excessive use of surfactants and soaps (Ananthapadmanabhan *et al.,* 2004; Froebe *et al.,* 1990) thus skin becomes dry and lose its ability to retain some or all of its water and starts to break down (Grubauer *et al.,* 1989; Imokawa *et al.,* 1991). So, a normal amount of moisture is necessary for the enzyme activities involved in desquamation and other processes. Dryness of the SC results in impaired desquamation and results in worsening of dry and unhealthy skin. Hence, exploring and identifying all the moieties present in the SC contributing towards the normal skin hydration and barrier function is of prime importance for the advancement of dermatological research. To improve barrier function and skin hydration status a class of skin lipids ceramides has already been incorporated in the skin formulations to recover skin abnormal barrier function (Meckfessel and Brandt, 2014). Other groups of scientists are working on molecules that are contained inside the corneocytes and are responsible for drawing and holding the water from the surrounding into the cells and thus keep the skin hydrated. These molecules are hygroscopic in nature and are also thought to play an important role in hydration and normal barrier function of the SC. This molecules include free amino acids (FAAs), derivatives of amino acids (AAs) such as pyrrolidone carboxylic acid, lactases and other molecules as urea, glycerol, inorganic salts of sodium, potassium, calcium and magnesium together called **natural moisturizing factors** (**NMFs**) of the skin (Harding *et al.,* 2000; Levin *et al.,* 2013; Robinson *et al.,* 2010; Sonoda *et al.,* 2012; Thyssen and Kezic, 2014; Visscher *et al.,* 2003).

1.3. NMFs of the skin and their role

The term 'NMFs' was first reported by blank in 1955 and then a number of research groups have been working in this specific area of research (Blank and Shappirio, 1955).

The NMFs, as mentioned earlier comprised of FAAs, derivatives of AAs as pyrrolidone carboxylic acid, urea, urocanic acid, lactic acid, citrate and sugars are produced inside the corneocytes (Clar and Fourtanier, 1981; Dapic *et al.,* 2013; Verdier-Sévrain and Bonté, 2007) and represent about 20-30 % dry weight of the SC (Trianse, 1974). They act as humectants by absorbing the environmental water and dissolving it into their own water of hydration and thus keeping the outermost surface of the skin hydrated even in the most desiccated environment (Bouwstra *et al.,* 2003). In 1982, Scott *et al.* while working on the skin of guinea pigs reported that free AAs are originated from a protein present in the keratohyline granules of the SC, that protein is most probably the histidine rich protein molecule, filaggrin (Scott *et al.,* 1982).

In the successive year Horii investigated FAAs in the mice epidermis and reported for the first time that FAAs were the degradation products of histidine rich protein molecule called filaggrin (Horii *et al.,* 1983). Filaggrin molecule (37 kDa) is SC protein and is synthesized in the keratohyaline granules from profilaggrin which is a large (> 500 kDa) and phosphorylated histidine rich protein molecule (Barrett *et al.,* 1983; Dale *et al.,* 1985; McAleer *et al.,* 2018; Scott and Harding, 1981; Scott *et al.,* 1982).

During the conversion of mature granular cells into the corneocytes, profilaggrin is dephosphorylated to convert into filaggrin , which is a transient component and persists only in the two to three deeper layers of the SC (Harding and Scott, 1983).

As the corneocytes maturation proceeds to the upper layers, complete proteolysis of filaggrin generates NMFs. This proteolysis is time controlled due to the shielding of filaggrin with keratin, which help filaggrin from premature proteolysis.

The short span of the filaggrin molecule is influenced by the turn over time of SC. The activity of protease which results in the conversion of filaggrin into a pool of NMFs is not initiated until the corneocytes get flattened, move to upper more dryer layers and the cornified envelope gets strengthened. Once all of these conditions are fulfilled and the corneocytes are ready to withstand the osmotic pressure that is produced as a result of releasing NMFs, filaggrin degrades (Harding and Scott, 2002). Other NMFs that are also

present extracellularly include urea, sugars, hyaluronic acid and especially lactate (Harding *et al.,* 2000).

1.3.1. Factors effecting the content of NMFs in the corneocytes

One of the factors effecting NMFs content is routine cleansing using soaps that wash out most of the NMFs from the skin (Rawlings and Harding, 2004). Low environmental humidity (<10 % relative humidity) impairs the functioning of enzymes that are responsible for the proteolysis of the filaggrin thus, ultimately effecting the NMFs content and results in the dry skin (Katagiri *et al.,* 2003). Ultra violet radiations has also been reported to damage the skin by interfering with the enzymatic breakdown of the filaggrin into NMFs and the amounts of NMFs in SC declines with age due to the reduce synthesis of filaggrin. Certain diseases such as atopic dermatitis, senile xerosis also exhibit decrease amount of AAs due to reduced synthesis of profilaggrin (Horii *et al.,* 1989). Besides AAs, other NMFs also play an important role, for example urea influences the hydration of the SC to a greater extent. It has been reported that the deficiency of urea, as in many dermatological diseases, can be corrected by the topical application of urea or arginine (precursor of urea) (Loden *et al.,* 2001; Nenoff *et al.,* 2004). Potassium and lactate also contribute in sustaining the hydration and physical properties, such as pH and turgidity of the SC (Nenoff *et al.,* 2004). FAAs, constituting about 40 % of total NMFs composition, are building block units of proteins (see Table 1). Each AA structurally consists of one amino group and one carboxylic group with a side chain `R´, specific to the AA. There are about 300 AAs exist naturally and only 20 AAs are found in proteins. These AAs chemically bind together to make peptides and polypeptides through a bond called peptide bond or amide bond (Damodaran, 2007). There are two types of AAs essential and non-essential ones. Essential AAs are those which are not synthesized by animal cells such as histidine, cysteine, arginine, iso-leucine, etc. while non-essential AAs can be prepared by animal cells examples of non-essential AAs are alanine, asparagine, aspartic acid and serine (Wu, 2013).

Table 1. Composition of NMFs in SC (Rawlings and Harding, 2004)

Compound	% Age contribution
FAAs	40
Pyrrolidone carboxylic acid	12
Lactate	12
Sugars	8.5
Urea	7
Chloride	6
Sodium	5
Potassium	4
Ammonia, Uric acid, Glucosamine, Creatinine	1.5
Calcium	1.5
Magnesium	1.5
Phosphate	0.5
Citrate and formate	0.5

AAs are classified based on the properties of the side chain. AAs are hydrophilic if the side chain is polar and hydrophobic in case of nonpolar side chain. These properties are necessary for proteins. Some of the proteins that have positively charged surface AAs such as lysine and arginine they interact with negatively charged molecules around them. While the proteins with negatively charges side like glutamic acid and aspartic acid they

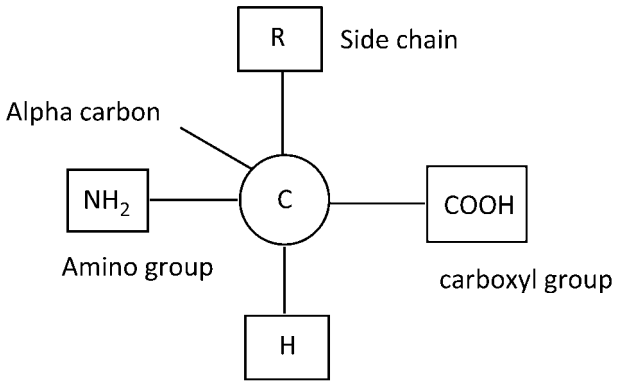

Figure 3. Basic structure of AA.

bind with positively charged molecules. As for example water soluble protein have their side chains exposed to the water solvents while the hydrophobic residue (leucine, iso-leucine, valine, phenylalanine ad tryptophane) are present in the middle of the protein structure. As example membrane proteins have hydrophobic surface AAs that help them

anchoring into the intercellular lipids (Urry, 2004). Some of the authors classify AAs according to their structures as AAs can be aliphatic, aromatic and cyclic or on the basis of the location of structural functional group as α (alpha-), β (beta-), γ (gamma-or δ (delta-) AAs. Protogenic AAs usually refer to the 22 AAs that are present in the protein structures (Urry, 2004).

1.4. Dermatogical disorders and barrier dysfunction

Dry skin conditions in various diseases is associated with abnormal barrier function, deficiency of NMFs, including FAAs/urea, and intercellular lipids which contribute to decreased water retaining capacity and increased TEWL of the SC (Berardesca *et al.,* 1990; Takahashi *et al.,* 2014; Verdier-Sévrain and Bonté, 2007). The two of the skin diseases associated with abnormal barrier function are described below.

1.4.1. Atopic dermatitis (AD)

AD is a chronic inflammatory, relapsing and highly pruritic skin disease, resulting in itchy, red, cracked and swollen patches on different body areas. The disease can occur at any age, may start in the childhood with repeated relapse and can persist for the whole life. Worldwide, AD has 20 % prevalence amongst children and 1-3 % in adults, which increased vastly in the last two decades (Simpson, 2010; Tollefson and Bruckner, 2014; Wolter and Price, 2014).

AD is characterized with barrier disruption, which ultimately makes the effected skin more prone to allergy and microbial attack. In a healthy skin the formation of cornified envelope and cleavage of large profilaggrin molecules by serine protease results in the release of functional filaggrin. Filaggrin aggregates the keratin cytoskeleton and facilitates the flattening of the keratinocytes, ultimately formation of the corneocytes, in the outermost layer of the epidermis. Furthermore, as the water content of the SC falls, filaggrin is proteolysed to produce NMFs including FAAs/urea of the SC to maintain the hydration of the skin (Boguniewicz and Leung, 2011; Elias and Wakefield, 2011; O'Regan *et al.,* 2008; Rawlings *et al.,* 1994).

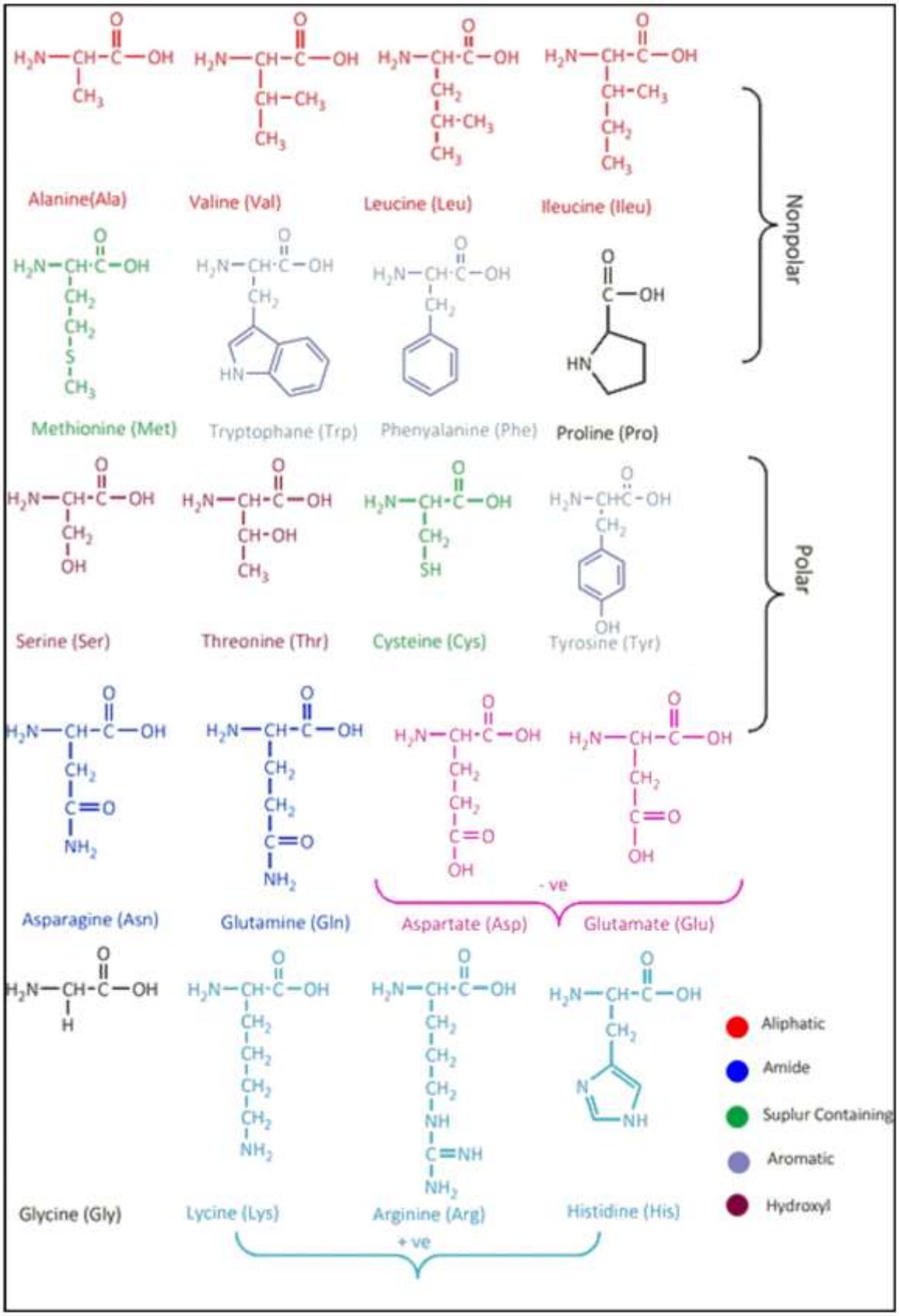

Figure 4. Structure and classification of AAs.

1.4.2. Physiological functions of AAs

Table 2. AAs and their physiological functions (Wu, 2009)

AA	Physiological functions
Alanine	Inhibition of pyruvate kinase and hepatic autophagy; gluconeogenesis; transamination; glucose–alanine cycle.
Arginine	Activation of mTOR signalling; antioxidant; regulation of hormone secretion; allosteric activation of NAG synthase (N-acetylglutamate) ammonia detoxification; regulation of gene expression; immune function; activation of BH4 (tetrahydrobiopterin), synthesis; N reservoir; methylation of proteins; deimination (formation of citrulline) of proteins.
Asparagine	Cell metabolism and physiology; regulation of gene expression and immune function; ammonia detoxification; function of the nervous system.
Aspartate	Purine, pyrimidine, asparagine, and arginine.
Citrulline	Antioxidant; arginine synthesis; osmoregulation; ammonia detoxification; N reservoir.
Cysteine	Disulfide linkage in protein; transport of sulfur.
Glutamine	Regulation of protein turnover through cellular mTOR (mammalian target of rapamycin) signalling, gene expression, and immune function; a major fuel for rapidly proliferating cells; inhibition of apoptosis; syntheses of purine, pyrimidine, ornithine, citrulline, arginine, proline, and asparagine; N reservoir; synthesis of Nicotinamide adenine dinucleotide phosphate (NAD(P)
Glutamate	Glutamine, citrulline, and arginine synthesis; bridging the urea cycle with the Krebs cycle; transamination; ammonia assimilation; flavour enhancer; activation of N-methyl-D-aspartate (NMDA) receptors; NAG synthesis.
Glycine	Calcium influx through a glycine-gated channel in the cell membrane; Purine and serine synthesis, Synthesis of porphyrins; inhibitory neurotransmitter in CNS; co-agonist with glutamate for NMDA receptors.
Histidine	Protein methylation; haemoglobin structure and function; anti-oxidative dipeptides; one-carbon unit metabolism
Ileucine	Synthesis of glutamine and alanine; balance among branched chain AA.
Leucine	Regulation of protein turnover through cellular mTOR signaling and gene expression; activator of glutamate dehydrogenase; branched chain AA balance; flavor enhancer
Lysine	Regulation of NO synthesis; antiviral activity (treatment of Herpes simplex); Protein methylation (e.g., trimethyllysine

AA	Physiological functions
	in calmodulin), acetylation, ubiquitination, and O-linked glycosylation
Methionine	Oxidant; independent risk factor for CVD (cardiovascular disease); inhibition of NO synthesis.
Phenylalanine	Activation of BH4 (a cofactor for NO synthase) synthesis; synthesis of tyrosine; neurological development and function.
Proline	Collagen structure and function; neurological function; osmoprotectant
Serine	One-carbon unit metabolism; syntheses of cysteine, purine, pyrimidine, ceramide and phosphatidylserine; synthesis of tryptophan in bacteria; gluconeogenesis (particularly in ruminants); protein phosphorylation.
Taurine	Antioxidant; regulation of cellular redox state; osmolyte
Threonine	Synthesis of the mucin protein that is required for maintaining intestinal integrity and function; immune function; protein phosphorylation and O-linked glycosylation; glycine synthesis.
Tryptophane	Neurotransmitter; inhibiting production of inflammatory cytokines and superoxide, N-acetylserotonin, Inhibitor of BH4 synthesis; antioxidant; inhibition of the production of inflammatory cytokines and superoxide
Tyrosine	Protein phosphorylation, nitrosation and sulfation
Valine	Synthesis of glutamine and alanine; balance among branched-chain AA.

However, as reported by Rawlings, loss of function mutation of filaggrin gene results in decreased NMFs level and thus increased dehydration and TEWL (O'Regan *et al.,* 2008; Rawlings, 2014). These produced NMFs contribute to the acidic pH of the skin required for normal functioning of various skin enzymes. However, in AD decreased NMFs result in increased pH of the SC, which leads to activation of number of serine proteases. Such as KLK_5 and KLK_7 associated with desquamation, exhibit a neutral pH optimum, a change in pH reduces their activity up to 50 % and hence results in poor desquamation and barrier disruption (Deraison *et al.,* 2007; Elisabeth *et al.,* 2000).

Conversely, cathepsin LZ and cathepsin D, also involved in desquamation, have acidic pH optimum (Bernard *et al.,* 2003; Horikoshi *et al.,* 1999). Lipid generating enzymes β-glucocerebrosidase and sphingomyelinase work well at low acidic pH. Additionally, the pH induced increased protease activity leads to T helper 2 cells (Th2) inflammation in AD. A study demonstrated that pH increase also cause colonization of pathogenic microbes to the SC and the releasing exogenous proteases of microbes further perpetuate barrier and

immunological abnormalities (Boguniewicz and Leung, 2011; Cork *et al.,* 2009; Danby and Cork, 2010; Elias and Schmuth, 2009).

1.4.3. Psoriasis (PS)

PS an autoimmune, chronic, inflammatory, multisystem disease with predominantly skin and joint manifestation with red, dry, itchy and scaly patches on the skin. It has worldwide prevalence of 1-2 %, which increased roughly over a lifetime as 0.12 % at the age 1 year to 1.2 % at age 18 years and effecting more men, than the women. PS can be classified as plaque, guttate, inverse, pustular and erythrodermic, with 90 % prevalence of plaque PS which is also called PS vulgaris (Barker, 2008; Boehncke and Schön, 2015; Grozdev and Korman, 2014; Lowes *et al.,* 2007; Menter *et al.,* 2008).

Excessive epidermal cell production and loss of cellular cohesiveness results in thickening of the SC in the form of scales, which makes it 10 times thicker than the normal skin. This abnormal growth of the cells leads to impaired barrier function and increased TEWL of the skin effected with PS (Lowes *et al.,* 2007).

It has been reported that in the SC effected with PS insufficient maturation of the corneocytes results in poor proteolysis of filaggrin and hence lesser production of NMFs. As discussed earlier in this chapter, that one of the major factors for retaining the water inside the corneocytes is NMFs that are produced by filaggrin, so in PS reduced content of NMFs leads to increased TEWL, reduced water content and ultimately dried skin. The evidence of lower water content in the PS lesional skin is provided by a study conducted by Egawa *et al.,* 2010, according to which water content in the involved skin was even lesser than the water of the uninvolved SC (Egawa *et al.,* 2010; Takenouchi *et al.,* 1986).

1.5. Extraction and quantification of FAAs/urea

AAs are a set of chemically diverse molecules and are building block units of proteins. Due to chemical diversity and many other factors (e.g physical properties), the quantitative analysis of AAs is a tedious and difficult work. A number of research groups developed analytical methods for quantification of AAs. Wilkerson conducted the first known study for determination of AAs in human SC in 1934. He investigated the acetone, alcohol and ether extract of human epidermis effected by atopic dermatitis. He determined cysteine, tyrosine and tryptophane upon direct protein hydrolysate using Folin-Marenzi technique (1929) for cysteine while were quantified using Folin and Ciocalteu (1927) for tyrosine

and tryptophan. Histidine, lysine and arginine were investigated by isolation and found to be in the molecular ratio of 1:5.6:15.1, respectively (Folin and Ciocalteu, 1927; Folin and Marenzi, 1929; Wilkerson, 1934). With the continuous progress of the technology and advancement in knowledge, researchers used the best available technique to get more precise picture of these molecules which effect the health of the skin. Paper chromatography with ninhydrin as detection reagent was used in analytical method by Spier and Pascher in 1955 and Burke *et al.,* in 1966 in their experiment on the SC and skin surface film in human beings to analyze FAAs. Burka *et al.,* analyzed FAAs by using sample extract from the skin of lower leg. The specific skin surfaces were washed with distilled water (DW), rubbed with gauze pads, which in turn was washed using alcohol and water, The extract thus obtained was observed for 20 AAs, urea, ammonia and several unidentified ninhydrine reactive substances. He presented his data for FAAs and soluble peptides in µmole/100 µmole in males and females (Burke *et al.,* 1966; Spier and Pascher, 1955). A successive investigation for FAAs was done by Wolferberger *et al.* in 1973 and determined the concentration of total FAAs in which epidermis was scrapped from autopsy skin samples of human and quantified by colorimetric ninhydrin method (Cocking and Yemm, 1954; Wolfersberger *et al.,* 1973).

With advancement of the technology, automated amino acid analyzer (AAA) was extensively used worldwide for determination of AAs in different research fields including dermatology. In 1989 Horii and colleagues investigated AAs contents in 30 elderly people and six individuals suffering from ichthyosis vulgaris to determine correlation between AAs content and skin hydration. AAs were extracted from tape stripped samples and homogenized with 0.3 N $HCLO_4$. The amounts of AAs were estimated by using AAA. They reported that dried skin contained lower amount of AAs that led to dehydration (Horii *et al.,* 1989). This was the first time when dry skin condition was associated with the AAs content of the epidermis. Meanwhile, a research was continued in developing better technology and improving analytical method for AAs quantifications. A lot of work has been done in the field of paper chromatography and resulted in the advancement of AAA and other chromatographic techniques. Different chromatographic techniques emerged to separate and quantify AAs in a sample, including ion-exchange chromatography, gas chromatography (GC), thin layer chromatography, reverse phase liquid chromatography.

In late 70´s chromatography is usually coupled with UV or fluorescence optical detection. However, due to non-chromophore nature of AAs the analysis is done using either pre-column or post column derivatization with selected reagent. This derivatization results in producing compounds, which are optically detectable and more hydrophobic. The derivatization of the AAs with a suitable reagent produce chromophore compounds which lead to increase sensitivity in the nano molar range (Kaspar *et al.,* 2009; Lee and Drescher, 1978; Rigas, 2013). To-date various derivatization reagents are used depending on the nature of samples as for example, phenylisothiocyanate (PITC), o-phthaldialdehyde (OPA), (fluoren-9-ylmethoxy) carbonyl chloride (FMOC-Cl) and diethyl ethoxymethylenemanolate. Where OPA is suitable only for primary AAs while FMOC-Cl reacts with primary as well as secondary AAs (Alaiz *et al.,* 1992; Carpino *et al.,* 1986; Cohen and Strydom, 1988; Lee and Drescher, 1978). A number of studies regarding quantification of AAs have been conducted using GC coupled with mass spectrometry (GC/MS) after derivatization, which reduced polarization (Dauner and Sauer, 2000; Kvitvang *et al.,* 2011; Persson and Nasholm, 2001). But for impure samples i.e., food need an extra clean up step prior to analysis with GC, because data generated using GC analysis produce more variability as compared to high performance liquid chromatography (HPLC) (Rutherfurd and Gilani, 2009).

In 1990, Jacobson *et al.* estimated FAAs in healthy, old and xerotic skin. Hydrolysed extract taken with scrapping the skin surface and analyzed with HPLC after post-column derivatization with OPA. Some of the AAs increased while a few decreased with increasing age. There was no significant relation between the AAs content of normal and xerotic skin was observed (Jacobson *et al.,* 1990).

Watanabe *et al.,* in their study conducted on AD, demonstrated the method of extraction and thereafter, the quantification of AAs using AAA. They stripped off the upper layer of the SC, removed the samples from strips by immersing in the toluene and dried. They reported the decrease in the quantities of FAAs in the uninvolved areas of the body of AD patients compared to healthy individuals (Watanabe, 1991).

Denda *et al.* also measured FAAs content in the experimentally induced scaly skin using high speed AAA and reported that FAAs content is reduced in scaly skin and it is responsible for this dry skin condition (Denda *et al.,* 1992). Rawlings and Harding *et al.,*

reported that FAAs decreases with age and virtually absent in the diseases state such as AD, PS and ichthyosis vulgaris. They further demonstrated that decrease in the FAAs in the SC of aged skin is due to the decrease in the filaggrin, attribute to the loss of function mutation in filaggrin gene (Harding, 2004; Harding *et al.,* 2000; Rawlings *et al.,* 1994; Rawlings, 2014). A study, conducted by Egawa and Tagawa for the measurement of NMFs, including FAAs/urea by in-vivo confocal Raman spectrotroscopy. They calculated the quantities of different NMFs using spectra from Raman spectrometer to analyze the effect of age on their quantities. Their results showed increase in the NMFs including FAAs and decrease in the urea amounts with increasing age (Egawa and Tagami, 2007).

Another work on quantification of FAAs obtained from healthy, ichthyosis vulgaris, senile xerosis and aged skin was done. FAAs were extracted from scratched skin of the lower legs, extraction was done with double distilled water (DDW) and analyzed by HPLC. The study reported an increased amount of FAAs in aged and skin effected by senile xerosis (Takahashi and Tezuka, 2004). Sugawara and colleagues also conducted the comparative study on healthy versus AD patients and measured the quantities of FAAs/urea along with other NMFs. He used the tape stripping method for sampling, extracted urea with H_2O that was analyzed using GC. While, 10 mM HCl extract was used to quantify FAAs after derivatization with OPA using HPLC. They concluded the results as no remarkable decrease in the quantities of FAAs in the AD, while amount of urea showed lowered trend in AD compared to healthy skin. The above mentioned controversial results regarding the quantification of FAAs pointed out an important research gap requiring standard analytical method with high selectivity and sensitivity. Most of the studies conducted for the quantification of FAAs/urea in SC used either AAA or HPLC after derivatization. HPLC method coupled with derivatization required longer separation times for individual AAs. These methods might not be very selective due to same retention times of two or more AAs and non-specific fluorescent signals associated with AAs. For more advancement of HPLC, in the recent years liquid chromatography-electrospray ionization/mass spectrometry/ mass spectrometry (LC- ESI-MS/MS) based methods coupled with multiple reaction monitoring (MRM) have been developed which is considered as convenient method to enhance selectivity. However, a wide range of charges and polarities of not derivatised AAs demands a separation system, which is also compatible

with the MS to utilize this methodology (Gu *et al.,* 2007; Nagy *et al.,* 2003; Piraud *et al.,* 2005, 2003). This problem was solved by using ion pair chromatography or reverse phase columns (Armstrong *et al.,* 2007; de Person *et al.,* 2008; Gu *et al.,* 2007; Piraud *et al.,* 2005, 2003). Jander *et al.,* in 2004 developed a HPLC-MS/MS method with separation time of only 1.5 min using phenyl-Hexyl column. However, the method resulted in poor separation of iso-leucine from leucine. All of these methods cause high ion suppression caused by either higher concentration of ion pair reagent or signals originated from (Jander *et al.,* 2004; Kaspar *et al.,* 2009; Pande *et al.,* 2014) matrix system and led to lower sensitivity. Unspecific signals derived from eluents or matrix are in the same range as molecular masses of most of the AAs. Additionally, the small sized AAs limits the choice of suitable and specific fragments from MRMs. Several derivatization techniques have been employed to facilitate the analysis of AAs using LC-MS/MS (Casetta *et al.,* 2000; Inagaki *et al.,* 2010; Leavens *et al.,* 2002; Shimbo *et al.,* 2009a, 2009b). In addition, to ions derived from chromatographic system and ions derived from unrelated compounds present in the sample result in suppression of ions and hence, higher detection limits. With the help of efficient sample clean up this issue can be resolved and maximum sensitivity can be achieved.

1.6. Drug diffusion across SC

Several researches done in the field of moisturizing technology, aimed at rejuvenation of the natural component FAAs/urea deficient skin via dermal rout. Dermal rout is being used for about one third of all the drugs under clinical evaluation and is a preferred over other routes (Cross and Roberts, 2004) due to several reasons including patient compliance and controlled drug delivery properties. One of the most prominent advantages is the avoidance of first pass effect as in case of oral route of drug administration. A large number of work still needed to be done to explore various aspects of this route. As penetration of the drug varies from individual to individual and at different sites of the same individual. The most pronounced and complex layer of the skin is the outer most layer of epidermis, SC. Which is composed of 18-20 layers of flattened, partially hydrated and interleaved cells called corneocytes (Wang, Kasting, & Nitsche) stacked in intercellular lipids. As described earlier in this chapter that intercellular lipids

of the SC consists of cholesterol, fatty acids and sphingolipids. This presence of hydrophilic (corneocytes) and lipophilic (intercellular lipids) alternative phases in the SC offers a rate-limiting component for the penetration of most of the dermally applied drugs (Wang *et al.,* 2006). Both of these structural elements play an important role for the transport of drugs across SC. In the Figure 5 below, two potential routes of transport through SC has been demonstrated. i) Intercellular rout that consisting of lipids and is suitable for the non-polar drugs and ii) intracellular is through the keratin filled coenocytes that allows only hydrophilic drugs to pass through it (Barry, 1987; Ng and Lau, 2015).

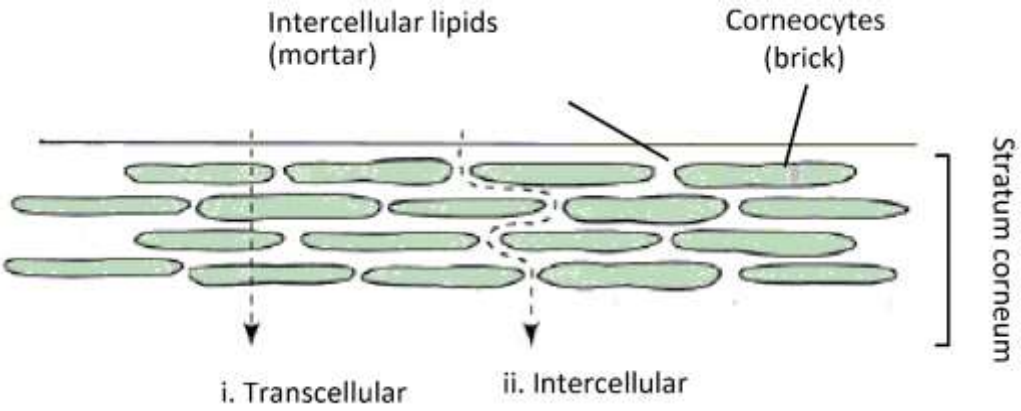

Figure 5. Dermal routes of drug transport through SC.

Some processes influence the transport of the drug through SC as molecular diffusion as natural diffusion under which the chemical substances in soln. move along the concentration gradient. The diffusion continues until the homogenous distribution of the diffusing substances takes place in the whole solvent. Another process is partitioning or relative distribution of the solvent molecules in two immiscible phases studied under Nernst ´s distribution law. For any substance `K´ the distributed in phases `A´ and `B´ depends on the lipophilicity and hydrophilicity of the substance and its distribution coefficient is described as $K_{\frac{A}{B}} = \frac{C_A^K}{C_B^K}$.Where, the concentration is also influenced by the pH of the solvents A and B.

Metabolism and phase changes is also considered as one of the important processes. As for example, dissolution in the solvent, evaporation, metabolism in the cells. The last

process is the binding and absorption of the drug molecules. As the corneocytes offer absorption depot for water soluble substances or adsorption occur at the surface of the cells which is a binding of the molecules to the surface proteins (Barry, 1987; Naegel *et al.,* 2013; Wang *et al.,* 2006).

A large work has been done over the past decades on mechanistic diffusion based modelling of skin permeation and various researchers developed a number of models to explain the transport of drug through skin and SC (Edwards and Langer, 1994; Michaels *et al.,* 1975; Yotsuyanagi and Huguchi, 1972). This transdermal permeation are explained by Naegel et al 2013 as processes that occur at four length scales as L1 (1-10 nm) processes at molecular level, L2 (0.1 µm) on sub cellular, L3 (0.1-1 µm) membrane level and L4 (1 cm) at compartmental /environmental level. The processes of L1 and L2 are considered as micro and L3 and L4 are referred to as macro scale models. These two types of models are further classified as one dimensional (1D), two dimensional (2D) and three dimensional (3D) diffusion models. 1D diffusion models are the simplest and treat the skin as homogenous entity, while for actual heterogeneous nature of complex skin 2D and 3D models were presented (Edwards and Langer, 1994; Naegel *et al.,* 2013; Nitsche, 1999; Nitsche and Frederick Frasch, 2011; Rim *et al.,* 2009).

A number of scientists combined inter- and trans-cellular transport with a macroscopic model system or from a capture mechanism to integrate the reservoir capacity of the corneocytes (Mollee and Bracken, 2007). The most used diffusion model in literature is brick and mortar based models, which distinguish between the corneocytes (brick) and intercellular lipids (mortar) arranged in an idealized geometry (Mollee and Bracken, 2007). These models comes under 2D class of models and allow basic morphological structures in a fully coupled fashion at a least computational expense. These models have the potential to cover broadly applicable class of chemicals including hydrophilic and hydrophobic molecules.

However, the brick and mortar model does not explain why the SC is extremely resistant against mechanical stress and inner pressure of the tissue neither it tells the cohesion of the layers and nor about the dynamics and mass transfer. Therefore, it was necessary to investigate this important skin structure sub-naturally with modern microscopic methods so this brick and mortar model is re-considered. Three dimensional models are

closer to the physical reality as they potentially illustrate more practical geometrical configurations of the corneocytes and lipids as well the transportation processes in the SC in more details (Naegel *et al.,* 2013). 3D models hold true as long as the effects such as partitioning, diffusion and metabolism has regularity and periodicity on microscopic (cellular) scale. However, violation in these assumptions are observed due to the hydration and swelling of the corneocytes , which are likely to influence the permeation processes (Richter *et al.,* 2004). This local effect of the corneocytes was reported by Hansen *et al.,* which explained that cornified envelope surrounding the corneocytes offer a large fraction of the binding sites for permeating molecules while transport through the SC, which are potentially also adsorbed to the keratin fibres of the corneocytes. Together with small hydrophilic hygroscopic molecules as urea, AAs, lactic acid and keratin which provide the major water holding capacity of the SC thus, regulating skin flexibility, firmness and smoothness. Hence, water is present inside the corneocytes thus helping entrapment of hydrophilic molecules inside the cells. On further occlusive conditions more water may be taken up by the corneocytes making their way to lipid bi-layer and inculcate there (Hansen *et al.,* 2009; Heard *et al.,* 2003).

1.7. Rationale of the study

FAAs/urea are decreased in the diseased and aged skin compared to healthy skin (Fowler, 2012; Rippke *et al.,* 1999; Sonoda *et al.,* 2012; Verdier-Sévrain and Bonté, 2007). Under the subject of section (sec.) 1.5 of this chapter controversial results regarding the quantification of FAAs/urea that are most abundantly found members of NMFs were reported. These controversial results are of the prime importance for further steps towards development of topical delivery of AAs or/and urea that is most considering remedy of today for diseased and ageing skin. However, previous studies have been conducting over whole SC rather than the isolated corneocytes. Additionally, acidic hydrolysis leads to proteolysis of the cells and produced more FAAs that were not related to actual NMFs. So, there is a need to develop a standard protocol of extraction for accurate determination of these indicating components using more sensitive and selective analytical method for quantification of FAAs/urea. So, in this study an extraction protocol has been developed, as the corneocytes were isolated and lysed without any chemically induced hydrolysis. In addition to this, analytical method, LC-ESI-MS/MS for

quantification of AAs has been used. Colorimetric quantification with coupled enzyme reaction with increased sensitivity has been done for urea. Dermal administration of AAs and urea is now a days more considering remedy for skin ailments such as AD and PS. However, due to hydrophilic nature of these molecules and structural complexity of SC the delivery of these molecules is not an easy task. Furthermore, being hydrophilic in nature AAs/urea has to undergo great resistance due to reservoir capacity of the corneocytes. For dermal administration of these molecules in diseased or ageing skin, it is utmost important to know the capacity of the corneocytes for these molecules. To the best of our knowledge to-date no study was conducted to determine the reservoir capacity of the corneocytes for AAs and urea.

1.8. Objectives of the research study are:

1. Isolation and microscopic study of the corneocytes from skin samples obtained after pedicure treatment and tape stripping.
2. Development of standard extraction protocol for FAA/urea from the isolated corneocytes
3. Quantification of FAAs to compare the amounts in healthy, diseased and aged skin using modern more sensitive and selective analytical method.
4. Determination of reservoir capacity and diffusion of AAs and urea in the corneocytes.
5. *In-vitro* diffusion model of model molecules i.e., taurine and urea with and without corneocytes.

Chapter 2. Materials and methods

2.1. Materials

2.1.1. Reagents and chemicals

	Manufacturer/ Supplier
9-Fluorenylmethoxycarbonyl chloride (Fmoc-Cl)	Sigma-Aldrich Chemie, GmbH, Taufkirchen, Germany
Acetone	Sigma-Aldrich, Chemie GmbH, Steinheim, Germany
Acetonitril	Baker, Deventer, Netherlands
Amino acid (AA) standards	Cambridge Isotope, Laboratories Andovar, MA, USA
Ammonium formate	Sigma-Aldrich, Chemie GmbH, Steinheim, Germany
Boric acid	Merck KGaA, Darmstadt Germany
Chloroform	VWR, International GmbH, Darmstadt, Germany
Ethanol (EtOH)	Merck KGaA, Darmstadt/ VWR International GmbH, Darmstadt, Germany
Glutaraldehyde	Sigma, Taufkirchen, Germany
KCl	Sigma-Aldrich, Chemie GmbH, Germany
Keratin Powder	Chroma Chemical Corp, Suqian, China
KH2PO4	Merck KGaA, Darmstadt, Germany
L. norvaline (NV)	Sigma-Aldrich, St. Louis, MO, USA
LiCl	Sigma-Aldrich, Chemie GmbH, Steinheim, Germany
Methanol (MeOH)	VWR, International GmbH, Darmstadt, Germany
Na2HPO4	Merck KGaA, Darmstadt, Germany
NaCl	Sigma-Aldrich, Chemie GmbH, Steinheim, Germany
NaHCO3	Sigma-Aldrich Chemie, GmbH, Taufkirchen, Germany
n-Pentane	Sigma-Aldrich, St. Louis, MO, USA
Osmium tetroxide	VWR, International GmbH, Germany
Sodium cacodylate	VWR, International GmbH, Germany
Taurine	VWR, International GmbH, Darmstadt, Germany.
Uranylacetate	VWR, International GmbH, Germany
Urea	Sigma-Aldrich Chemie, GmbH, Taufkirchen, Germany
Urea assay kit (MAK006)	Sigma-Aldrich Chemie, GmbH, Taufkirchen, Germany

2.1.2. Buffers

	Composition
Borate Buffer (pH, 7.9)	boric acid (0.5M), pH with NaOH to 7.9

Phosphate buffer saline (PBS) (pH, 7.4)	137 mM NaCl 2.68 mM KCl 10 mM Na2HPO4 1.76 mM KH2PO4 1 l DW,
0.1 M SCB- sodium cacodylate buffer (pH, 6.5)	Sodium cacodylate in water pH adjusted with HCl

2.1.3. Accessories

	Manufacturer/ Supplier
Chromabond® multi 96 well SPE (solid phase extraction) plates	Machery-Nagel GmbH & Co. KG, Düren, Germany
Chromabond® Sorbent HR-X	Machery-Nagel, GmbH & Co. KG, Düren, Germany
Column, Zorbax Eclipse Plus C18 Rapid Resoln. HD column	Agilent, Waldbronn, Germany
Column, YMC-diol-NP	YMC, Co, Ltd, Kyoto, Japan
Diffusion Apparatus	Mechanical workshop, Institute of Pharmacy, Martin Luther University, Halle-Wittenberg, Halle (Saale), Germany
Eppendorf tubes	Eppendorf AG, Hamburg, Germany
RC Dialysis membrane	Spectrm AG, Repligen coorporation, Waltham, MA, USA
Syringe filters 0.45µm	VWR, International GmbH, Darmstadt, Germany
Syringe needles	B. Braun, Injekt-F, B. Braun, Melsungen, Germany
Syringes	B. Braun, Injekt-F, B. Braun, Melsungen, Germany
Tape strips	Blenderm Surgical tapes, 3M Deutschland GmbH, Neuss, Germany

2.1.4. Commonly used lab equipment

	Model	**Manufacturer/ Supplier**
Multi sample Stirrer plate	Mix 15 eco	2mag AG, Muenchen, Germany
pH meter	inoLab pH 720	WTW GmbH, Weilheim, Germany
Vaccuum pump	Vacuubrand CVC2	Vacuubrand, Wertheim, Germany
		Mettler Toledo,

Weighing balance	Mettler Toledo, XA 150 Dual Range	Gießen, Germany
Ultrasonic bath	Sonorex, RK 100H	Bandelin electronic GmbH & Co. KG, Berlin, Germany
Rotary evaporator	Labrota 4000	Heidolph Instruments, GmbH & Co. KG, Schwabach, Germany
Ultra- Turrax	IKA, Ultra- Turrax	NeoLab Migge GmbH,
Ultra- Turrax dispersing element	S18N- 19G	Heidelberg, Germany
Mixer mill	MM301, mixer mill	Retsch, Haan, Germany
Centrifuge	Eppendorf centrifuge, 5417R	Eppendorf AG, Hamburg, Germany
Concentrator	Eppendorf, 5301	Eppendorf, Hamburg
Swing out rotor	Avanti J-26XP, centrifuge	Beckman Coulter, Fullerton, CA, USA
Nitrogen evaporator		MLU workshop, Halle, Germany

2.1.5. Special devices

	Model	**Manufacturer/ Supplier**
DAD (diod array detector)	DAD G1315A	HP Deutschland GmbH, Böblingen, Germany
Degasser	G1322A	HP Deutschland GmbH, Böblingen, Germany
ESI (electron spray ionization) Detector	ESI, Turbo Ion Spray interface	AB Sciex, Darmstadt, Germany
HPLC (High performance liquid chromatography)	Agilent, 1100 series	Agilent technologies, California, USA
Image recording camera	Variospeed SSCCD camera SM-1k-120	TRS, Moorenweis, Germany
Pump	G1312A	HP Deutschland GmbH, Böblingen, Germany
Scanning electrone microscope (SEM)	FEI/Philips XL-30 SEM	Leuven, Belgium
Transmission electron microscope (TEM)	EM900 transmission electron microscope	Carl Zeiss Microscopy, GmbH, Jena, Germany

UV-Spectrophotometer	EPOCH|2, microplate reader	BioTek, instruments, Winooski, USA
Variospeed SSCCD camera of TEM		TRS, Moorenweis, Germany

2.1.6. Waters

	Manufacturer/ supplier
DW (distilled water)	Distillation plant installed in the institute
DDW (double distilled water)	Double distillation plant installed in the institute
Ultra pure water	JWT-GmbH, Jena, Germany

2.1.7. Softwares

	Version	**Manufacturer/supplier**
Analysis software for HPLC to get response for urea	ChemStation for LC Rev.B.03.02.[341]	HP Deutschland GmbH, Böblingen, Germany
Analyst software of LC-ESI-MS/MS	Analyst 1.6 software	AB Sciex, Darmstadt, Germany
GraphPad	7.04	GraphPad prism software Inc., CA, USA.
MS-Excel	Excel, 2013	Microsoft, Santa Rosa, California, USA.
OriginLab	8.5.1	OriginLab Corperation Wellesley Hills,MA, USA.
SPSS	22	IBM Deutschland, GmbH, Ehningen, Germany
UV spectrophotometer microplate software	Gen5	BioTek, instruments, Winooski, USA

2.2. Methods

2.2.1. Isolation and microscopic study of the corneocytes

2.2.1.1. Isolation of the corneocytes from the skin samples obtained after pedicure treatment

The left over skin after pedicure treatment was obtained from a foot-care clinic (Neustadt Zentrum, Halle, Germany). The obtained material (1 g of skin) was crushed with the help of pestle and mortar with the twice addition of liquid nitrogen. After crushing, the material was washed five times with PBS (pH, 7.4) and subjected to extraction of intercellular lipids by adding 150 ml of chloroform/methanol (C/M) (2/1, V/V) mixture and stirred with the magnetic stirrer at 1200 rpm for 48 hrs. The above mixture then filtered through a sintered glass frit R4 under vacuum. The de-lipidized corneocytes , were again added with C/M (2/1, V/V) mixture and subjected to stirring by using IKA Ultra-Turrax homogenizer with S18N- 19G dispersing element, at 11000 rpm for 30 min and filtered with sintered glass frit under vacuum. The obtained isolated corneocytes were then sieved (mesh no. = 40, pore size 420 µm).

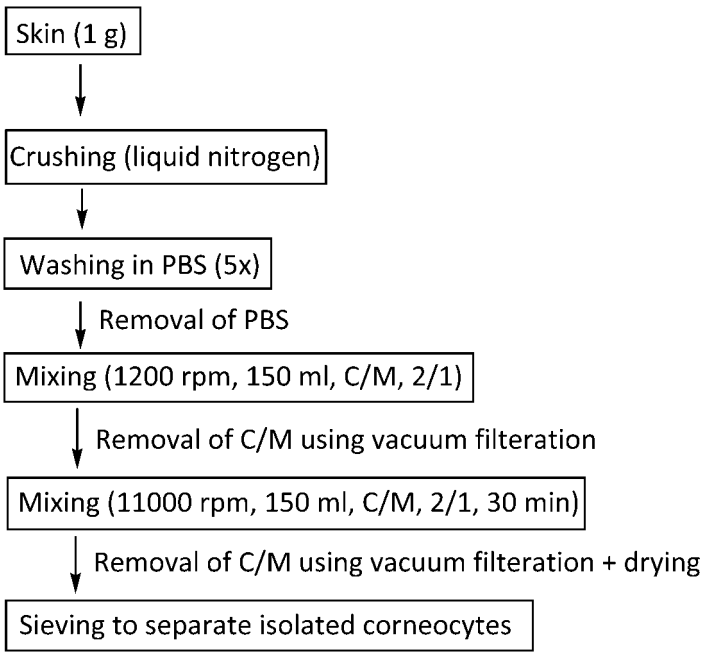

Figure 6. Isolation of the corneocytes from the skin obtained after pedicure treatment.

2.2.1.2. Microscopic study of the corneocytes from the skin samples obtained after pedicure using SEM

Microscopic images were obtained using dried sample of the isolated corneocytes sputtered with 20-30 nm Cr (chromium) layer and examined under high vacuum mode at 5 kV, using FEI/Philips XL-30 SEM.

2.2.1.3. Isolation of the corneocytes from the skin sample obtained after tape stripping

2.2.1.3.1. Skin sampling and isolation of the corneocytes

Samples were taken from healthy volunteers belonging to Caucasian race. Selected area of skin for sampling was cleaned with 70 % EtOH and a tape strip of 20×5 cm^2 was placed on palm side of the forearm for sampling with a slight pressure using spatula from each group. The first strip was discarded and the next eight strips were retained for further study. After sampling the strips were stored at -80 °C until processed.

Each sample strip was immersed into the 300 ml 90 % EtOH and then sonicated for 20 min until the SC detached from the strip and collected into the solvent. The solvent was evaporated using rotary evaporator and SC thus obtained, consisting of the corneocytes and intercellular lipids.

2.2.1.3.2. Removal of intercellular lipids from the corneocytes

The above dried SC was added with 10 ml C/M (2/1, V/V) mixer and stirred at 1200 rpm over a magnetic stirring plate for 48 hours to extract the lipids. After 48 hours the above sample was centrifuged at 2500 g for 15 min, the supernatant was discarded and the isolated suspended corneocytes without intercellular lipids were collected and subjected to TEM examination.

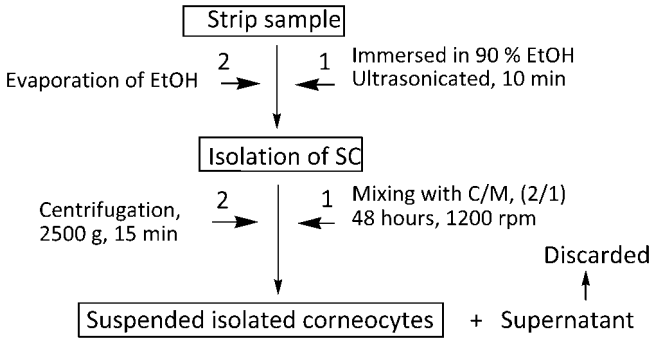

Figure 7. Isolation of the corneocytes without intercellular lipid lamella from skin obtained after tape stripping.

2.2.1.3.3. Removal of covalently bound lipids from the corneocytes

To remove covalently bound lipids the material from sec 2.2.1.3.2 was added with 10 ml 1M NaOH in 90 % MeOH and heated for 15 min. The flask was integrated with condensation system to keep the concentration of MeOH constant. After 15 min extracted lipids were removed by the addition C/M (2/1, V/V) mixture and centrifuged at 2000 rpm for 5 min, the suspended corneocytes collected and the supernatant consisting of lipids was discarded. The isolated corneocytes thus obtained, examined under TEM.

2.2.1.3.4. Removal of cornified envelope from the corneocytes

The above intact corneocytes obtained in sec 2.2.1.3.3 were mixed with 0.2 % sodium dodecyl sulphate- extraction buffer (SDS-EB) for 1 min and centrifuged at 1200 rpm this procedure was repeated again and the corneocytes without cornified envelope were examined by TEM.

2.2.1.4. Isolation of the corneocytes obtained after tape stripping of healthy young, aged and diseased skin

Skin sampling was done in the same way as described in sec. 2.2.1.3.1. Strip samples were collected from four groups HY (healthy young) HO (healthy old), AD and PS volunteer/patient (V/P) belong to caucasian race. From uninvolved skin areas. Each sample strip after sampling was immersed into the 100 ml 90 % EtOH, sonicated for 20 min until the SC detached from the strip and collected into the solvent. Evaporated of the solvent was carried out using rotary evaporator and SC thus obtained, consisting of the corneocytes with bound intercellular lipids which were removed by subjecting the above sample to the procedure mentioned in sec. 2.2.1.3.2 (see Figure 7) the isolated corneocytes thus obtained were examined by TEM.

2.2.2. Microscopic study of the isolated corneocytes from the skin obtained after tape stripping using TEM

The isolated corneocytes obtained in sec. 2.2.1.3.1, 2.2.1.3.2, 2.2.1.3.3, and 2.2.1.3.4 and sec. 2.2.1.4 were fixed directly with 3 % glutaraldehyde in 0.1 mM SCB for at least 4 hours, centrifuged at 5000 rpm for 5 min and taken up in 4 % agar/SCB, followed by 4 wash-steps with SCB-buffer for 10 min. After post fixation with 1 % osmium tetroxide in SCB for 1 hour, samples were dehydrated in a series of EtOH (10 %, 30 %, and 50 %). The sample corneocytes were treated with 1 % uranylacetate / 70 % EtOH for 1 hour, and further

dehydrated with a series of 70 %, 90 % and 100 % EtOH. Thereafter, the samples were infiltrated with epoxy resin according to Spurr (1969) and polymerized at 70 °C. The ultrathin sections (80 nm) were observed with EM900 TEM operating at 80 kV. (Spurr, 1969).

2.2.3. Extraction of FAAs/urea

2.2.3.1. Extraction of FAAs from isolated corneocytes of skin from pedicure

2.2.3.1.1. Extraction of FAAs/urea at different conditions from isolated corneocytes of skin from pedicure

The isolated corneocytes from the skin obtained after pedicure treatment (see isolation protocol in sec 2.2.1.1) subjected to extraction of FAAs at different conditions and using different solvents as shown in Table 3 to determine the optimum conditions at which maximum FAAs were obtained.

Table 3. Extraction of FAAs at different conditions of temperature and solvent

Sample	Temperature (°C)	Time (hours)	Solvent
1A	Ambient	24	DDW
2A	46	24	DDW
3A	70	24	DDW
4A	46	24	0.1 N, HCl
5A	Ambient	24	C/M, 1/1, V/V
6A	46	6	DDW

2.2.3.1.2. Extraction of FAAs/urea from the corneocytes isolated from skin from pedicure at optimum conditions

The corneocytes (50 mg/ml) as isolated in sec 2.2.1.1 incubated in DDW at 46 °C for 24 hours (defined optimum conditions as determined in previous sec.) to extract FAAs/urea. Thereafter, the corneocytes were centrifuged at 5,000 g for 10 min and the supernatant, containing extracted FAAs was separated from the suspended corneocytes. 25 µl supernatant was added with 2 µl of 10 mM NV and subjected to quantitative analysis of FAAs (see sec. 2.2.6.1) and urea (see sec. 2.2.6.3).

2.2.3.2. Extraction of FAAs/urea from the isolated corneocytes of skin obtained from tape stripping

Extraction of FAAs from the corneocytes isolated from four groups HY, HO AD and PS Sampling was done by tape stripping method as in section 2.2.1.3.1 from uninvolved skin of right and left arm of V/P, belonging to caucasian race, from each of the four groups HY. HO, AD and PS. First strip was discarded and the second strip was retained for further processing. Blenderm surgical tape was selected owing to its skin hyposensitivity and insolubility of the tape adhesive materials in the solvents used during extraction and analysis. All the sampling was carried out after approval of ethical committee of MLU, Halle (Saale), Germany. Each group comprised of five V/P with specific age group as mentioned in the Table 4 and 5. The corneocytes were isolated and processed following sec 2.2.1.4. The sample isolated corneocytes obtained in sec 2.2.1.4 were dried under laminar flow hood overnight and weighed by tare method before extraction of FAAs/urea. The corneocytes after weighing step were suspended in 150 µl of 70 % MeOH containing 2 nmol NV as an internal standard (IS) for quantification. Samples were transferred to 2ml eppendorf tubes containing a 5 mm diameter steel bead and lysed using a mixer mill at a speed of 25/s for 50 sec, the process was done twice.

The above lysed suspension was then subjected to vigorous shaking for 20 min and then centrifuged at 4 °C at 10,000 g for 1 min. 25 µl of the supernatant containing FAAs extract was collected and transferred to 1.5 ml eppendorf tubes. 25 µl were stored at -20 °C for FAAs analysis (see Figure 8 for extraction protocol).

2.2.3.2.1. Extraction of urea

To the remaining extract, 25 µl of DDW was added, stirred for 2 min and centrifuged twice at 4 °C at 10,000 g for 1 min to remove suspended lysed corneocytes by transferring the supernatant each time in another eppendorf tube. The extract was completely dried under nitrogen evaporator and stored at -80 °C for urea assay (see Figure 8) for urea assay see sec. 2.2.6.3.

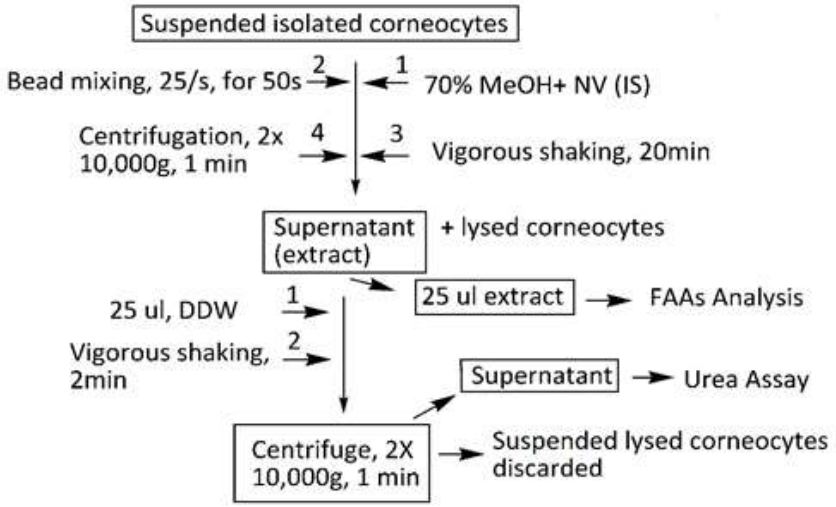

Figure 8. Protocol for extraction of FAAs/urea from the corneocytes obtained after tape stripping.

Table 4. Parameters of the study groups

Group	No. of volunteers V/P	Age (years)	Disease/PASI/ EASI score
HY(control)	5	18-40	n.a*
HO	5	65-75	n.a.
PS	5	18-65	PASI ≥ 10, PS Vulgaris
AD	5	18-65	EASI ≥ 12

*n.a, not applicable.

Table 5. Ages (years) and sex of V/P enrolled in the study

HY	HO	PS	AD
Age/sex			
28/f	69/f	50/f	48/m
19/f	69/m	60/m	43/f
19/f	73/f	52/m	53/m
31/f	72/m	62/m	38/f
24/f	65/f	62/m	27/m

2.2.4. Interaction of AAs and urea with the isolated corneocytes

2.2.4.1. Preparation of standard solutions and stability studies

Standard solns. of 100 µM for each of the 19 AAs, including taurine, and 500 µM for urea (for list of 19 AAs see Table 6) were prepared and subjected to stability studies after 24, 48 and 72 hours for taurine and urea while only 24 hours for remaining AAs incubated at conditions of 32 °C, 11.8 % humidity which was retained with saturated soln. of LiCl.

2.2.4.2. Interaction of AAs and urea with the corneocytes

The corneocytes isolated from the skin obtained after pedicure treatment as described in sec 2.2.1.1 and Figure 6 were used for interaction experiment owing to the sufficient quantity of the corneocytes for investigational purpose. We have selected 19 AAs including taurine and urea for the investigations (Table 6). After extraction of naturally present FAAs/urea as in sec 2.2.3.1 of the corneocytes the 10 mg of the cells were incubated with 100 µM standard soln. of 19 individual AAs including taurine and 500 µM urea (Table 6) as in an eppendorf tube for 24 hours at 32 °C temperature and 11.8 % humidity. Humidity was achieved by using saturated salt soln. of LiCl. Samples were centrifuged to collect supernatant and examined for the remaining amount of AAs and urea left after 24 hours of incubation with isolated corneocytes. The remaining amount was subtracted from the initial concentration of each of the respective AAs including taurine and urea will give the uptake of respective molecule by the corneocytes.

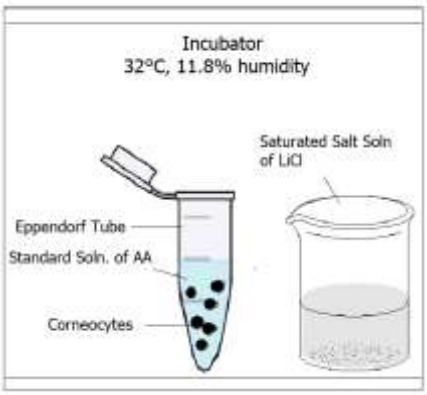

Figure 9. Schematic diagram of experimental design used in interaction of AAs and urea with the corneocytes.

2.2.4.3. Interaction of AA and urea with keratin

For this study keratin hydrolysate powder was used that was prepared from rams hoof. Two concentration of keratin (2 mg and 10 mg) were incubated with 100 µM standard solns. of 9 individual AAs including taurine and urea (500 µM) (Table 6) in an eppendorf tube using DDW (medium) for 24 hours at 32 °C and 11.8 % humidity (see Figure 9).

2.2.5. Development of *in vitro* diffusion model for hydrophilic molecules

2.2.5.1. Diffusion model of taurine

2.2.5.1.1. Uptake of taurine by isolated corneocytes

See sec 2.2.4.2 for uptake of taurine by the isolated corneocytes.

2.2.5.1.2. Interaction of taurine with keratin

See sec 2.2.4.3 for interaction of taurine with keratin.

2.2.5.1.3. In-vitro diffusion model of taurine

In vitro diffusion models `without corneocytes´ and `with corneocytes´ were a modification of previously used diffusion model of Neubert and Fürst (Neubert and Fürst, 1989) (Figure 10) and used for mathematical validation of uptake of taurine into the isolated corneocytes. Both *in-vitro* diffusion models `without corneocytes´ (taurine 100 µM) and `with corneocytes´ (taurine 100 µM + 10 mg/ml of the corneocytes) (Table 7) consisted of three diffusion cells each of the cells further comprised of acceptor (ACC) and donator (DON) sub-compartments with total volume of 20 ml, pH, 6.8 and the diffusion medium used was DDW. These compartments were immersed approximately 90 % in a water bath and were subjected to continuous stirring by integrated vibration system.

Table 6. List of AAs and urea included in each investigation

	Investigation		
Nr.	Quantification of AAs in the corneocytes	Stability study and interaction of AAs with the corenocytes	interaction of AAs with keratin
1.	Alanine	Alanine	Alanine
2.	Arginine	Arginine	-
3.	Aspartic acid	Aspartic acid	Aspartic acid
4.	Asparagine	Asparagine	Asparagine
5.	Citrulline	Citrulline	-
6.	Cysteine	-	-
7.	Glutamic acid	Glutamic acid	Glutamic acid
8.	Glutamine	Glutamine	Glutamine
9.	Glycine	Glycine	-
10.	Histidine	Histidine	Histidine
11.	Iso-leucine	Iso-leucine	-
12.	Leucine	Leucine	-
13.	Lysine	-	-
14.	Methionine	-	-
15.	Ornithine	-	-
16.	Phenylalanine	Phenylalanine	-
17.	Proline	Proline	Proline
18.	Serine	Serine	Serine
19.	Threonine	Threonine	-
20.	Tryptophane	Tryptophane	-
21.	Tyrosine	Tyrosine	-
22.	Taurine	Taurine	Taurine
23.	Valine	Valine	-
24.	Urea	Urea	Urea

Table 7. Composition of diffusion cells used in diffusion cells of taurine and urea

Model	Taurine	Urea	Taurine	Urea	
	100 µM	500 µM	100 µM	500 µM	1000 µM
DON	`Without the corneocytes ´		`With the corneocytes ´		
			10 mg/ml	50 mg/ml	
ACC	DDW		DDW	DDW	

The temperature of the water tank was maintained at 32 °C with inbuilt temperature regulator. DON and ACC were separated by a hydrophilic dialysis synthetic regenerated

cellulose (RC) membrane with total area of 15.9 cm^2 allowing the transport of taurine from DON to ACC compartment. Prior to the experiment the membrane was soaked in DDW for 30 min. Sample (1 ml) was drawn at specific time points (0.5, 1, 2, 4, 8, 12,…., 48 and 72 hours) from ACC and (24, 48 and 72 hours) from DON of both `without the corneocytes ´ and `with the corneocytes ´ models. After withdrawal samples were stored at 4 °C for one week and at -20 °C for longer duration. The withdrawn sample volume was refilled at every time with DDW to keep the total volume of the compartments constant.

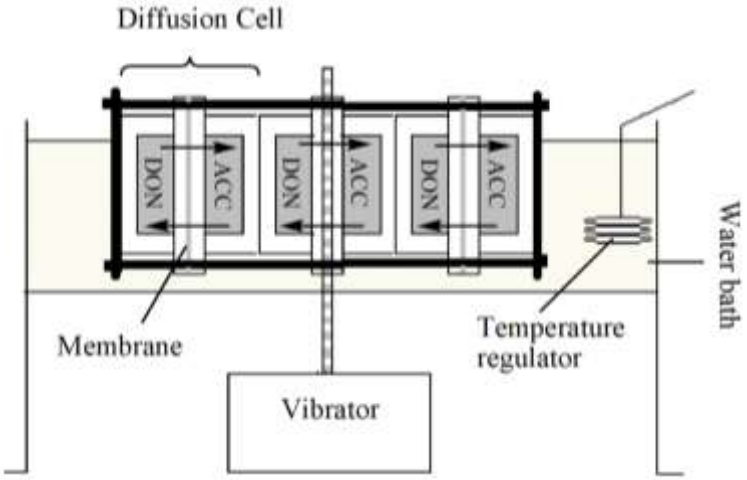

Figure 10. Schematic diagram of apparatus used in *in-vitro* diffusion profiles of taurine and urea.

2.2.5.1.4. Determination of correlation coefficient

Molecules diffused from DON through the dialysis membrane into the ACC following simple passive diffusion along the concentration gradient governed by FICK`s first law of diffusion as follows:

$$a_{DON} = -\mathrm{DA}\,\frac{dc}{dx} = -\mathrm{DA}\frac{(c_{DON} - c_{ACC})}{\triangle x} \qquad \text{Equ. (i)}$$

The total concentration of taurine will be equal to the sum of concentration distributed equally between both compartments at time when equilibrium is achieved. `$C_{eq}$´ is concentration at equilibrium that is half of the initial concentration `C_0´ if the volumes of DON and ACC are equal.

$$c_{eq} = \frac{C_0}{2} \qquad \text{Equ. (ii)}$$

With same volume and pH in both DON and ACC, the separating membrane is the only factor offering rate-limiting barrier for the transport of diffusing molecules across DON and ACC (Enderle, 2012; Fürst *et al.,* 1980, 1975; Neubert, 1978; Neubert and Fürst, 1989).

We have used `C_{cor}´ (corrected concentration) for curve fitting which was calculated using following formula:

$$C_{cor} = C_{tn} + C_{tn-1} . \frac{V_s}{V_{ACC}} + C_{tn-2} . \frac{V_s}{V_{ACC}} \ldots + C_{t1} . \frac{V_s}{V_{ACC}} \qquad \text{Equ. (iii)}$$

Where, `$C_{tn}$´ is concentration at final time point, `C_{tn-1}´ is concentration at point former to the last time point, `$V_s$´ is sample volume. Pearson´s correlation coefficient was calculated using corrected concentration of in vitro diffusion models `without corneocytes ´ and `with corneocytes ´ between the time points C_{24} to C_{72}, to observe the relative difference in the concentration curves of in vitro diffusion models.

2.2.5.2. Diffusion model of urea

2.2.5.2.1. Uptake of urea by the isolated corneocytes

See sec 2.2.4.2 for uptake of urea by the isolated corneocytes.

2.2.5.2.2. Interaction of urea with keratin

See sec 2.2.4.3 for interaction of urea with keratin.

2.2.5.2.3. In vitro diffusion model of urea

In vitro diffusion of urea `without corneocytes´ and `with corneocytes´ was same as in sec 2.2.5.1.3 and using diffusion apparatus presented in Figure 10, with only difference of concentration (500 µM and 1000 µM) were used. For *in-vitro* diffusion model of urea two concentration were used i) 500 µM ii) 1000 µM instead of 100 µM as in case of taurine only. While the concentration of the corneocytes used was 50 mg/ml in urea diffusion models instead of 10 mg/ml (for composition of diffusion cells see Table 7).

2.2.6. Analytics

2.2.6.1. Quantitative and qualitative analysis of amino acid after pre-column derivatization with FMOC-Cl using LC-ESI-MS/MS

2.2.6.1.1. Sample derivatization and processing

Pre-column derivatization was carried by adding 50 µl of sodium borate buffer (0.5 M, pH 7.9) in 25 µl samples and 100 µl of Fmoc-Cl (3 mM) soln. in acetone. After about 5-10 min, the reactions the samples were subjected to three times extraction with 500 µl n-pentane to remove organic layer. Thereafter, reaction mixture was left with open lid for 10 min to evaporate the remaining organic solvent. The aqueous phase left in the sample tube was added with 500 µl 5 % (V/V) of acetonitrile loaded onto the SPE resin. To distribute dry HR-X-resin into the wells of the 96-well filtration plate (50 mg/well) the SPE 96-well plate was prepared. 1 ml of MeOH followed by addition of 1 ml of DW to the plate for conditioning. In each of the above steps of conditioning and all the successive steps, after adding the liquid, the plates were allowed to centrifuge at 250 g for 5 min to allow the liquid to pass through the resin of the wells. After conditioning samples were loaded into this plate and the resin was washed with 1ml of water, and afterwards eluted with 1 ml of MeOH into a 96-deep well plate. The eluates containing extracted FAAs were transferred to 2 ml eppendorf vials, and the solvent was allowed to evaporate at 45 °C using vacuum in an eppendorf Concentrator till 50 µl of the sample is left in the tubes. The remaining concentrated samples were transferred to autosampler vials of LC–ESI-MS/MS for analysis.

2.2.6.1.2. LC-ESI-MS/MS Analysis

After concentration of the methanolic eluates, the analytes were separated by reverse phase chromatography on a Zorbax Eclipse Plus C18 Rapid Resolution HD column using a gradient consisting of eluent A (water + 0.02 % (V/V) acetic acid) and eluent B (acetonitrile + 0.02 % (V/V) acetic acid). At a flow rate of 700 µl min^{-1}, solvent B was held constant at 25 % for 0.3 min and increased to 50 % over the next 6.7 min. The column was washed by increasing solvent B to 98 % over 0.7 min, which was held for 1 min. Regeneration proceeded for 1 min at 25 % solvent B. The column temperature was set to 30 °C. Detection proceeded on-line by ESI–MS/MS using an API 3200 triple-quadrupole LC–ESI-MS/MS system equipped with an ESI Turbo Ion Spray interface, operated in the

negative ion mode. The ion source parameters were set as follows: curtain gas: 30 psi, ion spray voltage: −4,500 V, ion source temperature: 350 °C, nebulizing and drying gas: 50 psi. Triple-quadrupole scans were acquired in the multiple reaction monitoring (MRM) mode with Q1 and Q3 set at "unit" resolution Scheduled MRM was performed with a window of 90 s and a target scan time of 0.5 s. The MS parameters describing the MRMs for each amino acid are shown in Table A1 in appendices. Limit of quantification was below 20 nM for every analyte. Quantification was based on the signal intensities of the IS, NV.

Peak areas were integrated with IntelliQuant algorithm of the Analyst 1.6 software and adjusted manually if needed. All the calculations were done using MS-Excel. Calibration curves were recorded by taking six serial dilutions for each amino acid. The resulting response factor for each amino acid was used to correct for the deficiencies or differences in derivatization, sample clean up and detection between different series of measurements. The corrected values were then used to calculate the amounts based on the area of the added IS NV. For histidine and tyrosine, we have achieved two types of response signals mono and double derivatized AAs that were calculated independently and the values of Tyr-1 and Tyr-2 as well as Histidine-1 and Histidine-2 were summed; giving the final value for Tyrosine and Histidine, respectively. Similarly, the analysis generated two signals for methionine i.e., methionine and methionine-oxide that were also treated independently and added to get the final value of total methionine present.

2.2.6.2. Quantitative analysis of urea using HPLC

Urea was determined using HPLC Agilent 1100 series incorporated with G1312 pump and DAD G1315A and G1322 degasser. Separation was performed on Diol-NP/S Column (150× 3 mm and particle size of 5 µm) using 95/5 acetonitrile/water V/V as mobile phase. Flow rate was adjusted at 0.5 ml/min with injection volume of 20 µl and column temperature 30 °C. DAD was operated at 200 nm UV wavelength. Limit of detection and quantification were 0.5 µg/ml and 1 µg/ml, respectively. Standard were first prepared in water in six serial dilutions and the water that was replaced with mobile phase acetonitrile/water. Samples were also dried and added with mobile phase. The total run time was 12 min including last 2 min of equilibration and urea retention time at about 5.1

min. Calibration curve was recorded, method was validated for interday and intraday day precision before the actual samples run.

2.2.6.3. Calorimetric determination of urea

Concentration of urea was determined by coupled enzyme reaction, using urea assay kit provided with 25 ml of urea assay buffer along with four vials of reagents and one 100 µl vial of urea standard. The reagents consisted of oxiRed probe in DMSO, enzyme mix (lyophilized), developer, converting enzyme each with volume of 100 µl. Urea assay buffer was equilibrated at room temperature prior analysis and oxiRed added with DMSO was thawed at 37 °C for 1-5 min before analysis. Each of the enzyme mix, developer and converting enzyme reagent vials were reconstituted with 220 µl of urea assay buffer and stored at -20 °C. During use all the reagents and standard were kept on ice. 0.5 mM standard was prepared by adding 5 µl into 995 µl of urea assay buffer and for calibration serial dilutions from 1- 5 nmol/well were prepared to final volume of 50 µl made up with urea assay buffer. Each of the standard and sample were added with 42 µl buffer, 2 µl each of the all four reagents to obtain final volume of 50 µl designated as reaction mix. This reaction mix with amount of 50 µl was added to each of the sample and standard including one blank to get background response so the total final volume was 100 µl. Standards were prepared in triplicate to get the precise results. The standard and samples were added in 96-well microplate and placed in microplate reader of EPOCH 2 UV-spectrophotometer inculcated with Gen5 software to retrieve absorption data. The wavelength was set at 540 nm. After getting values for standards absorption vs concentration calibration curve was recorded to calculate the concentration of urea in the samples using following formula using excel.

$$Sa = \frac{corrected\ conc. - (y - intercept)}{slope} \quad \text{..... Equ (i)}$$

Concentration of urea was determined using:

$$\text{Urea Concentration} = \frac{Sa}{Sv} * D \quad \text{.....Equ (ii)}$$

Where `Sa´ was sample amount from standard curve, `Sv´ was sample volume added into the wells and `D´ was dilution factor. The assay can detect > 0.5 nmol/well of urea with 0.5 nmol/well – 5 nmol/well of linear quantification range.

2.2.7. Statistical analysis of data

For data obtained in quantification of FAAs/urea in the isolated corneocytes distribution of the data was tested by Shapiro-Wilk normality test using SPSS. Statistical significance was determined by Kruskal-Wallis test followed by post-hoc Mann- Whitney test. The difference was considered significant and highly significant at $p < 0.05$ and $p < 0.01$, respectively, using GraphPad.

The comparison of the FAAs/urea values between left and right arm was carried out using Bland and Altman analysis with the help of MS- Excel. The Bland and Altman plot analysis was used to evaluate a bias between the mean differences, and to estimate an interval, within which 95 % of the differences of the second measurement, compared to the first one, fall (Giavarina, 2015). Data related to urea and taurine diffusion profile was analysed by curve fitting was performed using originLab statistical software. For descriptive statistics MS-excel was used.

Chapter 3. Isolation and microscopic study of the corneocytes

3.1. Introduction

Keratinocytes the cells of lower layers of the epidermis are filled with filaggrin, a histidine rich protein, which binds with the keratin and results in the flattening of the keratinocytes by a process called desquamation. These flattened cells of the epidermis are called the corneocytes and the layer thus formed is called SC, representing the outermost layer of the epidermis (Jepps *et al.,* 2013; McGrath *et al.,* 2008; Piérard *et al.,* 2000). the corneocytes are surrounded by a protein shell called cornified envelope (Kalinin *et al.* 2002; Mojumdar *et al.* 2017) along with covalently bound lipid monolayer (Elias *et al.,* 2014). The layers of the corneocytes are (Sylvestre *et al.,* 2010) embedded in multilamellar lipid matrix or intercellular lipid comprised of ceramides, free fatty acids, cholesterol and its derivatives (Elias *et al.,* 2014).

In this study we have the isolated corneocytes from two types of skin samples i) from pedicure treatment ii) tape stripping of the forearms of HY, HO, AD and PS. The former kind of the corneocytes were isolated for two purposes. Firstly, to conduct preliminary studies of protocol development for extraction of FAAs/urea and secondly, to use them for the interaction studies with AAs and in diffusion profile of taurine and urea due to their sufficient quantities. The later type of the isolated corneocytes were used in microscopic and comparative study to observe effect of disease and ageing on the content of FAAs/urea. SEM was done for first kind of the corneocytes while, the other type of the corneocytes were studied by TEM. Selection of the respective microscopic technique is based on the type of sample, its density and limitations of the technique.

3.2. Microscopic images of the corneocytes isolated from skin obtained after pedicure treatment obtained with SEM.

SEM images were obtained for the corneocytes isolated from skin sample obtained from pedicure treatment. Figure 11 showing the isolated corneocytes before treatment while, Figure 12 presented images of the isolated corneocytes after treatment with C/M, (2/1, V/V).

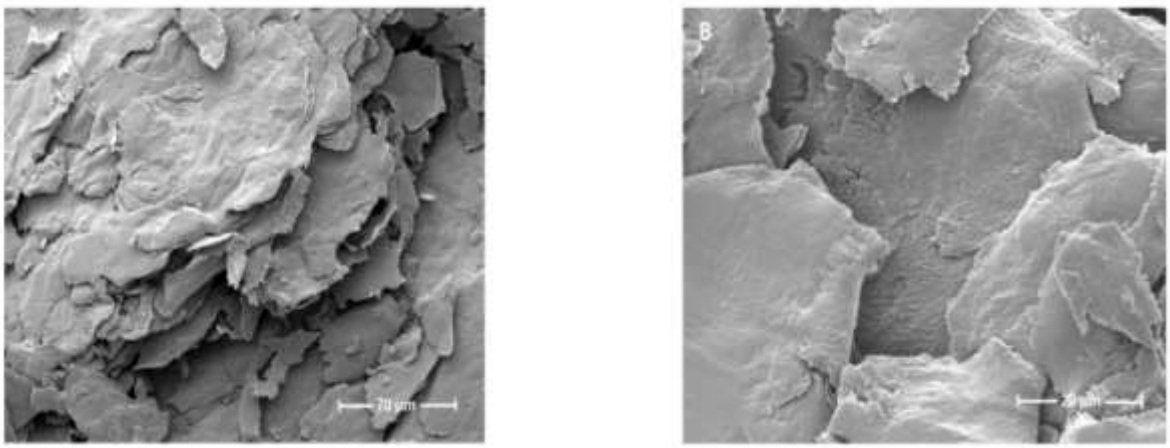

Figure 11. SC sample of the skin obtained from pedicure treatment. The sample crushed and washed with PBS and consisted of the corneocytes with intercellular lipids at A) lower magnification B) at higher magnification.

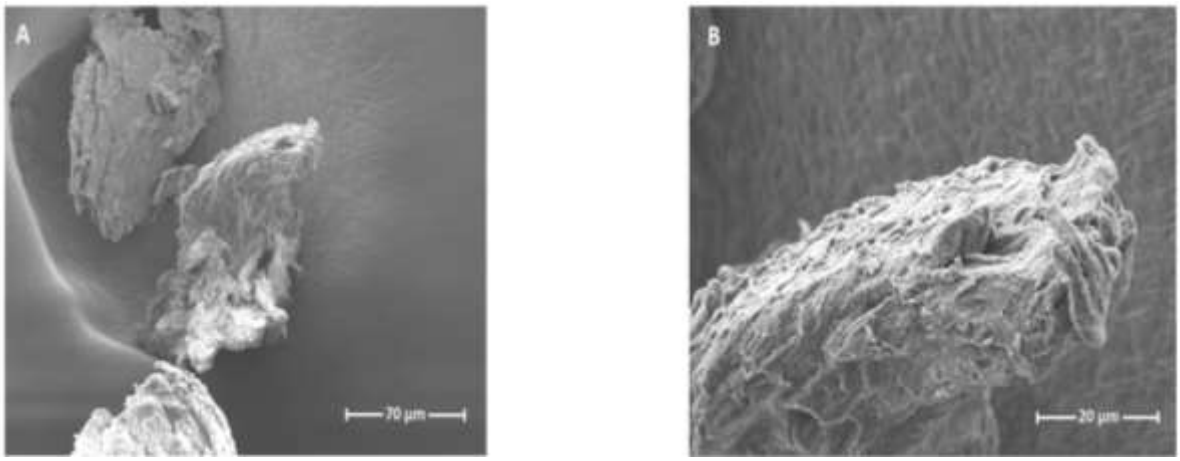

Figure 12. SC sample after treatment with C/M (2/1, V/V) mixture to remove intercellular showed the isolated corneocytes without intercellular lipids A) at lower magnification B) at higher magnification.

Figure 12 A and B showed the segregated corneocytes without intercellular lipids. These corneocytes were used for preliminary studies for the development of extraction protocol as well as in the experiments related to interaction of AAs and diffusion profile of taurine and urea.

3.3. Isolation and microscopic study of the corneocytes from the skin obtained after tape stripping using TEM

TEM of the corneocytes isolated from the stratum corneum obtained after tape stripping showed elongated cells filled with keratin. In literature it has not yet been clearly mentioned that whether the second layer of the SC contains intercellular lipid or not but according to some researchers second tape strip also contained lipids present intercellularly particularly ceramides (T'Kindt *et al.,* 2012). In this study we used second strip for the isolation of the corneocytes and removed intercellular lipids to get isolated corneoctytes.

3.3.1. Microscopic images of the corneocytes isolated at different morphological levels taken from tape stripping

3.3.1.1. SC sample without any treatment taken with tape stripping

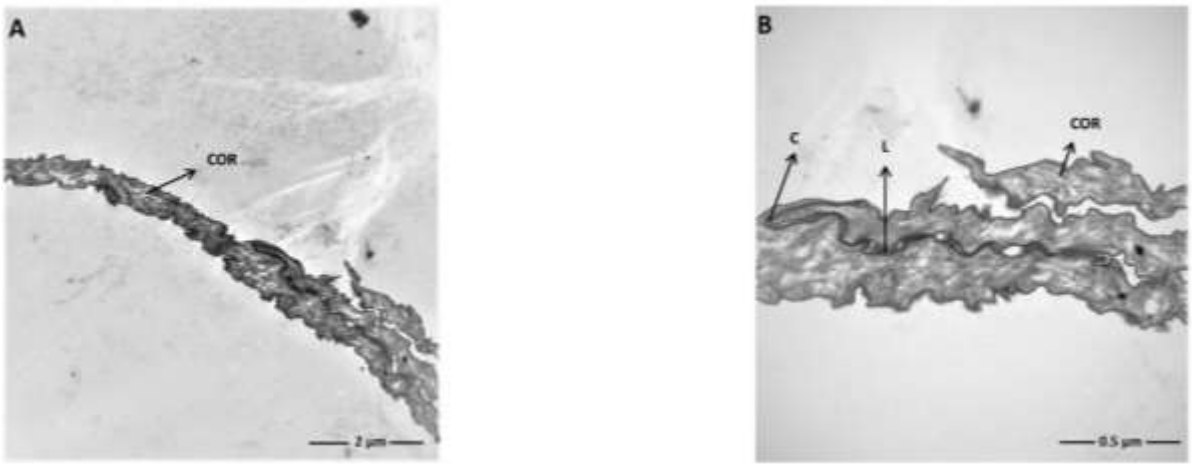

Figure 13. SC taken with the help of tape stripping method A) SC sample without any treatment at lower magnification `COR´ showing the corneocytes B) at higher magnification `C´ is indicating the hook like structure corneodesmosome `L´ is indicating the intercellular lipids.

Figure 13. Showed elongated structures which are the corneocytes and in between these corneocytes are the lipids. Corneodesmosomes are the structures derived from desmosomes after molecular modifications, persist in the upper layers of the SC and function to bind coenocytes together (Haftek *et al.,* 1998, 1997; Serre *et al.,* 1991).

3.3.1.2. Isolated corneocytes without intercellular lipids

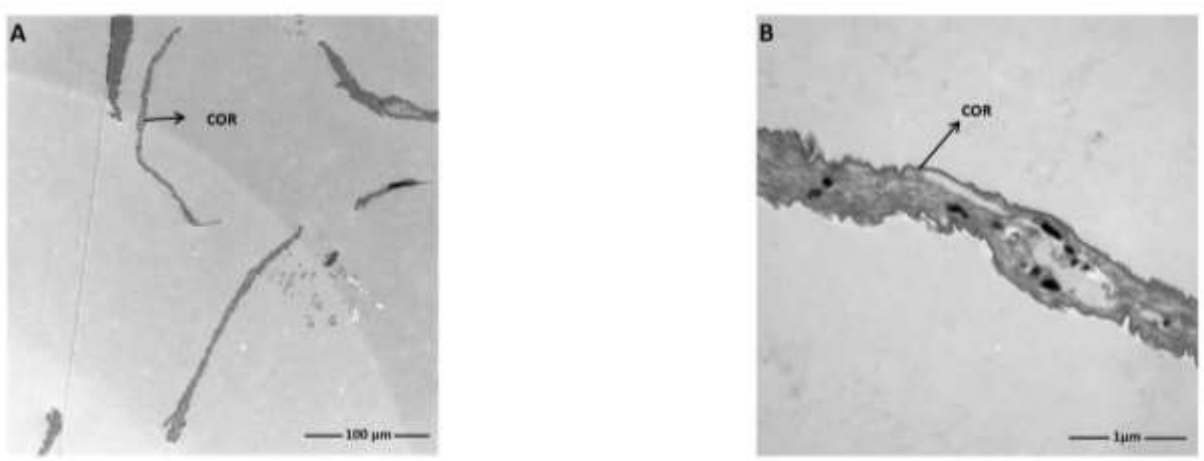

Figure 14. Isolated corneocytes without intercellular lipids.

SC sample after tape stripping treated with C/M, (2/1, V/V) mixture resulted in the isolation of the corneocytes without intercellular lipids.

3.3.1.3. Isolated corneocytes without esterified lipids

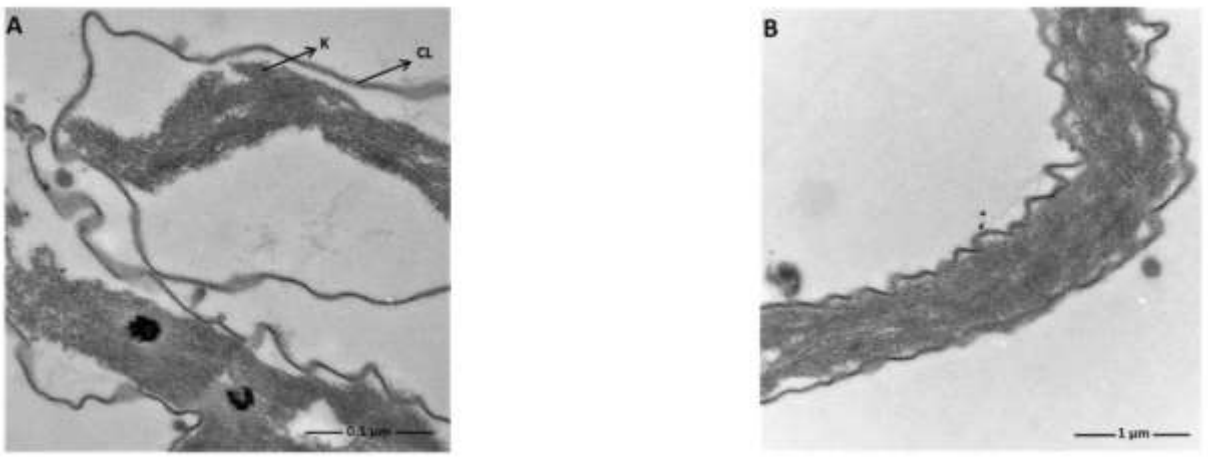

Figure 15. Isolated corneocytes without covalently bound lipids.

Figure 15 showed the covalently bound lipids `CL´ and detachment of covalently bound lipids from keratin `K´ present inside the corneocytes.

3.3.1.4. Isolated corneocytes without cornified envelope

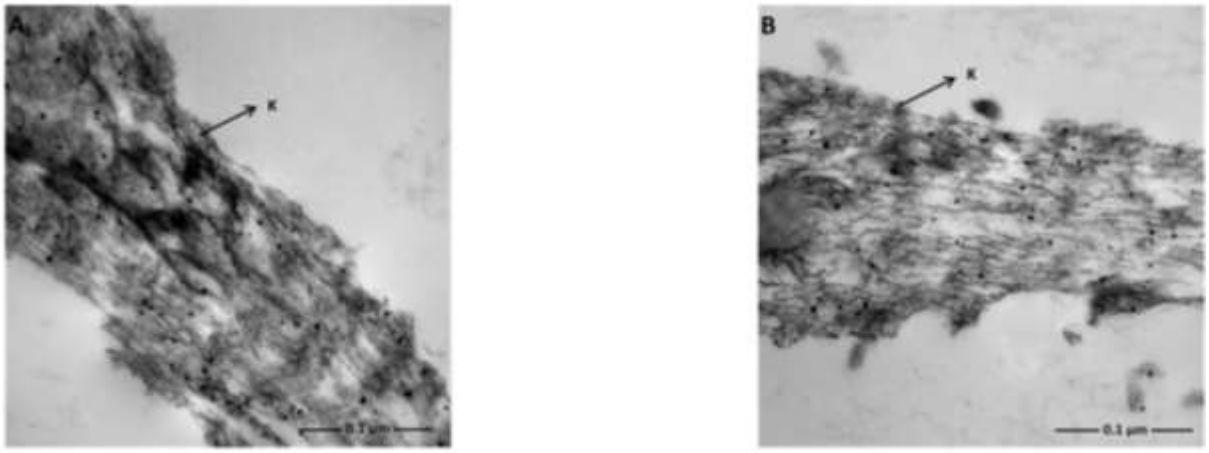

Figure 16. Isolated corneocytes without cornified envelope.

Cornified envelope is the first most boundary surrounding the keratin and thus shaping the corneocytes. The corneocytes samples with tape stripping were treated with 0.2 % SDS EB as mentioned in methods resulted in complete removal of cornified envelope which surrounds the keratin of the corneocytes (Candi *et al.,* 2005; Harding *et al.,* 2003).

3.4. Microscopic study of the corneoytes isolated from HY, HO, AD and PS group using TEM.

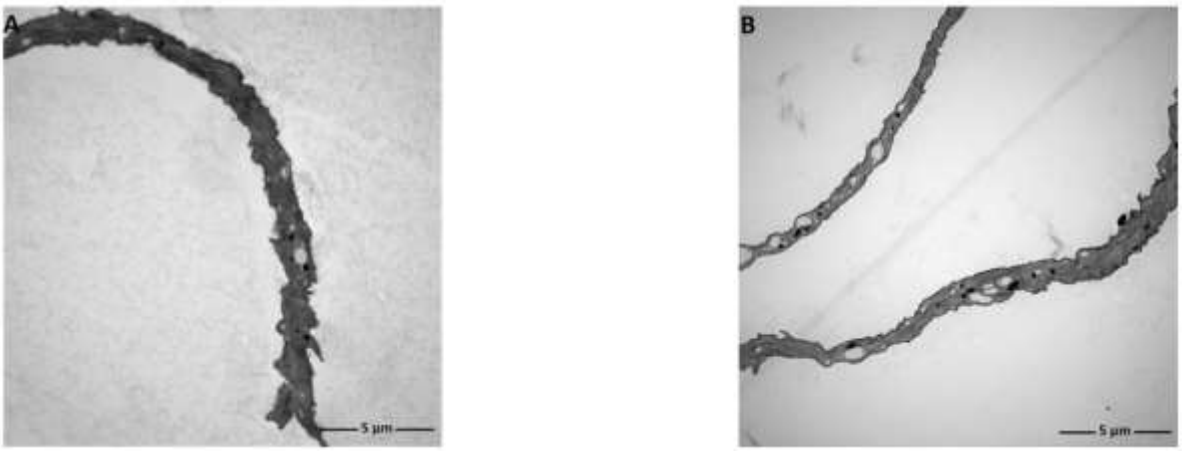

Figure 17. TEM images of the corneocytes isolated from healthy skin of HY group and SC sample was treated with C/M, (2/1, V/V) to remove intercellular lipids.

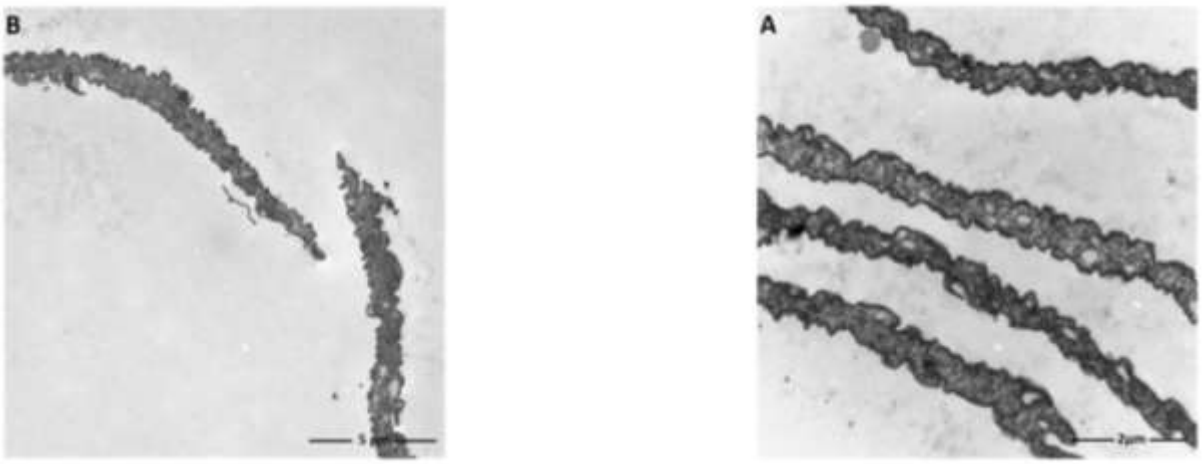

Figure 18. TEM images of the corneocytes isolated from aged skin of HO group and SC sample after tape stripping was treated with C/M, (2/1, V/V) to remove intercellular lipids.

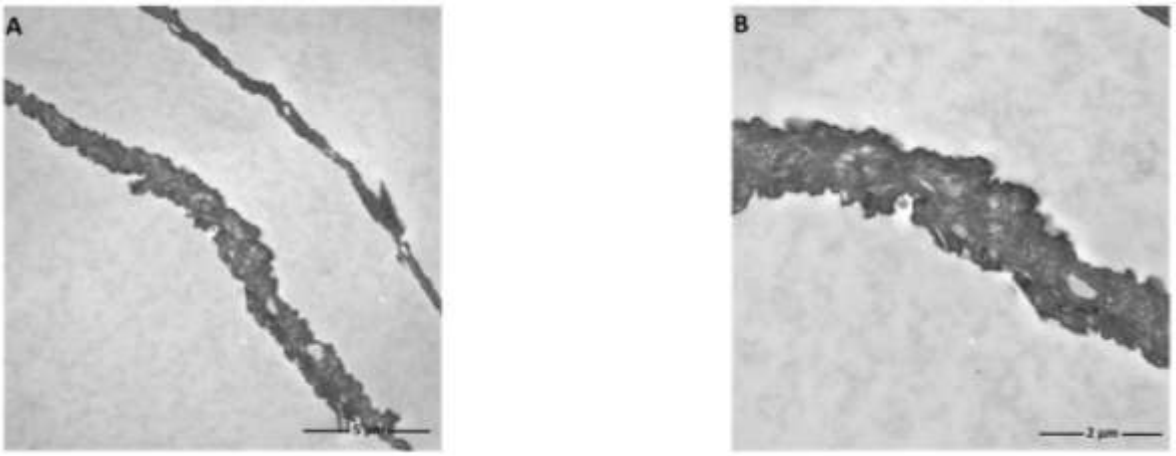

Figure 19. TEM images of the corneocytes isolated from diseased skin of the AD group and SC sample after tape-stripping was treated with C/M, (2/1, V/V) to remove the intercellular lipids.

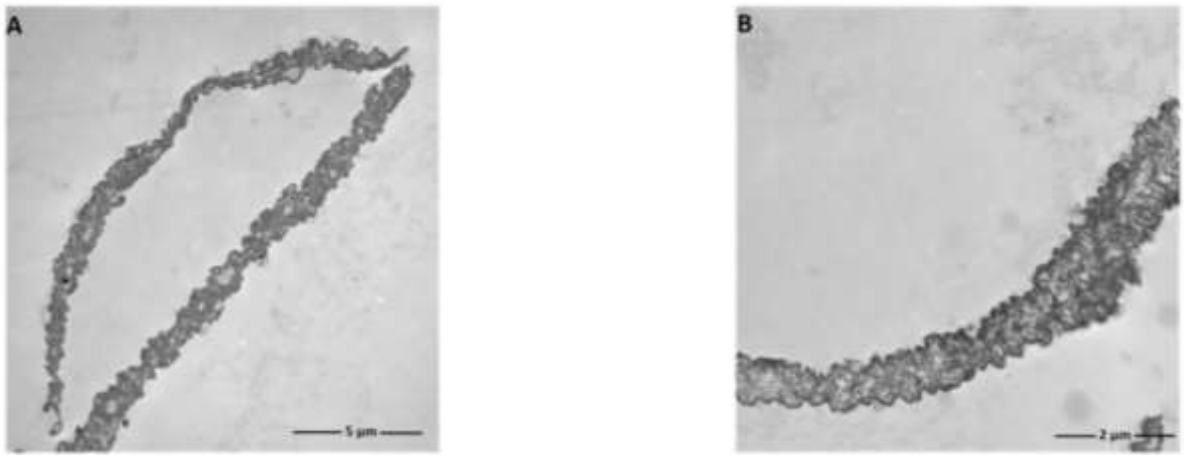

Figure 20. TEM images of the corneocytes isolated from diseased skin of PS group and SC sample after tape-stripping was treated with C/M, (2/1, V/V) to remove intercellular lipids.

The corneocytes were isolated from the SC sample taken from the tape stripping of forearm skin of four groups were examined by TEM for any visual differences in morphology or size of the corneocytes. In old literature studies described correlation of corneocyte size with the age. Three dimensional parameters of the corneocytes were examined by atomic force microscopy obtained from healthy, aged AD and PS skin. The study reported an increase in the size of the cells with age, while the corneocytes of uninvolved area of AD also showed differences from that of the corneocytes of healthy skin (Fartacsh, 1997; Kashibuchi *et al.,* 2002; Marks *et al.,* 1981). However, contrary to these reports there were no visual differences in the size and morphology of the isolated corneocytes of healthy versus aged or uninvolved skin the corneocytes of AD and PS observed in our study.

3.5. Conclusions

No visual difference in the size or morphology in any of the corneocytes isolated from HO, AD or PS group was identified. Moreover, the corneocytes isolated from skin samples obtained after pedicure treatment can be utilized in the dermatological studies requiring sufficient amount of the corneocytes.

Chapter 4. Extraction and quantification of FAAs/urea in the isolated corneocytes

4.1. Introduction

FAAs are present at about 40 % and urea being 7 % of total molecular composition of the SC and hence, are the most abundantly found molecules amongst other NMFs in the corneocytes (Rawlings *et al.,* 1994). Already reported FAAs in NMFs include alanine, asparagine, arginine, aspartic acid, cysteine, citrulline, glutamine, glutamic acid, histidine, iso-leucine, leucine, lysine, methionine, ornithine, phenylalanine, proline, serine, threonine, tyrosine, tryptophan and valine (Caspers *et al.,* 2001; Joo *et al.,* 2012; Sylvestre *et al.,* 2010; Visscher *et al.,* 2011).

As mentioned in the sec. 1.5 a number of studies demonstrated that the level of NMFs including FAAs/urea is decreased in dry skin conditions such as Ichthyosis vulgaris, AD, PS and dehydrated skin of aged compared to healthy skin (Fowler, 2012; Rippke *et al.,* 2004; Schölermann *et al.,* 1998; Sonoda *et al.,* 2012; Verdier-Sévrain and Bonté, 2007). While some of the researchers reported contrary results regarding the quantitative level of FAAs in the SC of the old and diseased skin (Jacobson *et al.,* 1990; Sugawara *et al.,* 2012; Takahashi and Tezuka, 2004). Most of the studies conducted for the analysis of FAAs/urea in the SC used HPLC, AAA and other less efficient analytical methods with limited selectivity and sensitivity. In this study LC-ESI-MS/MS-MRM method was used, which circumvents the limitations associated with selectivity, sensitivity and comprehensiveness compared to already used methods in this field. Other interventions were made at the level of extraction of FAAs/urea from the isolated corneocytes without hydrolysis of the cell proteins. Which in most of the studies, as mentioned above, are producing unclear results related to FAAs/urea quantification. For protocol development, preliminary studies were conducted on the corneocytes isolated from the skin samples obtained from pedicure treatment. The protocol thus developed, was implemented on the isolated corneocytes from skin samples obtained from tape strips with slight modifications. After preliminary work, the major study was conducted on the skin sample taken with the help of tape strips from right and left arm of HY, HO, AD and PS group. A comparative analysis of FAAs/urea was done to observe the correlation between the quantities of FAAs/urea obtained from right and left arm between the groups.

4.2. Qualitative and quantitative analysis of FAAs from the corneocytes using LC-ESI-MS/MS-MRM analysis after pre-column derivatization with FMOC-Cl

4.2.1. Quantification of FAAs isolated from pedicure skin n

4.2.1.1. FAAs determined at different conditions of temperature, incubation time and solvent

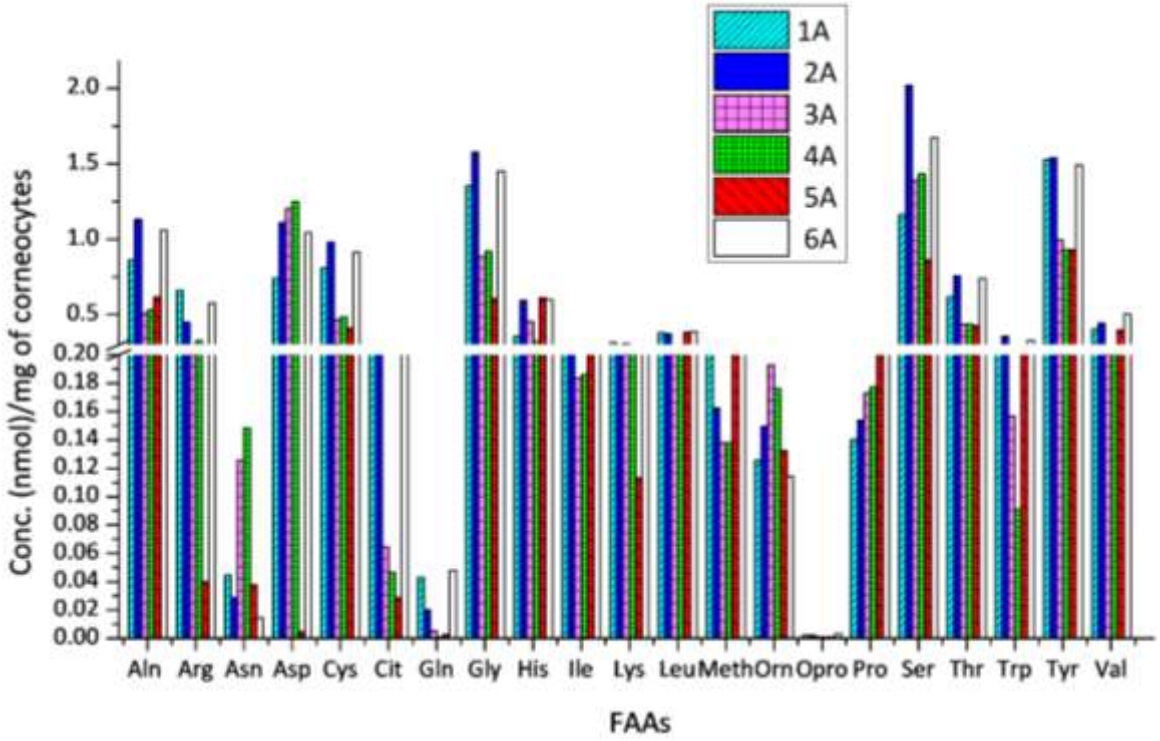

Figure 21. FAAs quantified from the corneocytes isolated from pedicure skin at different temperatures, incubation time and solvents (n = 1).

The corneocytes isolated from the skin samples obtained after pedicure treatment and extraction of FAAs/urea was carried out without being subjected to acidic hydrolysis at different temperatures, incubation time and solvents. The maximum concentration of FAAs was obtained at 46 °C incubating for 24 hours in DDW as shown in Figure 21.

4.2.1.2. Extraction and quantification of FAAs from the corneocytes isolated from pedicure skin at optimum conditions

4.2.1.2.1. FAAs/ urea

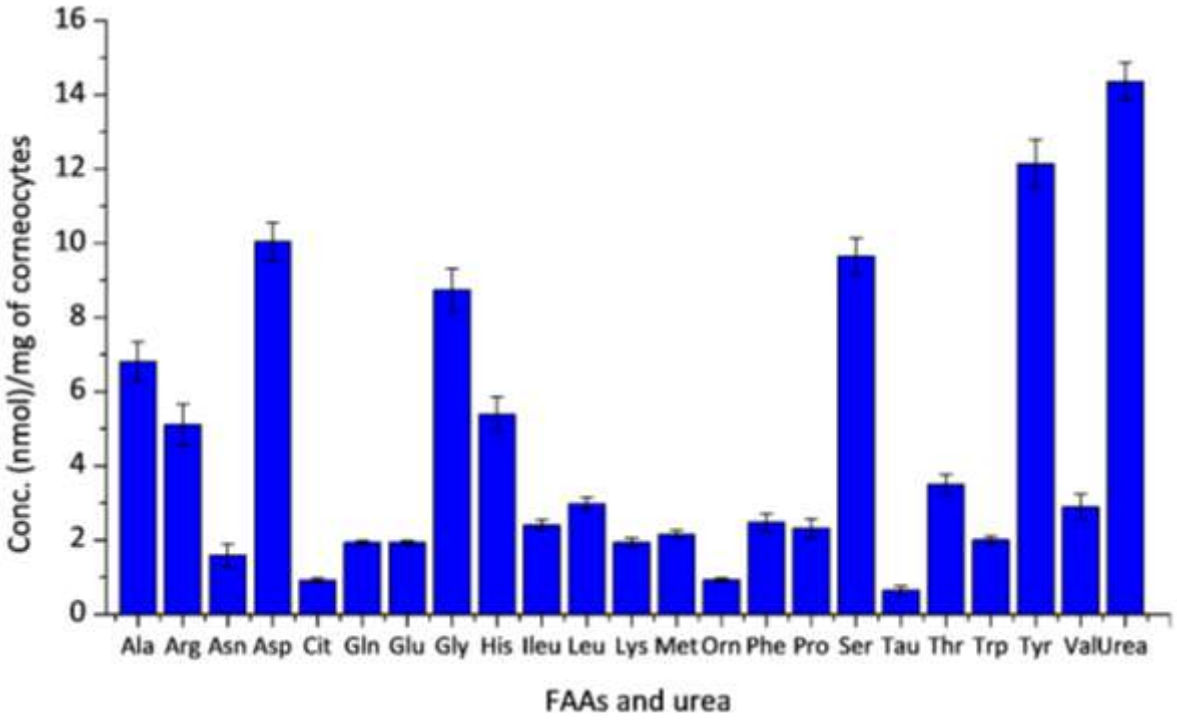

Figure 22. FAAs/urea quantified at optimum conditions (46 °C, 24 hours in DDW) from the corneocytes isolated from the skin obtained after pedicure treatment (n = 5, RSD < 20 %).

FAAs/urea were determined in the isolated corneocytes at optimum conditions of 46 °C with incubation time of 24 hours in DDW, as shown in Figure 22. Which showed the presence of 23 AAs. The amount of each AA is expressed in (nmol)/mg of the corneocytes and alanine, arginine, aspartic acid, histidine, serine and tyrosine found in higher amounts. While citrulline, ornithine and taurine were amongst AAs, that were present in lower concentration. FAAs of the SC have been determined by various investigators in the past, however, to the best of our knowledge to-date no work is done on the quantification of FAAs content of the corneocytes isolated from the skin obtained after pedicure treatment. The isolated corneocytes thus obtained can be used not only for objective analysis of horny skin of the feet but also for preliminary protocol developments in various studies. In previous researches, scientists used hydrolysis to extract the AAs which proteolysed most of the epidermal proteins resulted in production of hydrolyzed

AAs rather than FAAs only. We have used only DDW and an optimum temperature to extract the FAAs that resulted in the extraction and quantification of FAAs. At 46° C the corneocytes results in segregation from each other and maximum extraction of FFAs/urea (Warner *et al.,* 2003). DDW was selected due to the solubility of AAs in it.

4.3. Extraction of FAAs/urea from skin samples obtained from tape stripping

4.3.1. Quantification of FAAs/urea in HY group

Extraction and quantification of FAAs/urea from the isolated corneocytes obtained after tape stripping of HY group resulted in the following amounts.

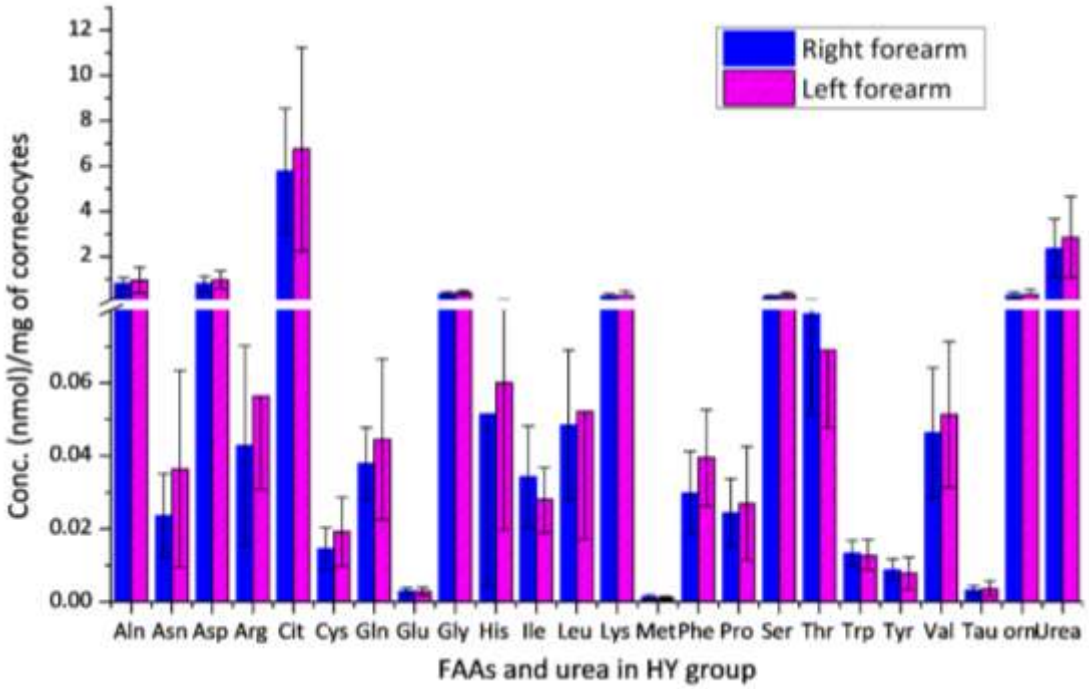

Figure 23. FAAs/urea measured in the isolated corneocytes obtained from both left and right forearm of HY group (n= 5, RSD ≤ 70 %).

Figure 23 showed, FAAs/urea content in the HY skin (18- 40 years) obtained from right and left forearm of the volunteers. The extraction was done by lysis of the corneocytes with 70 % MeOH which results in 100 % solubility of FAAs in the solvent and thus avoiding any chemically induced acid hydrolysis. 23 FAAs included alanine, asparagine,

arginine, aspartic acid, citrulline, cysteine, glutamine, glutamic acid, glycine, histidine, isoleucine, leucine, lysine, methionine, phenylalanine, proline, serine, threonine, tryptophane, tyrosine, valine, taurine, ornithine and urea have been quantified in the corneocytes isolated from forearm skin of HY. Predominantly found FAAs were alanine, aspartic acid, citrulline, glycine, lysine, serine. While the FAAs that were found to be in lower amounts are cysteine, glutamic acid, methionine, taurine, tryptophane and tyrosine, whose quantities are less than 0.02 (nmol)/mg of the corneocytes. The quantity of citrulline is the highest up to 7 (nmol)/ mg of the corneocytes. The concentration of urea was about 3.5 nmol/ml in the right and left forearm respectively.

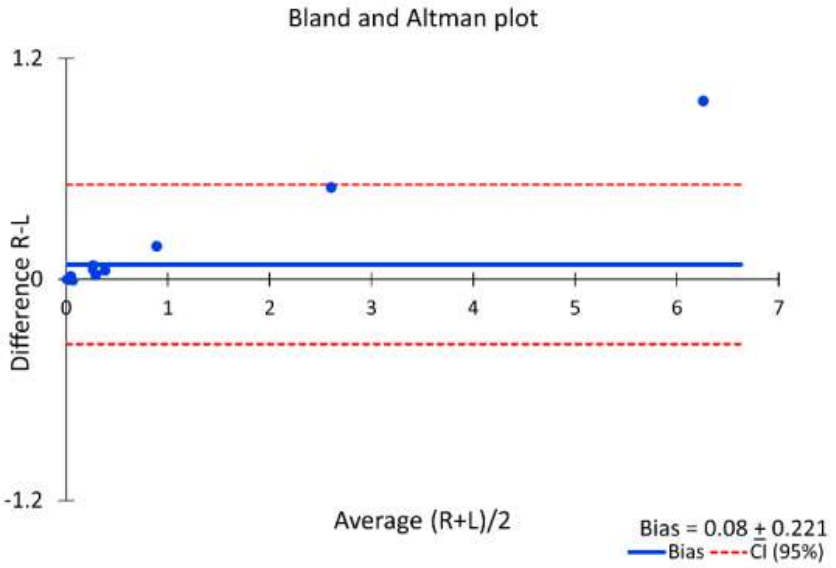

Figure 24. Bland-Altman plot for comparative analysis of FAAs/urea in right and left forearm of HY group. The horizontal lines represents the mean difference, and at the limits of agreement (95 % correlation).

As shown by Figure 24 the quantities of FAAs/urea both left and right forearm showed strong correlation. There was a good agreement in the FAAs/urea amounts between both forearms with the average bias (average of the difference between left and right arm) of 0.08. The fact that average bias close to zero indicates that the measured values for right and left forearms do not produce systematically different results.

4.3.2. Quantification of FAAs/urea in HO group

HO skin samples were obtained from the volunteers with age between 65-75 years old. The above results showed the presence of all 23 AAs in addition to urea as identified in HY group. Alanine, citrulline and serine found up to 10 (nmol)/mg of the corneocytes. While the amount of urea is even more than 10 (nmol)/mg of the corneocytes. While arginine, glutamine, and taurine are found in the lower concentration. Unlike HY group HO group contains urea the most abundant molecule in the corneocytes. The reason for the highest amount of urea in the old age may be due to the reason other than that FAAs/urea were only produced by filaggrin degradation.

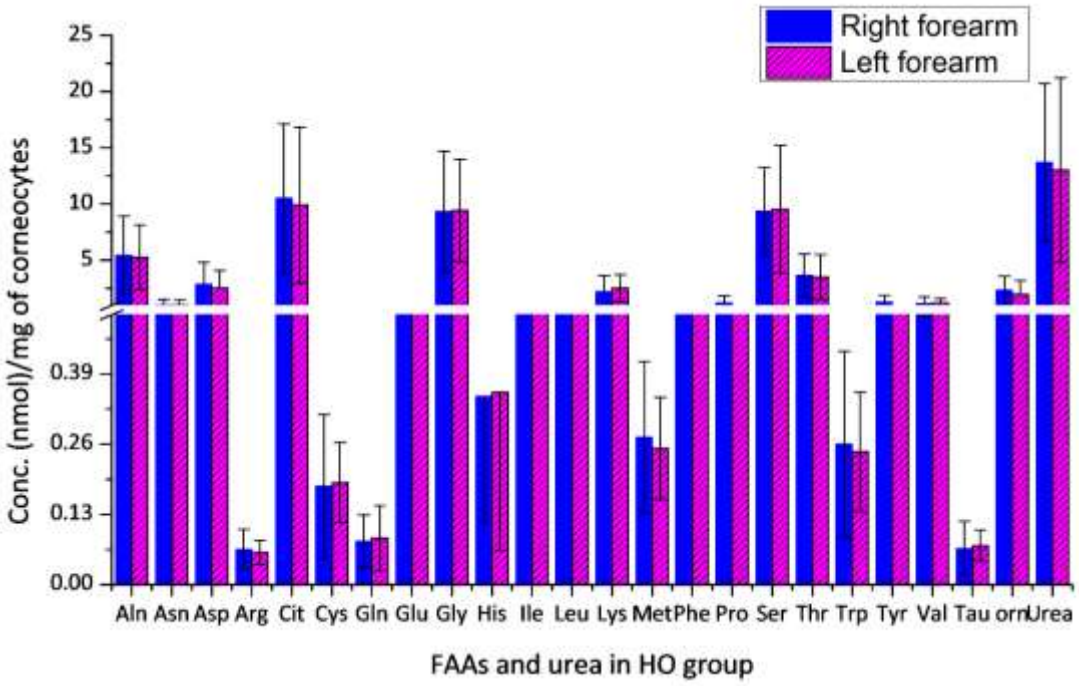

Figure 25. FAAs/urea measured in the cornecytes isolated from skin sample of right and left forearm of HO group (n= 5, RSD < 70 %).

The Bland and Altman plot showed a strong correlation between the concentrations of

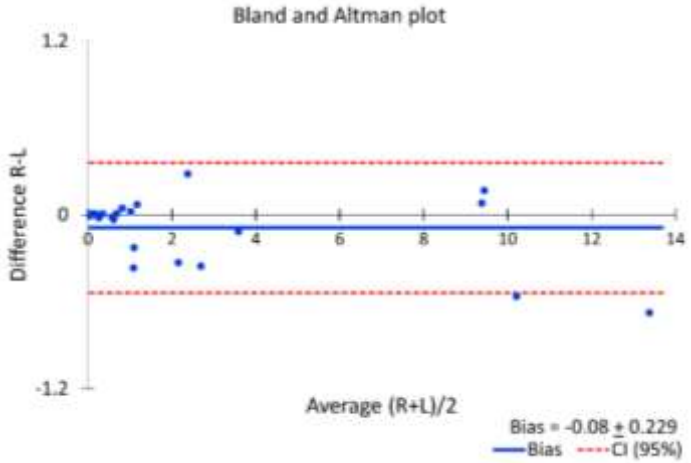

Figure 26. Bland and Altman analysis of FAAs/urea in right and left forearm of HO group. The horizontal lines represents the mean difference, and at the limits of agreement (95 % correlation).

FAAs/urea obtained in the isolated corneocytes from both forearms in AD group with average bias of -0.08. Which showed that the measurements of FAAs/urea both forearms do not produce systematically different results.

4.3.3. Quantification of FAAs/urea in AD group

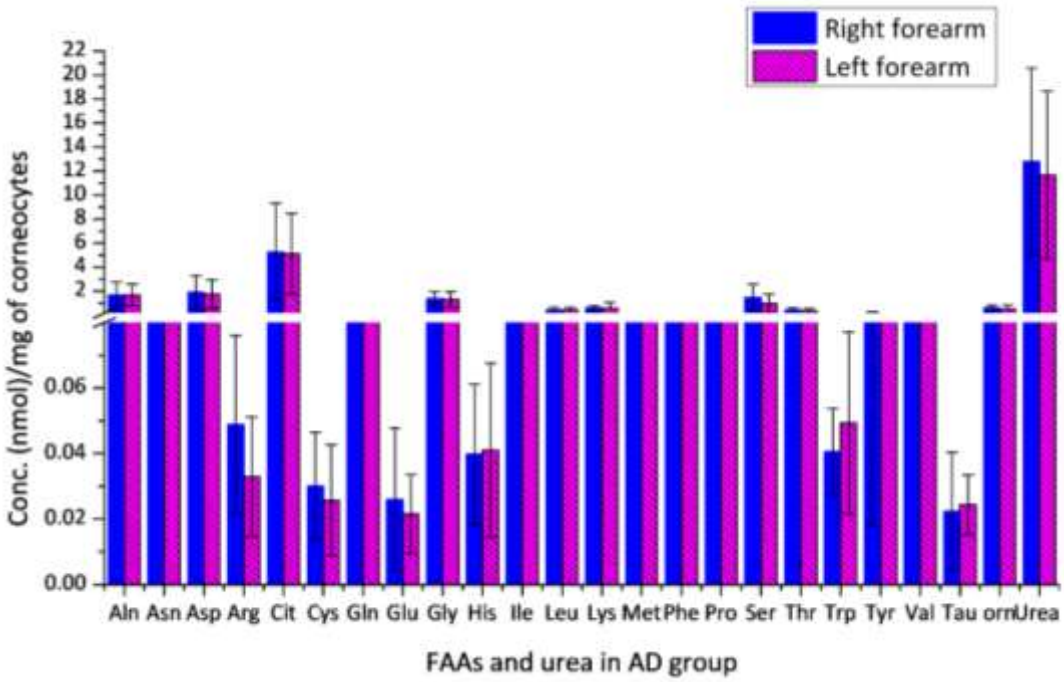

Figure 27. FAAs/urea measured in the cornecytes isolated from skin sample of right and left forearm of AD group (n = 5, RSD = 70 %).

Extraction of FAAs/urea has been done from the corneocytes isolated from right and left forearms of AD patients and analyzed. All of the 23 FAAs, as mentioned above, along with urea were observed and quantified. Figure 27 showed the highest concentration, up to 12 (nmol)/mg of the corneocytes, was shown by urea. Citrulline was also quantified to be about 6 (nmol)/mg of the corneocytes. The amount of taurine was present in the lowest, arginine, glutamic acid histidine and tryptophane were also observed in lower concentrations however, greater than 0.02 (nmol)/mg of the corneocytes.

A strong correlation in the amounts of FAAs/urea between right and left forearms have been observed by Bland and Altman analysis with bias of -0.1 as presented by Figure 28.

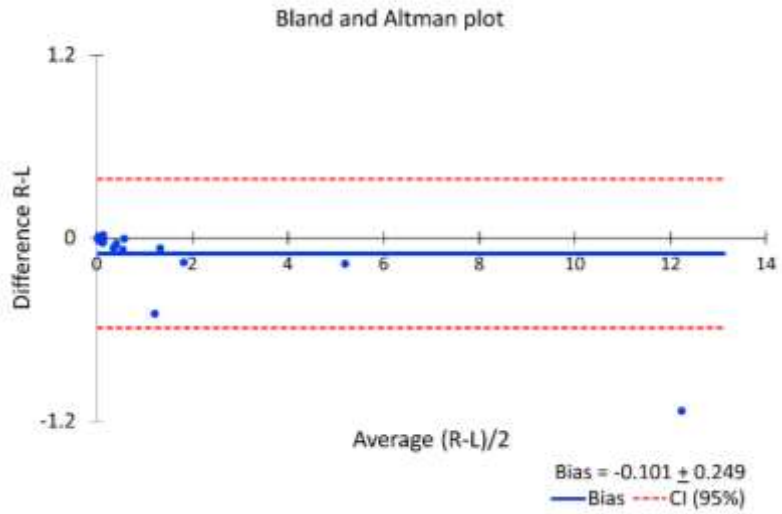

Figure 28. Bland and Altman analysis of FAAs/urea measure in right and left arm of AD group. The horizontal lines represents the mean difference, and at the limits of agreement (95 % correlation).

4.3.4. Quantification of FAAs/urea in PS group

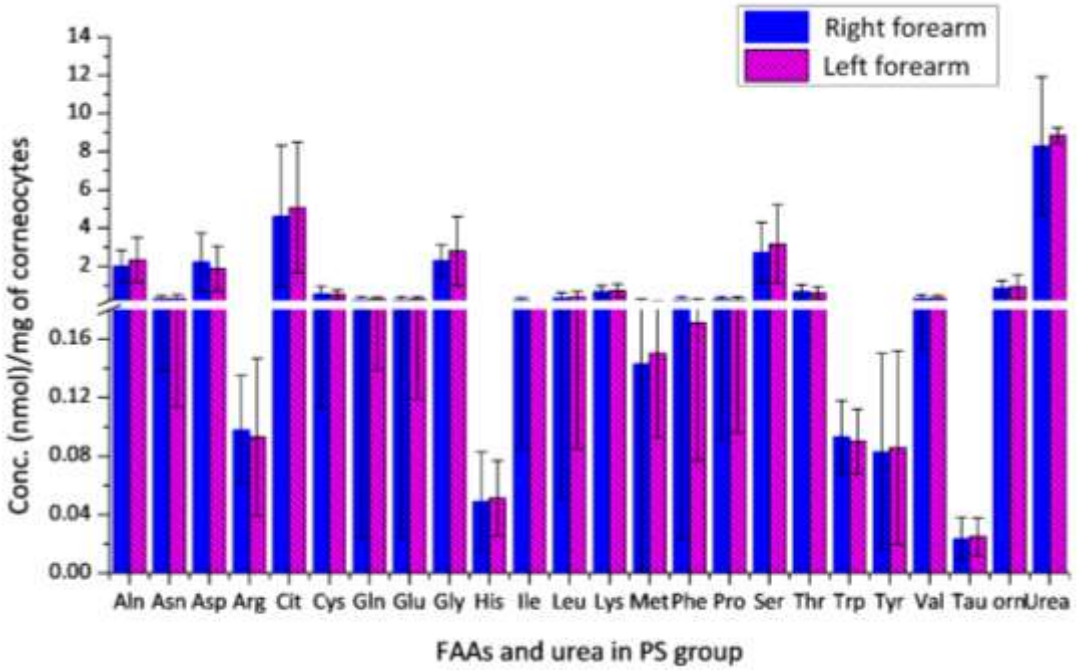

Figure 29. FAAs/urea measured in the cornecytes isolated from skin sample of right and left forearm of PS group (n = 5, RSD < 70 %).

FAAs/urea were extracted from the corneocytes isolated from tape stripping samples of right and left forearms of PS patients. The results showed all 23 AAs in addition to urea to be present in the isolated corneocytes of this group.

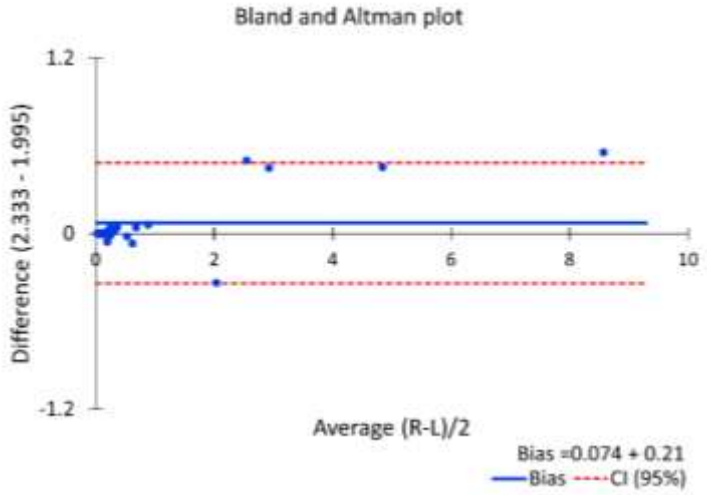

Figure 30. Bland and Altman analysis of FAAs/urea in right and left forearm of PS group. The horizontal lines represents the mean difference, and at the limits of agreement (95 % correlation). In PS group again the amount of urea was found to be highest amongst others which is about 8 (nmol)/mg of the isolated corneocytes. The second and the third highest concentration molecules of the corneocytes were citrulline, 5 (nmol)/mg and serine, 4 (nmol)/mg, respectively. Although taurine, arginine and histidine were amongst the FAAs found in concentration, however, more than 0.02 (nmol)/mg of the corneocytes. There was no difference identified between the quantities of FAAs/urea measured in right and left forearm of the skin samples of PS group after bland and Altman analysis (see Figure 30).

4.3.5. Comparative analysis of FAAs/urea in four groups (HY, HO. AD and PS)

Extraction of FAAs/urea were carried out in four groups HY, HO. AD and PS for comparative analysis and to observe any relation between the skin conditions and quantities of FAAs/urea. FAAs/urea concentration were determined in per mg of the corneocytes obtained from the SC of four groups, HY, HO, AD and PS. There was significant difference for FAAs/urea concentration observed amongst all the groups. Alanine, aspartic acid, citrulline, glycine, lysine, serine and urea were found predominantly in all the groups as shown in Figure 31 and see supporting information Table A6 in appendices. The results showed highest concentration of total FAAs/urea in the HO group while the significantly ($p < 0.01$) lowest concentration was observed in HY group compared to all groups Figure 32. Higher concentration of FAAs/urea is also in line with the most recent researches done in the past regarding aged skin (Egawa and Tagami, 2007; Jacobson *et al.,* 1990; Takahashi and Tezuka, 2004) According to Kashima *et al.* Cathepsin D and epidermal serine proteinase may play a role in the degradation of filaggrin and processing of profilaggrin (Kashima *et al.,* 1988). So, this increase in the amount of FAAs/urea in HO group may be due to the increased expression of cathepsin B and cathepsin L enzyme activity towards the degradation of filaggrin in the stratum spinosum of the aged epidermis (Kawada *et al.,* 1995a, 1995b).

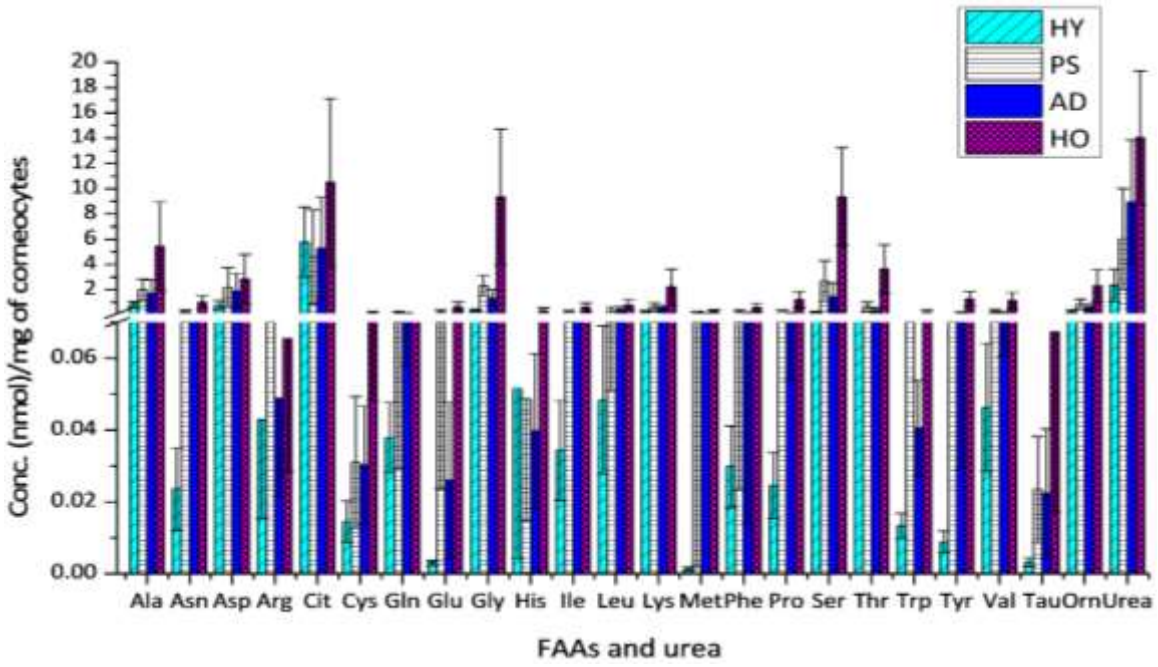

Figure 31. Comparative analysis of quantities of FAAs/urea (nmol)/ mg of the corneocytes in right forearm measured in four groups HY, HO, AD and PS (n = 5, RSD < 70 %).

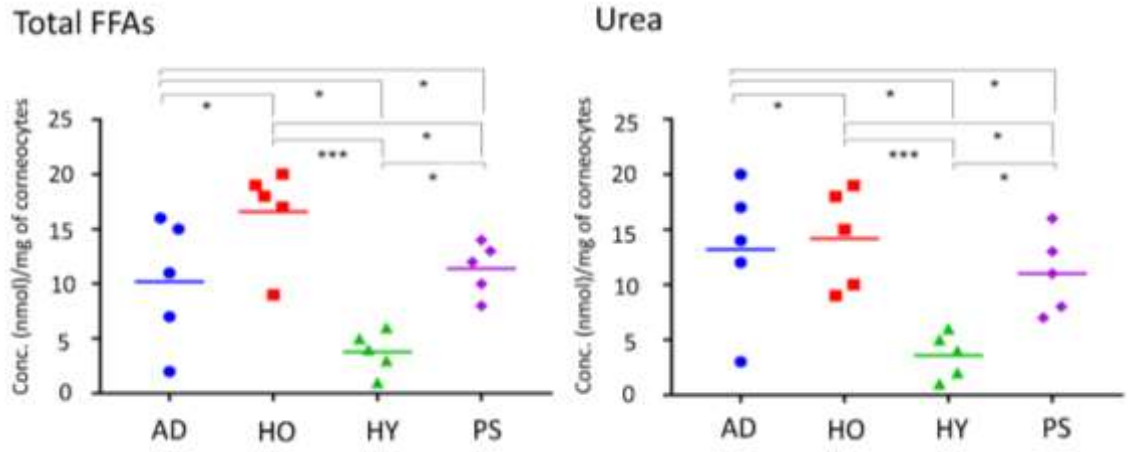

Figure 32. Graph showing significance difference for total concentration of FAAs/urea in the corneocytes from all the four groups with difference * not significant, ** P < 0.05, *** P < 0.01.

While in diseased groups (PS and AD) the concentration of FAAs/urea was non-significantly greater than that in HY group but lower than the HO group. The overall skin pH of the forearm in the healthy individuals is 5.4- 5.9 that is slightly acidic and contribute to the optimal barrier function of the skin (Braun-Falco and Korting, 1986; Schade and Marchionini, 1928; Schmid-Wendtner and Korting, 2006). Literature showed that in AD

skin pH is slightly increased compared to the skin of healthy individuals even in the uninvolved skin areas (Braun-Falco and Korting, 1986; Eberlein-Konig *et al.,* 2000; Schade and Marchionini, 1928; Schmid-Wendtner and Korting, 2006; Seidenari and Giusti, 1995). In agreement with previous reports and studies serine protease enzymes are involved in regulation of desquamation by controlling the degradation of corneodesmosomes present at the junctions of the corneocytes at optimum pH of the SC. But as mentioned earlier that in AD the pH of SC is increased that leads to increased degradation of corneodesmosomes and hence disrupted SC (Cork *et al.,* 2009; Hachem *et al.,* 2005; Rawlings and Voegeli, 2013; Rippke *et al.,* 2004; Schmid-Wendtner and Korting, 2006). This degraded desmosomes produce AAs. So, the overall amino acid content of SC is increased in the deeper layers that can seep into the corneocytes of upper layers thus resulted in the slight increase in the concentration of FAAs/urea of the corneocytes in AD and PS. In the present study the level of citrulline was observed to be higher in the HY and HO groups compared to the other two groups. Earlier in this study it has been demonstrated that FAAs/urea are produced inside the corneocytes from filaggrin, that is a histidine and arginine rich protein molecule. It has been reported that the histidine and arginine are converted to citrulline and urocanic acid by the histidase and peptidyl deiminase, respectively, in healthy skin (Girbal-Neuhauser *et al.,* 1999; Masson-Bessière *et al.,* 2001; Takahashi and Tezuka, 2004). So, the increased level of citrulline in HY and HO groups was a sign of higher filaggrin amount. In various researches, filaggrin has been reported to be in lower amount in the skin of AD patients (Danby *et al.,* 2010; Seguchi *et al.,* 1996) That is why the level of citrulline is lesser in the AD group when compared with HY and HO groups. The other reason for the decreased citrulline in AD and PS groups could be the immune dysregulation in the SC of these patients as in some studies it was reported that citrulline is produced from arginine that undergoes catabolism following two pathways i) by arginase (I or II) to produce urea and ornithine ii) by nitric oxidize synthase to create nitric oxide and citrulline. Arginase I activity is induced by T-helper cell type Th2 cytokines whereas nitric oxide synthase activity is induced by Th1 cytokines. As in both of these diseases the amount of Th2 and Th1 cytokines is disturbed so does the quantities

of citrulline is decreased (Boguniewicz and Leung, 2011; Dimitriades *et al.,* 2014; Girbal-Neuhauser *et al.,* 1999; Masson-Bessière *et al.,* 2001). Cysteine, glutamine, glutamic acid tryptophan and taurine are amongst the FAAs that were found in comparatively lesser amounts in all the groups. The above results are attributed to either enzyme activities or pH of the skin. The pH of the SC is in turn effected by a number of environmental, pathological and physiological factors such as humidity, age, disease or genetics which require further research (Schmid-Wendtner and Korting, 2006).

4.4. Conclusions

It can be interpreted from this study that total FAAs/urea were higher in HO as compared to the HY group. While there was no change in the amounts of FAA/urea was observed in the isolated corneocytes of left and right forearms. The high level of citrulline in both groups of healthy skin (young and old) could be attributed to higher amount of filaggrin present in the corneocytes compared to diseased skin (AD and PS). However, further quantitative investigations are suggested to establish the effects of aging and skin diseases on the amount of FAAs/urea.

Chapter 5. Interaction of AAs, urea with isolated corneocytes and keratin

5.1. Introduction

Various studies have reported the presence of FAAs/urea in the epidermis as member of NMFs (Harding *et al.,* 2000; Rawlings *et al.,* 1994) and constitute 40 % and 7 %, respectively, by total weight of all NMFs. These hygroscopic molecules of NMFs along with other compounds attract the water into the corneocytes even at the relative humidity of as low as 50 %. Hence, NMFs maintains the hydration status of the SC (Harding *et al.,* 2000; White-Chu and Reddy, 2011) Reduction in the level of FAAs/urea, which constitute major part of the NMFs , leads to dry skin condition in diseases such as atopic dermatitis, PS and ichthyosis vulgaris (Kwan *et al.,* 2012; Levin *et al.,* 2013; Takahashi *et al.,* 2014; Takahashi and Tezuka, 2004).

These compounds are present inside the corneocytes of the SC, the corneocytes are embedded in between the lipid lamella, both of these components of SC (lipids and the corneocytes) are organized to maintain the barrier function of the skin. Many of the researchers described this arrangement of the corneocytes and lipids as 'brick and mortar' (respectively) model (Anissimov *et al.,* 2013; Hachem, 2006; White-Chu and Reddy, 2011) which represents the heterogeneous nature of the SC (Bolzinger *et al.,* 2012; Chen *et al.,* 2009; Williams and Barry, 2004) consisting of the polar the corneocytes and non-polar SC highly ordered lipid matrix.

Drugs applied dermally have mainly to cross the SC in order to reach the living epidermis and the dermis. It is well accepted in the literature that drug penetration across the SC occurs intercellularly via the lipid lamella which will naturally favor only the penetration of lipophilic molecules. In contrast, the transcellular or corneocytary pathway via the corneocytes and the corneodesmosomes is not well studied to date. However, this pathway would allow the diffusion of hydrophilic molecules to pass the SC (Barry, 1987; Moser *et al.,* 2001). The transcellular route has limitations and is not clear as how to influence this pathway because the corneocytes accompanying this route act as reservoir for most of the hydrophilic molecules. As described earlier in elsewhere that keratin, due to their binding affinity towards hydrophilic molecules, present inside the corneocytes can play a vital role in the reservoir property of these cells. Thus, the molecules passing

the corneocytes are entrapped inside the corneocytes and the time taken by the molecules to get into and out of the corneocytes ultimately effects the total transfer rate, of dermal drugs, (Sznitowska *et al.* 1998; Heard *et al.* 2003; Seif and Hansen 2012; Patel *et al.* 2015; Choe *et al.* 2017).

To date various studies have been conducted to explore the diffusion of hydrophilic molecules across SC, however, the reservoir capacity of the corneocytes for AAs and urea is still not been measured. AAs and urea are of great dermatological significance and intensively considered for rejuvenation of the skin for a number of diseased conditions including AD and PS. However, without going into the details of their entrapment by the corneocytes during dermal transport it is useless to develop dermal formulations using these compounds. So, in this study we have investigated reservoir capacity of the corneocytes for 19 AAs including taurine and urea. The stability of AAs and urea have been studied at the same conditions which were used to determine the reservoir capacity of the corneocytes and interaction with keratin. The isolated corneocytes used in the study were extracted of naturally present FAAs/urea so as to get their maximum uptake by the corneocytes without being interfered by already present FAAs and urea. The compounds giving maximum uptake into the corneocytes were further used to study their interaction with keratin to determine their binding with keratin of the corneocytes.

5.2. Interaction of AAs and urea with the corneocytes isolated from the skin obtained after pedicure treatment and keratin.

5.2.1. Stability studies of AAs and urea

Incubation of selected AAs and urea after 24 hours at the said conditions, given in methods section, resulted in no degradation. Taurine and urea after 72 hours were also observed to be stable as shown in the Table 8.

Table 8. Stability studies of AAs and urea used in the study after incubation for 24 hours at 32 °C and 11.8 % humidity.

AAs	Initial concentration (µM)	Concentration(µM) after 24 hours ±SD	AAs	Initial concentration (µM)	Concentration(µM) after 24 hours ±SD
Aln	120 ± 1.8	118 ± 1.5	Ser	310 ± 0.0	311 ± 0.9
Arg	70 ± 1.9	72 ± 0.5	Tau	108 ± 0.1	24 h-99 ± 0.78
Asp	100 ± 0.5	101 ± 1.2			48 h-101± 1.1
Asn	120 ± 0.9	105 ± 1.6			72 h- 97± 1.7
Gln	110 ± 1.4	108 ± 0.9	Thr	90 ± 0.8	88 ± 1.2
Glu	100 ± 1.5	99.9 ± 0.4	Trp	70 ± 0.3	71 ± 0.5
Gly	90 ± 0.8	92 ± 0.7	Tyr	210 ± 0.1	208 ± 0.7
His	64 ± 1.9	65 ± 0.8	Val	80 ± 0.9	80 ± 0.9
Ileu	110 ± 1.1	110 ± 0.5	Cit	180 ± 0.8	177 ± 0.5
Leu	150 ± 0.8	149 ± 1.3	Urea	475 ± 5.1	24 h- 476 ± 9.8
Phe	150 ± 0.8	148 ± 1.6			48 h- 472± 8.1
Pro	70 ± 0.05	69 ± 0.5			72 h- 468 ± 6.4

As the results showed (Table 8) all the AAs soln. in DDW are stable for the 24 hours at 32 °C and 11.8 % humidity. Taurine and urea were incubated for 72 hours and both of them were also observed to be stable with only a negligible reduction in the amount that was present at the initial time. So, none of the experimental conditions were interfering with the reduction of the concentration during the interaction of AAs with the corneocytes and keratin experiment. Hence, all the study molecules were stable at the selected conditions.

5.2.2. Interaction and uptake of AAs and urea with the corneocytes

Incubation of selected AAs and urea with isolated corneocytes was carried out to determine the reservoir capacity of the corneocytes for these molecules. Reduction in the amounts of AAs in the soln. after 24 hours of incubation with isolated corneocytes was observed which showed that remaining amount of the respective molecule was either absorbed into the corneocytes. Different AAs showed different concentration left after incubation with isolated corneocytes (see Table 9).

Table 9. Interaction and uptake of AAs and urea by the corneocytes after incubation for 24 hours at 32 °C and 11.8 % humidity.

AAs	Initial Concentration (µM)	Concentration (µM) left after 24 hours ± SD	% age of AAs uptake by the corneocytes
Aln	120 ± 1.8	56 ± 9.4	51.6
Arg	70 ± 1.9	55 ± 2.4	16.9
Asp	100 ± 0.5	4 ± 2.3	95.4
Asn	120 ± 0.9	2 ± 0.6	98.6
Gln	110 ± 1.4	6 ± 1.6	94.1
Glu	100 ± 1.5	4 ± 1.6	95.6
Gly	90 ± 0.8	66 ± 11.1	27.1
His	64.0 ± 1.9	6.1 ± 38	90.1
Ileu	110 ± 1.1	102 ± 5.5	7.5
Leu	150 ± 0.8	137 ± 3.2	8.9
Phe	150 ± 0.8	119 ± 8.3	20.7
Pro	70 ± 0.0	4 ± 24	94.6
Ser	310 ± 0.0	85 ± 8.7	72.9
Tau	108 ± 0.1	45.4 ± 20.8	57.8
Thr	90 ± 0.8	84.3± 23.7	6
Trp	70 ± 0.3	69 ±9.6	1.2
Tyr	210 ± 0.1	152 ± 8.5	27
Val	80 ± 0.9	72 ± 10.2	9.8
Cit	180 ± 0.8	170 ± 2.9	5.2
Urea	444 ± 10.5 992 ± 14.6	99 ± 26.7 225.87 ± 18.6	77.7 77.2

The results were presented in Table 9 showing the initial concentration of each AAs and urea along with the concentration left after 24 hours. The table also showed % age of each AAs and urea uptake by isolated corneocytes. Alanine, aspartic acid, asparagine, glutamine, glutamic acid, histidine, proline, serine, taurine, and urea showed uptake of 51.6, 95.4, 98.6, 94.1, 95.6, 90.1, 94.6, 72.9, 57.8 and 77.7 %, respectively. AAs are chemically diverse group of molecules and thus exhibits different behaviour in same experimental conditions. So, nine AAs amongst 19 showed uptake into the isolated corneocytes while remaining AAs either had none or very negligible amount diffused into the corneocytes. All of these AAs which with higher uptake into the corneocytes belong to the non-essential class of AAs except histidine and aspartic acid. Non-essential AAs are those AAs which are synthesized in the human body. The reason they were showing higher uptake may be they are more natural to human body with respect to pH, osmotic properties of the cellular content. Asparagine showed the maximum uptake (98.6 %) into the isolated corneocytes, is a polar AA. The other observed property in these AAs which showed uptake is all of them are polar except proline. The corneocytes serve as absorption depot for hydrophilic molecules which was demonstrated by a scientific study on visualization of the corneocytes using TEM and photon microscopy (Boddé *et al.,* 1991; Jacobi *et al.,* 2006; Yu *et al.,* 2003) so is the case with AAs and urea. A lot of efforts have been done in research related to prediction of permeability of hydrophilic drugs across SC. However, to the best of our knowledge none of the studies was carried out using AAs and urea uptake into the isolated corneocytes. However, reported measurement data of more than 50 hydrophilic molecules, other than AAs and urea, of dermatological value for predicting their skin permeability is available (Chen *et al.,* 2009; Lian *et al.,* 2008; Mitragotri, 2003; Potts and Guy, 1992; Wilschut *et al.,* 1995).

5.2.3. Interaction of AAs and urea with keratin

All of the AAs and urea which showed a good amount of uptake into the corneocytes were tested for their interaction with keratin. As in literature it has been mentioned that after entering into the corneocytes the drugs crossing the SC bind with the keratin of the corneocytes and the binding results in hindered transport of drugs across SC (Banning and Heard, 2002; Hashiguchi *et al.,* 1998)

Table 10. Interaction of selected AAs and urea with keratin for the 24 hours at 32 °C and 11.8 % humidity.

AA	Initial Concentration (µM)	Concentration(µM) after 24 hours ± SD	AA	Initial concentration (µM)	Concentration (µM) after 24 hours ± SD
Interaction with Keratin					
Ala	128.0 ± 1.5	121 ± 5.5	His	134.8 ± 0.9	140 ± 5.5
Asp	120.4 ± 1.9	132 ± 10.3	Pro	93.3 ± 0.5	89.5 ± 6.3
Asn	101.1 ± 0.6	121 ± 11.2	Ser	70.4 ± 0.7	70.9 ± 0.5
Gln	97.7 ± 0.8	103 ± 1.6	tau	99.8 ± 1.0	95.1 ± 10.0
Glu	94.3 ± 1.2	94.6 ± 0.0	Urea	445 ± 5.6	443 ± 6.3

Incubation of selected AAs and urea standard soln. with keratin after 24 hours resulted in the negligible difference in the initial concentration and concentration left after 24 hours. Which showed AAs has no binding infinity with the keratin. The results are presented in the Table 10.

5.3. Conclusions

AAs has a great potential to be diffused into the corneocytes including taurine and urea which gave 57.8 % and 77.7 %, respectively. However, none of the AAs and urea showed binding with the keratin at the same conditions as uptake experiment was conducted. This property of the AAs and urea can be employed in further dermatological research on diseased or aged skin conditions requiring these molecules.

Chapter 6. *In-vitro* diffusion study of hydrophilic molecules

6.1. Introduction

Being the member NMFs, taurine is found intracellular while, urea is also found extracellularly to the corneocytes (Caspers *et al.,* 2001; Jacobson *et al.,* 1990; Jassoy *et al.,* 2015; Joo *et al.,* 2012; Sylvestre *et al.,* 2010; Visscher *et al.,* 2011).

Urea is a non-protein organic compound, chemically structured as a carbonyl group attached to two amine residues (Brahma and Kumar Pankaj, 2014; Pan Ba *et al.,* 2013). Numerous researches reported dermatological significance of urea as to increase the permeability of the SC, improving dry skin condition in diseased and ageing. Such as promoting the normal healing of keratotic surface lesions developed in healing retarding conditions as for example in local skin infection, necrotic tissues and fibrinous debris or in hyperkeratotic conditions such as dry rough skin, atopic dermatitis, PS, ichthyosis vulgaris (Björklund *et al.,* 2013; Peju and Rajat, 1906; Wilson, 1906). A number of topical products, containing up to 50 % of urea, are available in the market to support already established benefits of urea in dermatological ailments. However, the mechanism of action of urea is still not known. According to the reported studies topically applied urea creates keratolytic and hydrating effects in the SC produced due to the breakage of hydrogen bonds in the SC which leads to loosening of epidermal keratin and increasing water-binding sites (Gloor *et al.,* 2002). Taurine (2-aminoethanesulfonic acid) is the second most considering molecule in today's dermatological world due to its unique properties. Taurine is also classified as not protein and highly hygroscopic molecule in nature compared to other AAs of the NMFs, in addition to its osmoregulatory and antioxidant properties. In one of the studies it was also reported that taurine stimulates the synthesis of all three barrier lipids (ceramides, fatty acid and cholesterol) in reconstructing epidermis (Boelens *et al.,* 2003; Jassoy *et al.,* 2015; Nishimura *et al.,* 2009; Odetti *et al.,* 2003) So, taurine is beneficial in re-establishing the hydration status of the skin in conditions like AD and PS by reconstructing the lipids content and as strenuous humectant.

However, both of the above important molecules are water soluble and hydrophilic and can only cross SC via transcellular or corneocytary pathway via the corneocytes and corneodesmosomes. As mentioned earlier in the previous chapter section 5.1 hydrophilic

molecules, undergoe resistance to their transport across SC due to entrapment by the corneocytes. In the previous chapter reservoir concentration of taurine and urea in isolated corneocytes have already been measured. In this chapter, time dependent diffusion profile of taurine and urea have been studied using in vitro diffusion model with and without the corneocytes. To date various studies have been conducted for the development of in vitro diffusion models for hydrophilic molecules across the SC following transcellular route (Couto *et al.,* 2014; Marquez-Lago *et al.,* 2010; Wang *et al.,* 2006; Xiao and Imhof, 2012). However, none of the studies used isolated corneocytes for predicting the diffusion of hydrophilic molecules into the corneocytes.

In this study a diffusion apparatus consisting of three cells was used each cell was further comprised of two compartments ACC and DON. For taurine, 100 µM while for urea two concentrations (500 and 1000 µM) were used. A comparative diffusion profile was created (with and without the corneocytes) for both of the molecules which helped in calculating the pearson´s correlation coefficient `r´ as a measure of reservoir capacity of the taurine and urea.

6.2. *In-vitro* diffusion study

6.2.1. *In-vitro* diffusion of taurine and urea without the corneocytes

In *in-vitro* diffusion model `without corneocytes´ the DON was filled with standard soln. of the study molecule. While ACC contained only DDW, as a diffusion medium, separated by a porous membrane. The graphical fitting of diffusion of study molecule across membrane showed that concentration of both taurine and urea increased exponentially in the ACC compartment for the first 12 hours (See Figure 33). After 12 hours the concentrations reached at dynamic equilibrium with regression values R^2, 0.99 and 0.997 (see table 11) for taurine and urea, respectively.

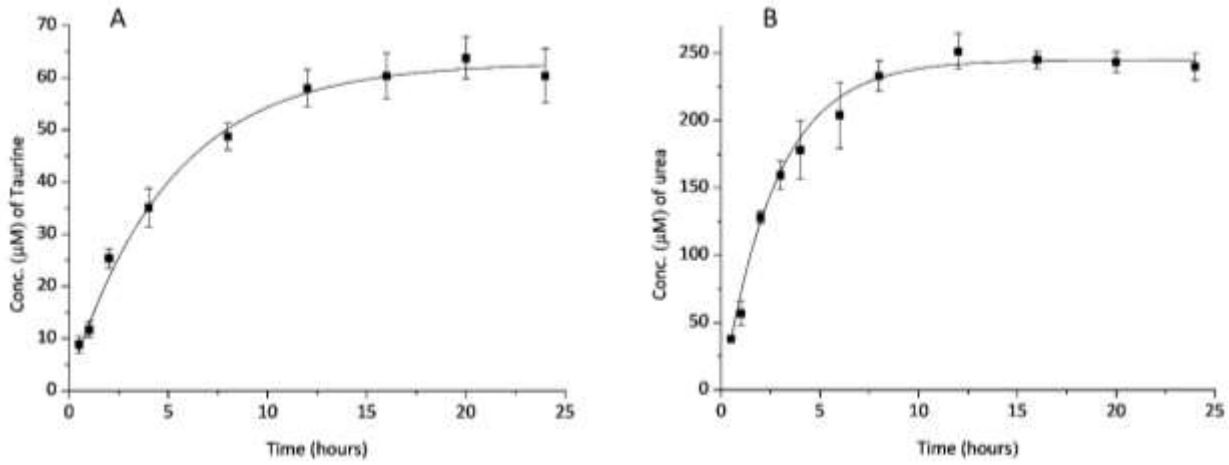

Figure 33. Diffusion profile of *in-vitro* diffusion model `without corneocytes´ in ACC compartment for taurine (A) and urea (B) for first 24 hours (n = 3, RSD ≤ 15 %).

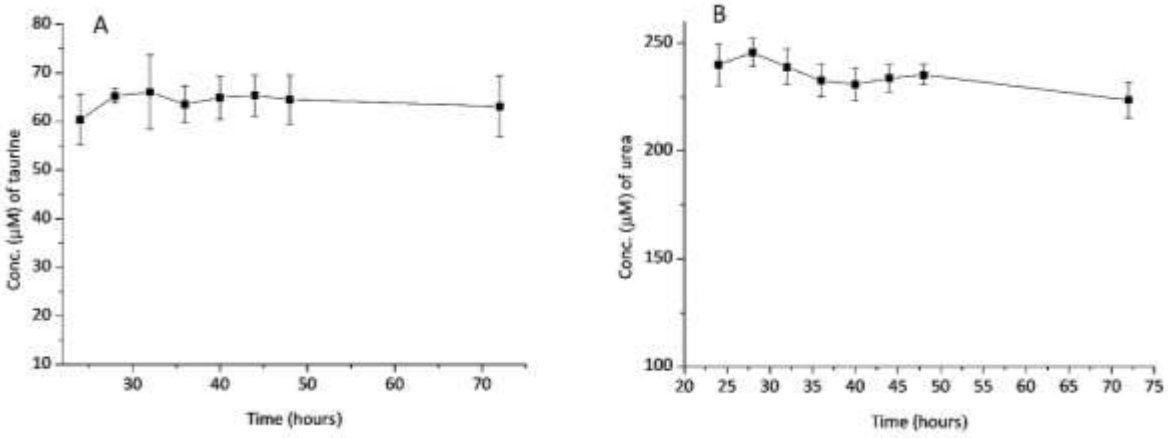

Figure 34. Diffusion profile of *in-vitro* diffusion model `without corneocytes ´ in ACC compartment for taurine (A) and urea (B) for 72 hours (n = 3, RSD ≤ 15 %).

The equilibrium was a point where the concentration of study molecules distributed, exactly the half of the total initial concentration `C_0´ between ACC and DON.

The experiment was continued for the next 72 hours (see Figure 34), no change in the dynamic equilibrium was observed. The reduction in the total concentration of taurine and urea measured in both ACC and DON at different time points was C_{24} = 100 %, C_{48} = 94 %, C_{72} = 94 % and for urea was C_{24} = 96 %, C_{48} = 89 %, C_{72} = 86 %), respectively, also not significant (Table 12).

6.2.2. *In-vitro* diffusion model with the corneocytes

While in in vitro diffusion `with corneocytes´ we have introduced the corneocytes (10 mg/ml in taurine and 50 mg/ml in urea diffusion cell) in the DON in addition to standard soln. of the study molecules under same experimental conditions.

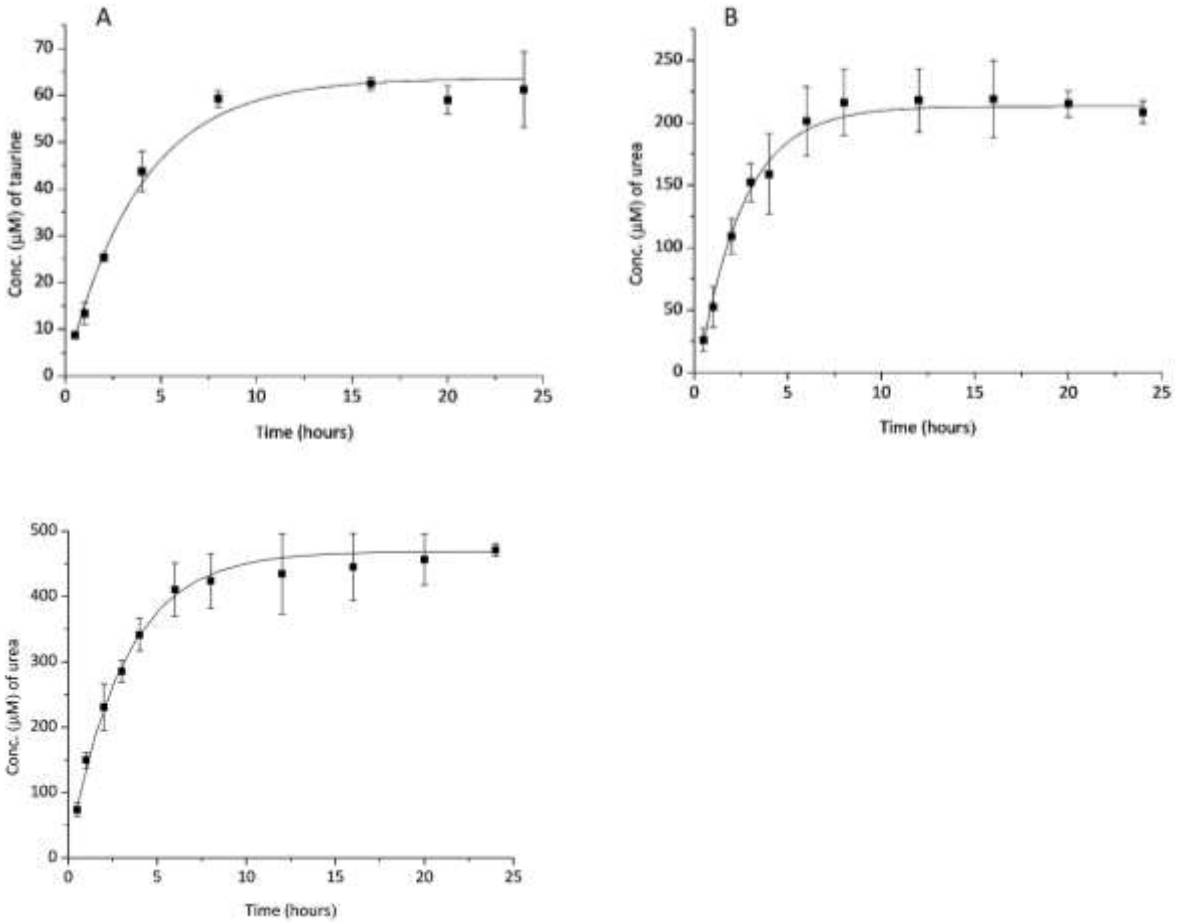

Figure 35. Diffusion profile of (A) taurine (B) urea 500 µM and (C) urea 1000 µM in ACC after 24 hours `with corneocytes´.

This time we expected the change in the diffusion profile across membrane due to the introduction of the corneocytes. Figure 35 A, B and C showed again exponentially increasing concentration of both the study molecules taurine and urea (both concentrations) for 24 hours. The concentration of both the study molecules reached at 50 % of the initial concentration in 8 hours and dynamic equilibrium was established. This concentration was continued to be the same for the next 24 hours. The regression values R^2 for exponential growth curve of taurine and urea were 0.993, 0.995 and 0.997, respectively (see Table 11).

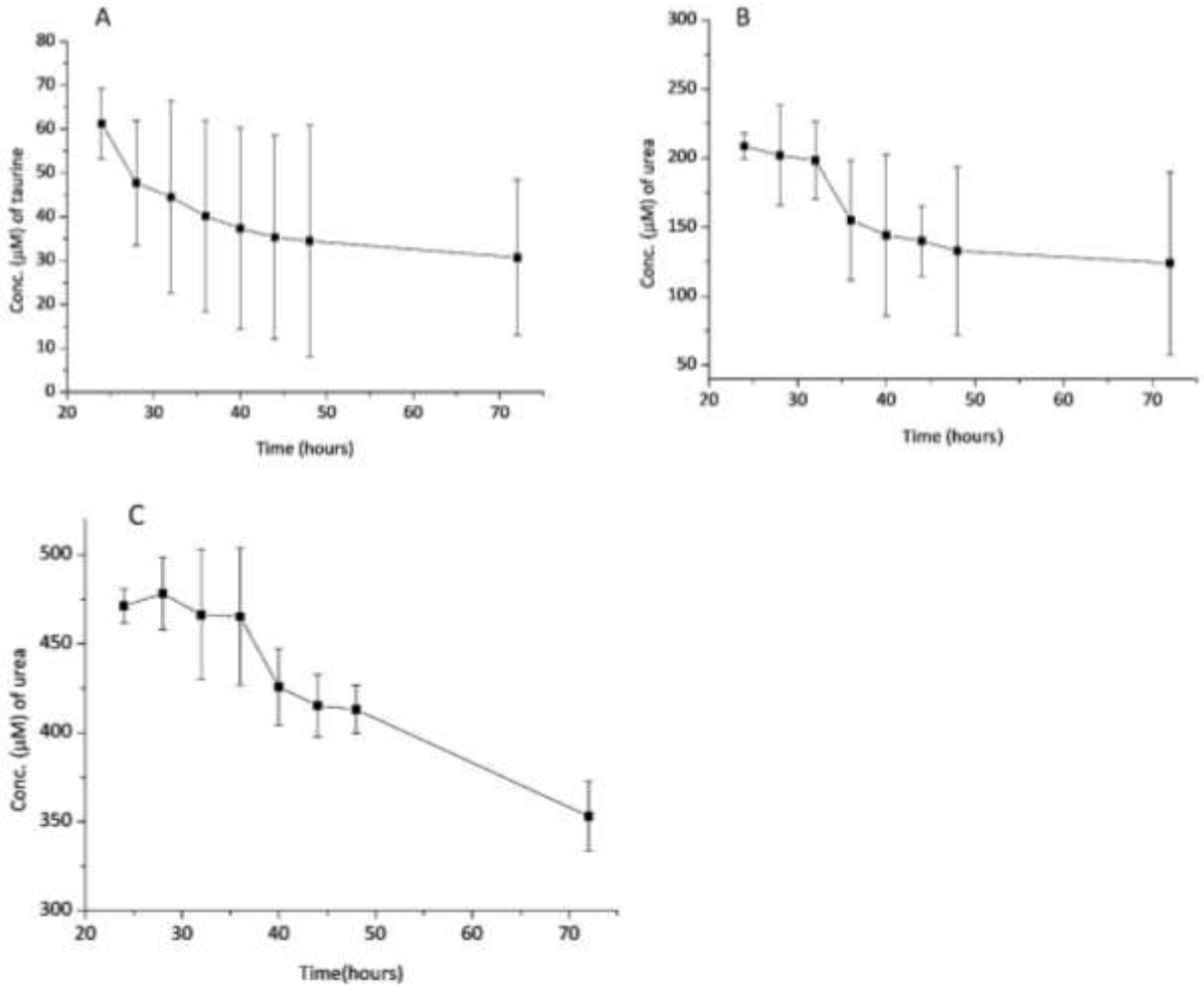

Figure 36. Diffusion profile of (A) taurine (B) urea 500 µM and (C) urea 1000 µM in ACC after 72 hours `with corneocytes´.

Figure 36 A, B and C are the graphical representation of diffusion profile of taurine and both concentrations of urea with the corneocytes after 24 hours. The graph showed that

after 24 hours the concentration of both taurine and urea started decreasing. In taurine diffusion cell concentration was decreased to 47 %, 50 % and 76 % in taurine, urea 500 µM and 1000 µM (see Table 12). In the literature it has been reported that the corneocytes swell when immersed or come in contact with water for a longer period of time and this swelling can change the morphology of the corneocytes (Richter *et al.,* 2001) which attributes to the increased permeability of the corneocytes for hydrophilic taurine and urea. Thus, the corneocytes started taking up the taurine and urea and the concentration of both of these molecules started decreasing in DON. The corneocytes uptake capacity for taurine has arrived at 72 hours and concentrations decreased maximum to 37.8 %, 40 % and 63 %, while 81 %, 50 % and 40 % urea 500 µM and 89 %, 76 % and 63 % for 1000 µM urea (see Table 12). At 72 hours the equilibrium was again established with the remaining diffusion molecules in both compartments.

Table 11. Parameters of diffusion profiles of taurine and urea

	Taurine	Urea	Taurine	Urea	
	100 µM	500 µM	100 µM	500 µM	1000 µM
Model	Without corneocytes		With corneocytes		
Time (hours)	24	24	24	24	24
R^2	0.99	0.997	0.993	0.995	0.997
Pearson´s correlation coefficient `r´			-0.54	0.84	
Equation	$y = A_1 * \exp(x/t_1) + Y°$				

Table 12. Concentration comparison of taurine and urea in both experiments `without corneocytes ´ and `with corneocytes in ACC and DON at different time points

% age of concentration left in ACC and DON					
Time points (hours)	Taurine	Urea	Taurine	Urea	
	100 µM	500 µM	100 µM	500 µM	1000 µM
	`Without corneocytes ´		`With corneocytes ´		
			10 mg/ml	50 mg/ml	
C0	100	100	100	100	100
C24	99	92	94	81	89
C48	94	89	47	50	76
C72	94	86	37.8	40	63

Comparing taurine, urea is left in the ACC and DON compartment in more percentage which shows high solubility of urea than taurine. Secondly, urea is smaller molecule as compared to taurine and thus crossing the hydrophilic membrane between ACC and DON more rapidly than taurine and that is the reason it is found comparatively in more quantity in the compartments rather than absorbed in the corneocytes.

6.2.3. Calculation of correlation coefficient

When comparing the both curves in Figure 34 A with 36 A and 34 B with 36 B (72 hours curves) of in vitro diffusion `without corneocytes´ and `with corneocytes´ for taurine and urea, respectively. It is clear that there is significant change in concentration observed from 24 to 72 hours. We have quantified this difference in both curves for each of the model molecule taurine and urea in the form of Pearson´s co-relation coefficient (r) between 24 to 72 hours. For *in-vitro* diffusion `without corneocytes ´ and `with corneocytes ´ the value of `r´ calculated for taurine is -0.54 and 0.84 for urea.

The results showed that the corneocytes exhibit high resistance for the transport of hydrophilic molecules across transcellular route due to their higher reservoir property. This reservoir property can be utilized positively for targeted delivery of many hydrophilic molecules in dermatological disorders with the NMFs deficiency to replenish the effected corneocytes. The measurement of `r´ value based on these *in-vitro* diffusion models is a useful prediction tool and can be used in evaluating other hydrophilic test molecules with significant uptake into the corneocytes.

Furthermore, these models can also be used to evaluate various controlled release matrix systems used in nanocarrier formulations as well as for the identification of penetration enhancers showing maximum diffusion into the corneocytes.

6.3. Conclusions

Diffusion profile of taurine and urea showed exponential increase in the ACC compartment in *in-vitro* diffusion model with and without corneocytes. In *in-vitro* diffusion model without corneocytes no significant change in total concentration in ACC and DON was observed in 72 hours. While in the *iv-vitro* diffusion model with the corneocytes after 24 hours the concentration decreased significantly in both ACC and DON for both taurine and urea. Pearson´s coefficients calculated were -0.54 and 0.84 for taurine and urea, respectively. The model developed based on correlation coefficient of

with and without the corneocytes profiling of molecules can be helpful, along with AAs, for a number of other dermatologically significant hydrophilic molecules.

Summary and perspectives

Natural moisturizing factors (NMFs) are hygroscopic molecules which function to keep the skin hydrated. They do so by drawing water inside the corneocytes even at a humidity as low as 50 %. FAAs (free amino acids)/urea are the predominant members amongst the NMF molecules. They not only act as humectants but are also responsible to maintain the acidic pH of the skin. Decreased amounts of FAAs/urea have been reported in pathological dry skin associated with atopic dermatitis (AD), psoriasis (PS) and in ageing skin. This decreased quantity of FAAs/urea was attributed to the loss-of-function mutation of the filaggrin gene in the diseased skin conditions and low production of keratohyaline granules in the ageing skin. Scientists are searching for treatment options for dry skin by trying to reconstruct the natural chemical composition of the skin with topical application of e.g. AAs (amino acids) and urea. However, controversial reports regarding the concentration of FAAs/urea engrossed the attention of dermatologists. These controversial results are due to lack of a standard extraction protocol of FAAs/ urea and quantification based on low sensitivity and selectivity of analytical methods.

The present work therefore, aimed at the development of a standard extraction protocol, for FAAs/urea from the corneocytes, isolated from healthy, aged and diseased skin of AD and PS patients without being subjected to hydrolysis. Sampling of the SC was carried out by tape stripping. Quantification of FAAs was done using LC-ESI-MS/MS MRM, which is not only a highly selective but also very sensitive method with LOQ lower than 20 nM. The concentration of urea was determined by coupled enzyme reaction. The results showed a significantly highest concentrations of FAAs/urea in aged skin, while they were not decreased in the corneocytes taken from uninvolved areas of diseased skin, compared to the healthy skin. A large amount of citrulline was observed in healthy and ageing skin, which may be attributed to the higher amount of filaggrin in both of these groups. The higher quantities of FAAs/urea in both diseased groups (AD and PS) were a result of hyperactivity of the proteolytic enzymes due to high skin pH for the diseased groups. The pH is thought to be increased due to reduced amount of FAAs/urea in diseased skin which can be rebuilt by topical administration of these molecules.

However, due to the heterogeneous nature of the SC and reservoir function of the corneocytes, dermal application of these hydrophilic molecules is a challenging task. To-date no study was conducted to determine the reservoir capacity of AAs including taurine

or urea. In the present work, reservoir capacity of the corneocytes for AAs and urea was calculated, as a measure of concentration of molecules diffused into the corneocytes. Investigation was carried out for 19 AAs and urea, nine AAs along with urea showed more than 90 % uptake by the corneocytes. Asparagine did show the highest uptake into the corneocytes while taurine and urea exhibited 77.7 % and 57.8 %, respectively.

Moreover, diffusion profiles of taurine and urea were studied with the help of an in-vitro diffusion model without and with corneocytes to measure the reservoir capacity of corneocytes in terms of Pearson's correlation coefficient 'r'. Pearson's correlation coefficient 'r' of taurine and urea were determined to be -0.54 and 0.84 respectively, which showed a sufficient amount of uptake of both molecules into the corneocytes. The results showed that the corneocytes exhibit greater resistance for the transport of hydrophilic molecules across the transcellular route due to their higher reservoir property. This reservoir property can be utilized for targeted delivery of AAs/urea to the corneocytes. AAs and urea are promising molecules for maintaining the pH of the diseased skin and thus hindering proteolysis of the corneodesmosomes, regulating desquamation. The measurement of `r´ value based on these in-vitro diffusion models is a useful prediction tool and can be used in evaluating other hydrophilic test molecules with significant uptake into the corneocytes.

These models can furthermore, be used to evaluate various controlled release matrix systems used in nano-carrier formulations as well as for the identification of penetration enhancers showing maximum diffusion into the corneocytes.

Zusammenfassung

Natural moisturizing faktors (NMFs) sind hygroskopische Moleküle, die den natürlichen Feuchtigkeitsgehalt der Haut erhalten. Sie sind hierfür in der Lage, dazu Wasser, selbst bei geringer Feuchtigkeit von nur 50 %, in die Korneozyten zu ziehen. FAAs/Harnstoff sind die häufigsten Mitglieder der Molekülgruppe der NMFs. Sie wirken nicht nur als Feuchthaltemittel, sondern sind auch dafür verantwortlich, den sauren pH-Wert der Haut aufrechtzuerhalten. Bei trockener Haut, die mit AD, PS und alternder Haut einhergeht, wurde eine verminderte Menge an FFAs/Harnstoff nachgewiesen. Die verringerte Menge an FAAs/Harnstoff ist bei Hautkrankheiten (AD und PS) auf den Funktionsverlust durch Mutation des Filaggrin-Gens zurückzuführen, während sie bei alternder Haut von einer verringerten Produktion von Keratohyalin-Granula herrührt. Wissenschaftler suchen nach Behandlungsmöglichkeiten für trockene Haut durch die Wiederherstellung der natürlichen chemischen Zusammensetzung der Haut z.B. mit AAs oder FFAs. Allerdings erregen kontroverse Berichte über die Konzentration von FAAs/Harnstoff die Aufmerksamkeit von Dermatologen. Diese kontroversen Ergebnisse können auf das Fehlen eines standardisierten Extraktionsprotokolls für FAAs/Harnstoff und deren Quantifizierung, welche auf wenig empfindlichen und selektiven Analysemethoden basiert, zurückgeführt werden.

Die vorliegende Arbeit zielte daher auf die Entwicklung eines Standard-Extraktionsprotokolls für FAAs/Harnstoff aus Korneozyten ab, welche aus gesunder, gealterter, sowie pathologisch veränderter Haut von AD und PS Patienten isoliert wurden, ohne diese einer Hydrolyse auszusetzen. Die Probenahme aus dem SC erfolgte mittels tape stripping (Abziehen eines Klebestreifens vom Unterarm der Probanden). Die Quantifizierung der FAAs erfolgte mittels LC-ESI-MS/MS-MRM, was nicht nur hochselektiv, sondern auch hochsensitiv ist und einen LOQ von weniger als 20 nM bietet. Die Harnstoffkonzentration wurde durch eine gekoppelte Enzymreaktion bestimmt. Die Ergebnisse zeigten eine signifikant höhere Konzentration von FAAs/Harnstoff in der Gruppe der gealterten Haut verglichen mit der Gruppe der jungen, gesunden Haut. In den Korneozyten, aus nicht betroffenen Bereichen der Haut erkrankter Patienten, zeigte sich im Vergleich zur gesunden Haut, keine reduzierte FFA/Harnstoff Konzentration. Eine erhöhte Menge an Citrullin wurde in den Gruppen der gesunden und gealterten Haut beobachtet und könnte auf eine höhere Menge an Filaggrin in diesen beiden Gruppen

zurückzuführen sein. Die erhöhten Mengen an FAAs/Harnstoff in beiden erkrankten Gruppen waren eine Folge der Hyperaktivität der proteolytischen Enzyme aufgrund eines zu hohen Haut-pH-Werts. Es wird angenommen, dass der pH-Wert, aufgrund einer verringerten Menge an FAAs/Harnstoff erhöht ist, und durch eine topische Administration dieser Moleküle wieder aufgebaut werden könnte.

Aufgrund der heterogenen Natur des SC und der Reservoirfunktion der Korneocyten ist die dermale Anwendung dieser hydrophilen Moleküle (AAs und Harnstoff) jedoch eine Herausforderung auf dem Gebiet der Dermatologie. Bisher wurde keine Studie zur Bestimmung der Reservoirkapazität von Korneozyten für AA einschließlich Taurin oder Harnstoff durchgeführt. In der vorliegenden Arbeit wurde die Reservoirkapazität von Korneozyten für AAs und Harnstoff als Maß für die Konzentration der jeweils in die Korneozyten diffundierten Moleküle berechnet. 19 AAs und Harnstoff wurden in die Studie einbezogen, wobei 9 AAs zusammen mit Harnstoff eine mehr als 90 %ige Aufnahme in die Korneozyten zeigten. Asparagin zeigte die höchste Aufnahme, während Taurin und Harnstoff jeweils 77,7 % bzw. 57,86 % Aufnahme aufwiesen.

Darüber hinaus wurden zeitabhängige Diffusionsprofile für Taurin und Harnstoff mit Hilfe eines In-vitro-Diffusionsmodells ohne und mit Korneozyten generiert und die Reservoirkapazität von Korneozyten anhand des Pearson-Korrelationskoeffizienten „r“ validiert. Der Pearson-Korrelationskoeffizient, ``r´´ von Taurin und Harnstoff wurde mit -0,54 bzw. 0,84 bestimmt, was eine ausreichende Penetration beider Moleküle in die Korneozyten ergab. Die Ergebnisse zeigten, dass Korneozyten aufgrund ihrer höheren Speicherkapazität eine hohe Resistenz gegen den Transport hydrophiler Moleküle (AAs und Harnstoff) über den transzellulären Weg aufweisen. Diese Reservoir-Eigenschaft kann zur gezielten Einbringung dieser Moleküle in Korneozyten genutzt werden. AAs und Harnstoff sind vielversprechende Moleküle, um den pH-Wert der erkrankten Haut aufrechtzuerhalten und somit die Proteolyse der Korneodesmosomen zu verhindern, welche die Desquamation reguliert. Die Messung des ``r´´-Wertes, basierend auf den In-vitro-Diffusionsmodellen, ist ein nützliches Vorhersagewerkzeug und kann zur Bewertung anderer hydrophiler Testmoleküle mit signifikanter Aufnahme in die Korneozyten verwendet werden.

Darüber hinaus können diese Modelle auch zur Bewertung verschiedener Matrixsysteme mit kontrollierter Freisetzung wie Nanotransportformulierungen angewandt werden,

sowie zur Identifizierung von Penetrationsverstärkern, welche die Diffusion in die Korneozyten verstärken, verwendet werden.

References

Alaiz, M., Navarro, J., Girón, J., Vioque, E., 1992. Amino acid analysis by high-performance liquid chromatography after derivatization with diethyl ethoxymethylenemalonate. J. Chromatogr. A 591, 181–186.

Albery, W., Hadgraft, J., 1979. Percutaneous absorption: in vivo experiments. J. Pharm. Pharmacol. 31, 140–147.

Ananthapadmanabhan, K., Moore, D., Subramanyan, K., Misra, M., Meyer, F., 2004. Cleansing without compromise: the impact of cleansers on the skin barrier and the technology of mild cleansing. Dermatol. Ther. 17, 16–25.

Anderson, R., Cassidy, J., Hansen, J., Yellin, W., 1973. Hydration of stratum corneum. Biopolymers 12, 2789–2802.

Anissimov, Y., Jepps, O., Dancik, Y., Roberts, M., 2013. Mathematical and pharmacokinetic modelling of epidermal and dermal transport processes. Adv. Drug Deliv. Rev. 65, 169–190.

Armstrong, M., Jonscher, K., Reisdorph, N., 2007. Analysis of 25 underivatized amino acids in human plasma using ion-pairing reversed-phase liquid chromatography/time-of-flight mass spectrometry. Rapid Commun. Mass Spectrom. 21, 2717–2726.

Banning, T., Heard, C., 2002. Binding of doxycycline to keratin, melanin and human epidermal tissue. Int. J. Pharm. 235, 219–227.

Barker, J., 2008. Psoriasis as a systemic disease. Expert Rev. Dermatol. 3, 25–29.

Baroni, A., Buommino, E., De Gregorio, V., Ruocco, E., Ruocco, V., Wolf, R., 2012. Structure and function of the epidermis related to barrier properties. Clin. Dermatol. 30, 257–62.

Barrett, J., And, I., Scott, M., 1983. Pyrrolidone Carboxylic Acid Synthesis in Guinea Pig Epidermis, J. Invest. Dermatol. 81, 122-124.

Barry, B., 1987. Mode of action of penetration enhancers in human skin. J. Control. Release 6, 85–97.

Berardesca, E., Fideli, D., Borroni, G., Rabbiosi, G., Maibach, H., 1990. In vivo hydration and water-retention capacity of stratum corneum in clinically uninvolved skin in atopic and psoriatic patients. Acta Derm. Venereol. 70, 400-404.

Bernard, D., Méhul, B., Thomas-Collignon, A., Simonetti, L., Remy, V., Bernard, M.A., Schmidt, R., 2003. Analysis of Proteins with Caseinolytic Activity in a Human Stratum Corneum Extract Revealed a Yet Unidentified Cysteine Protease and Identified the

So-Called “Stratum Corneum Thiol Protease” as Cathepsin L2. J. Invest. Dermatol. 120, 592–600.

Björklund, S., Engblom, J., Thuresson, K., Sparr, E., 2013. Glycerol and urea can be used to increase skin permeability in reduced hydration conditions. Eur. J. Pharm. Sci. 50, 638–645.

Blank, I., Shappirio, E., 1955. The water content of the stratum corneum. III. Effect of previous contact with aqueous solutions of soaps and detergents. J. Invest. Dermatol. 25, 391–401.

Boddé, H., BI., van den, Koerten, H., de Haan, F., 1991. Visualization of in vitro percutaneous penetration of mercuric chloride; transport through intercellular space versus cellular uptake through desmosomes. J. Control. Release 15, 227–236.

Boehncke, W.-H., Schön, M., 2015. Psoriasis. Lancet 386, 983–994.

Boelens, P., Houdijk, A., De Thouars, H., Teerlink, T., Van Engeland, M., Haarman, H., Van Leeuwen, P., 2003. Plasma taurine concentrations increase after enteral glutamine supplementation in trauma patients and stressed rats. Am. J. Clin. Nutr. 77, 250–256.

Boguniewicz, M., Leung, D., 2011. Atopic dermatitis: a disease of altered skin barrier and immune dysregulation. Immunol. Rev. 242, 233–246.

Bolzinger, M.-A., Briançon, S., Pelletier, J., Chevalier, Y., 2012. Penetration of drugs through skin, a complex rate-controlling membrane. Curr. Opin. Colloid Interface Sci. 17, 156–165.

Bouwstra, J., de GraaBouwstra, J., Gooris, G., Nijsse, J., Wiechers, J., van Aelst, A., 2003. Water Distribution and Related Morphology in Human Stratum Corneum at Different Hydration Levels. J. Invest. Dermatol. 120, 750–758.

Brahma, B., Kumar Pankaj, P., 2014. Evaluation of Milk Urea Concentration as Useful Indicator for Dairy Herd Management: A Review. Asian J. Anim. veternary Adv. 6, 1–19.

Braun-Falco, O., Korting, H., 1986. Der normale pH-Wert der Haut Hautarzt. Hautarzt 3, 126–129.

Burke, R., Lee, T., Buettner-Janusch, V., 1966. Free amino acids and water soluble peptides in stratum corneum and skin surface film in human beings. Yale J. Biol. Med. 38, 355–73.

Candi, E., Schmidt, R., Melino, G., 2005. The cornified envelope: A model of cell death in the skin. Nat. Rev. Mol. Cell Biol. 6, 328–340.

Carpino, L., Cohen, B., Stephens, K., Sadat-Aalaee, S., Tien, J., Langridge, D., 1986. (Fluoren-9-ylmethoxy)carbonyl (Fmoc) amino acid chlorides. Synthesis, characterization, and application to the rapid synthesis of short peptide segments. J. Org. Chem. 51, 3732–3734.

Casetta, B., Tagliacozzi, D., Shushan, B., Federici, G., 2000. Development of a Method for Rapid Quantitation of Amino Acids by Liquid Chromatography-Tandem Mass Spectrometry (LC-MSMS) in Plasma. Clin. Chem. Lab. Med. 38, 391–401.

Caspers, P., Bruining, H., Puppels, G., Lucassen, G., Carter, E., 2001. In Vivo Confocal Raman Microspectroscopy of the Skin: Noninvasive Determination of Molecular Concentration Profiles. J. Invest. Dermatol. 116, 434–442.

Chan, Y., Yu, Q., LeBlanc-Straceski, J., Christiano, A., Pulkkinen, L., Kucherlapati, R., Uitto, J., Fuchs, E., 1994. Mutations in the non-helical linker segment L1-2 of keratin 5 in patients with Weber-Cockayne epidermolysis bullosa simplex. J. Cell Sci. 107, 765-774.

Chen, L., Lian, G., Han, L., 2009. Modeling transdermal permeation. Part I. Predicting skin permeability of both hydrophobic and hydrophilic solutes. AIChE J. 56, 1136–1146.

Choe, C., Schleusener, J., Lademann, J., Darvin, M., 2017. Keratin-water-NMF interaction as a three layer model in the human stratum corneum using in vivo confocal Raman microscopy, Scientific Reports. Nature Publishing Group 7, 15900.

Clar, E., Fourtanier, A., 1981. L'acide pyrrolidone carboxylique (PCA) et la peau. Int. J. Cosmet. Sci. 3, 101–113.

Cocking, E., Yemm, E., 1954. Estimation of amino acids by ninhydrin. Biochem. J. 58, xii.

Cohen, S., Strydom, D., 1988. Amino acid analysis utilizing phenylisothiocyanate derivatives. Anal. Biochem. 174, 1–16.

Cork, M., Danby, S., Vasilopoulosnnis, Y., Hadgraft, J., Lane, M., Moustafa, M., Guy, R., MacGowan, A., Tazi-Ahnini, R., Ward, S., 2009. Epidermal Barrier Dysfunction in Atopic Dermatitis. J. Invest. Dermatol. 129, 1892–1908.

Couto, A., Fernandes, R., Cordeiro, M., Reis, S., Ribeiro, R., Pessoa, A., 2014. Dermic diffusion and stratum corneum: A state of the art review of mathematical models. J. Control. Release 177, 74–83.

Cross, S., Roberts, M., 2004. Physical Enhancement of Transdermal Drug Application: Is Delivery Technology Keeping up with Pharmaceutical Development. Curr. Drug Deliv. 1, 81–92.

Dale, B., Resing, K., Lonsdale-Eccles, J., 1985. Filaggrin: A Keratin Filament Associated Protein. Ann. N. Y. Acad. Sci. 455, 330–342.

Damodaran, S., 2007. Amino acids, peptides and proteins., in: Damodaran, S., Parkin, K.L., Owen Fennema, R. (Eds.), Fennema's Food Chemistry. CRC Press, Taylor& Francis group PP.425-439.

Danby, S., Cork, M., 2010. A New Understanding of Atopic Dermatitis : The Role of Epidermal Barrier Dysfunction and Subclinical Inflammation. J. Clin. Dermatology 1, 33–46.

Danby, S., Danby, S.G., Cork, M.J., 2010. A New Understanding of Atopic Dermatitis: The Role of Epidermal Barrier Dysfunction and Subclinical Inflammation. J. Clin. Dermatology 1, 33–46.

Dapic, I., Jakasa, I., Yau, N., Kezic, S., Kammeyer, A., 2013. Evaluation of an HPLC Method for the Determination of Natural Moisturizing Factors in the Human Stratum Corneum. Anal. Lett. 46, 2133–2144.

Dauner, M., Sauer, U., 2000. GC-MS Analysis of Amino Acids Rapidly Provides Rich Information for Isotopomer Balancing. Biotechnol. Prog. 16, 642–649.

de Person, M., Chaimbault, P., Elfakir, C., 2008. Analysis of native amino acids by liquid chromatography/electrospray ionization mass spectrometry: comparative study between two sources and interfaces. J. Mass Spectrom. 43, 204–215.

Denda, M., Hori, J., Koyama, J., Yoshida, S., Nanba, R., Takahashi, M., Horii, I., Yamamoto, A., 1992. Stratum corneum sphingolipids and free amino acids in experimentally-induced scaly skin. Arch. Dermatol. Res. 284, 363–367.

Deraison, C., Bonnart, C., Lopez, F., Besson, C., Robinson, R., Jayakumar, A., Wagberg, F., Brattsand, M., Pierre Hachem, J., Leonardsson, G., Hovnanian, A., 2007. LEKTI Fragments Specifically Inhibit KLK5, KLK7, and KLK14 and Control Desquamation through a pH-dependent Interaction D. Mol. Biol. Cell 18, 3607–3619.

Dimitriades, V., Rodriguez, P., Zabaleta, J., Ochoa, A., 2014. Arginase I levels are decreased in the plasma of pediatric patients with atopic dermatitis. Ann. Allergy. Asthma Immunol. 113, 271–5.

Eberlein-Konig, B., Schafer, T., Huss-Marp, J., Darsow, U., Mohrenschlager, M., Herbert, O., Abeck, D., Kramer, U., Behrendt, H., Ring, J., 2000. Skin surface pH, stratum corneum hydration, trans-epidermal water loss and skin roughness related to atopic eczema and skin dryness in a population of primary school children. Acta Derm. Venereol. 80,

188–191.

Eckert, R., Crish, J., Robinson, N., 1997. The epidermal keratinocyte as a model for the study of gene regulation and cell differentiation. Physiol. Rev. 77, 397–424.

Edwards, D., Langer, R., 1994. A Linear Theory of Transdermal Transport Phenomena. J. Pharm. Sci. 83, 1315–1334.

Egawa, M., Kunizawa, N., Hirao, T., Yamamoto, T., Sakamoto, K., Terui, T., Tagami, H., 2010. In vivo characterization of the structure and components of lesional psoriatic skin from the observation with Raman spectroscopy and optical coherence tomography: A pilot study. J. Dermatol. Sci. 57, 66–69.

Egawa, M., Tagami, H., 2007. Comparison of the depth profiles of water and water-binding substances in the stratum corneum determined in vivo by Raman spectroscopy between the cheek and volar forearm skin: effects of age, seasonal changes and artificial forced hydration. Br. J. Dermatol. 158, 251–260.

Elias, P., Gruber, R., Crumrine, D., Menon, G., Williams, M., Wakefield, J., Holleran, W., Uchida, Y., 2014. Formation and functions of the corneocyte lipid envelope (CLE). Biochim. Biophys. Acta - Mol. Cell Biol. Lipids 1841, 314–318.

Elias, P., Schmuth, M., 2009. Abnormal skin barrier in the pathogenesis of atopic dermatitis. Curr. Allergy aand Asthma Reports 9, 265–272.

Elias, P., Wakefield, J., 2011. Therapeutic Implications of a Barrier-Based Pathogenesis of Atopic Dermatitis. Clin. Rev. Allergy Immunol. 41, 282–295.

Elisabeth, E., Brattsand, M., Egelrud, T., 2000. Stratum Corneum Tryptic Enzyme in Normal Epidermis: a Missing Link in the Desquamation Process? J. Invest. Dermatol. 114, 56–63.

Enderle, J.D., 2012. Compartmental Modeling, in: Enderle, J., Bronzino, J. (Eds.), Introduction to Biomedical Engineering. Elsevier, pp. 359–445.

Fartacsh, F., 1997. Epidermal Barrier in Disorders of the Skin. Microsc. Res. Tech. 372, 361–372.

Folin, O., Ciocalteu, V., 1927. On tyrosine and tryptophane determination in proteins. J. Biol. Chem. 73, 627.

Folin, O., Marenzi, A., 1929. Tyrosine and tryptophane determination in one tenth gram of protein. J. Biol. Chem. 83, 89–102.

Fowler, J., 2012. Understanding the Role of Natural Moisturizing Factor in Skin Hydration. Pract. dermatology 9, 36–40.

Froebe, C.L., Simion, F.A., Rhein, L.D., Cagan, R.H., Kligman, A., 1990. Stratum corneum Lipid Removal by Surfactants: Relation to in vivo Irritation. Dermatology 181, 277–283.

Fuchs, E., 1994. Intermediate filaments and disease: mutations that cripple cell strength. J. Cell Biol. 125, 511–6.

Fürst, W., Falk, M., Neubert, R., Klapper, I., 1975. [Drug permeation through synthetic lipoid membranes. 6. The influence of volume on the permeation equation]. Pharmazie 30, 614–5.

Fürst, W., Neubert, R., Reppel, L., 1980. [Drug permeation through synthetic lipid membranes. Part 10: The effects of diffusion layers on the permeation process (author's transl)]. Pharmazie 35, 106–9.

Giavarina, D., 2015. Understanding Bland Altman analysis. Biochem. Medica 25, 141–151.

Girbal-Neuhauser, E., Durieux, J., Arnaud, M., Dalbon, P., Sebbag, M., Vincent, C., Simon, M., Senshu, T., Masson-Bessière, C., Jolivet-Reynaud, C., Jolivet, M., Serre, G., 1999. The epitopes targeted by the rheumatoid arthritis-associated antifilaggrin autoantibodies are posttranslationally generated on various sites of (pro)filaggrin by deimination of arginine residues. J. Immunol. 162, 585–94.

Gloor, M., Fluhr, J., Lehmann, L., Gehring, W., Thieroff-Ekerdt, R., 2002. Do urea/ammonium lactate combinations achieve better skin protection and hydration than either component alone? Skin Pharmacol. Appl. Skin Physiol. 15, 35–43.

Grozdev, I., Korman, N., 2014. Psoriasis as a systemic disease. Clin. Dermatol. 32, 343–350.

Grubauer, G., Elias, P., Feingold, K., 1989. Transepidermal water loss: the signal for recovery of barrier structure and function. J. Lipid Res. 30, 323–333.

Gu, L., Jones, A., Last, R., 2007. LC–MS/MS Assay for Protein Amino Acids and Metabolically Related Compounds for Large-Scale Screening of Metabolic Phenotypes. Analytical chemistry 79, 8067-8075.

Hachem, J., Houben, E., Crumrine, D., Man, M., Schurer, N., Roelandt, T., Choi, E., Uchida, Y., Brown, B., Feingold, K., Elias, P., 2005. Sustained Serine Proteases Activity by Prolonged Increase in pH Leads to Degradation of Lipid Processing Enzymes and Profound Alterations of Barrier Function and Stratum Corneum Integrity. J. Invest. Dermatol. 125, 510–520.

Hachem, J.P., 2006. The two compartment model of the stratum corneum: biochemical aspects and pathophysiological implications. Verh K Acad Geneeskd Belg. 68, 287–

317.

Haftek, M., Simon, M., Kanitakis, J., Marechal, S., Claudy, A., Serre, G., Schmitt, D., 1997. Expression of corneodesmosin in the granular layer and stratum corneum of normal and diseased epidermis. Br. J. Dermatol. 137, 864–873.

Haftek, M., Teillon, M.-H., Schmitt, D., 1998. Stratum corneum, corneodesmosomes and ex vivo percutaneous penetration. Microsc. Res. Tech. 43, 242–249.

Hansen, S., Naegel, A., Heisig, M., Wittum, G., Neumann, D., Kostka, K.-H., Meiers, P., Lehr, C.-M., Schaefer, U., 2009. The Role of Corneocytes in Skin Transport Revised—A Combined Computational and Experimental Approach. Pharm. Res. 26, 1379–1397.

Harding, C., 2004. The stratum corneum: structure and function in health and disease. Dermatol. Ther. 17, 6–15.

Harding, C., Long, S., Richardson, J., Rogers, J., Zhang, Z., Bush, A., Rawlings, A.V., 2003. The cornified cell envelope: an important marker of stratum corneum maturation in healthy and dry skin. Int. J. Cosmet. Sci. 25, 157–167.

Harding, C., Scott, I., 2002. Stratum Corneum Moisturizing Factors, in: Leyden, J., Rawlings, A.V. (Eds.), Skin Moisturization. Boca Raton, FL: CRC Press, pp. 61–80.

Harding, C., Scott, I., 1983. Histidine-rich proteins (filaggrins): Structural and functional heterogeneity during epidermal differentiation. J. Mol. Biol. 170, 651–673.

Harding, C., Watkinson, A., Rawlings, A.V., Scott, I., 2000. Dry skin, moisturization and corneodesmolysis. Int. J. Cosmet. Sci. 22, 21–52.

Hashiguchi, T., Kodama, A., Ryu, A., Otagiri, M., 1998. Retention capacity of topical imidazole antifungal agents in the skin. Int. J. Pharm. 161, 195–204.

Heard, C., Monk, B., Modley, A., 2003. Binding of primaquine to epidermal membranes and keratin. Int. J. Pharm. 257, 237–244.

Heisig, M., Lieckfeldt, R., Wittum, G., Mazurkevich, G., Lee, G., 1996. Non steady-state descriptions of drug permeation through stratum corneum. I. The biphasic brick-and-mortar model. Pharm. Res. 13, 421–426.

Horii, I., Kawasaki, K., Nakayama, Y., Morikawa, Y., Mitsui, T., Kumagai, H., Kawasaki, K., Koyama, J., Nakayama, Y., Nakajima, K., Okazaki, K., Seiji, M., 1983. Histidine-Rich Protein as a Possible Origin of Free Amino Acids of Stratum Corneum. Curr Probl Dermatol, in: Seiji, M., Bernstein, I. (Eds.), Normal and Abnormal Epidermal Differentiation. Karger Publishers, pp. 301–315.

Horii, I., Nakayama, Y., Obata, M., Tagami, H., 1989. Stratum corneum hydration and amino

acid content in xerotic skin. Br. J. Dermatol. 121, 587–592.

Horikoshi, T., Igarashi, S., Uchiwa, H., Brysk, H., Brysk, M., 1999. Role of endogenous cathepsin D-like and chymotrypsin-like proteolysis in human epidermal desquamation. Br. J. Dermatol. 141, 453–9.

Imokawa, G., Abe, A., Jin, K., Higaki, Y., Kawashima, M., Hidano, A., 1991. Decreased Level of Ceramides in Stratum Corneum of Atopic Dermatitis: An Etiologic Factor in Atopic Dry Skin? J. Invest. Dermatol. 96, 523–526.

Inagaki, S., Tano, Y., Yamakata, Y., Higashi, T., Min, J., Toyo'oka, T., 2010. Highly sensitive and positively charged precolumn derivatization reagent for amines and amino acids in liquid chromatography/electrospray ionization tandem mass spectrometry. Rapid Commun. Mass Spectrom. 24, 1358–1364.

Jacobi, U., Tassopoulos, T., Surber, C., Lademann, J., 2006. Cutaneous distribution and localization of dyes affected by vehicles all with different lipophilicity. Arch. Dermatol. Res. 297, 303–310.

Jacobson, T., Yüksel, K., Geesin, J., Gordon, J., Lane, A., Gracy, R., 1990. Effects of Aging and Xerosis on the Amino Acid Composition of Human Skin. J. Invest. Dermatol. 95, 296-300.

Jander, G., Norris, S., Joshi, V., Fraga, M., Rugg, A., Yu, S., Li, L., Last, R., 2004. Application of a high-throughput HPLC-MS/MS assay to Arabidopsis mutant screening; evidence that threonine aldolase plays a role in seed nutritional quality. Plant J. 39, 465–475.

Jarnik, M., Simon, M.N., Steven, A.C., 1998. Cornified cell envelope assembly: a model based on electron microscopic determinations of thickness and projected density. J. Cell Sci. 111, 1051–1060.

Jassoy, C., Ag, H., Jassoy, C., Waldmann-laue, M., Forster, T., Wadle, A., Doering, T., Kgaa, H., 2015. Taurine improves epidermal barrier properties stressed by surfactants - A role for osmolytes in barrier epidermal barrier properties. j. Cosmet. Sci. 57, 1-10.

Jepps, O., Dancik, Y., Anissimov, Y., Roberts, M., 2013. Modeling the human skin barrier — Towards a better understanding of dermal absorption. Adv. Drug Deliv. Rev. 65, 152–168.

Joo, K., Han, J., Son, E., Nam, G., Jeong, H., Lim, K., Cho, J., 2012. Study on the Relationship between Skin Dryness and Amino Acids in Stratum Corneum. J. Soc. Cosmet. Sci. Korea 38, 75–82.

Kalinin, A., Kajava, A., Steinert, P., 2002. Epithelial barrier function: Assembly and

structural features of the cornified cell envelope. Bioessays 24, 789-800.

Kalinin, A., Marekov, L., Steinert, P., 2001. Assembly of the epidermal cornified cell envelope. J. Cell Sci. 114, 3069–3070.

Kanitakis, J., 2002. Anatomy, histology and immunohistochemistry of normal human skin. Eur. J. dermatol 12, 390-399.

Kashibuchi, N., Hirai, Y., O'Goshi, K., Tagami, H., 2002. Three-dimensional analyses of individual corneocytes with atomic force microscope: Morphological changes related to age, location and to the pathologic skin conditions. Ski. Res. Technol. 8, 203–211.

Kashima, M., Fukuyama, K., Kikuchi, M., Epstein, W.L., 1988. Limited Proteolysis of High Molecular Weight Histidine-Rich Protein of Rat Epidermis by Epidermal Proteinases. J. Invest. Dermatol. 90, 829–833.

Kaspar, H., Dettmer, K., Gronwald, W., Oefner, P., 2009. Advances in amino acid analysis. Anal. Bioanal. Chem. 393, 445–452.

Katagiri, C., Sato, J., Nomura, J., Denda, M., 2003. Changes in environmental humidity affect the water-holding property of the stratum corneum and its free amino acid content, and the expression of filaggrin in the epidermis of hairless mice. J. Dermatol. Sci. 31, 29–35.

Kawada, A., Hara, K., Hiruma, M., Noguchi, H., Ishibashi, A., 1995a. Rat epidermal cathepsin L-like proteinase: Purification and some hydrolytic properties toward filaggrin and synthetic substrates. J. Biochem. 118, 332–337.

Kawada, A., Hara, K., Morimoto, K., Hiruma, M., Ishibashi, A., 1995b. Rat epidermal cathepsin B: Purification and characterization of proteolytic properties toward filaggrin and synthetic substrates. Int. J. Biochem. Cell Biol. 27, 175–183.

Kvitvang, H., Andreassen, T., Adam, T., Villas-Bôas, S., Bruheim, P., 2011. Highly Sensitive GC/MS/MS Method for Quantitation of Amino and Nonamino Organic Acids. Analytical Chemistry 83, 2705-2711.

Kwan, P., Sills, G., Brodie, M., 2012. Understanding the Role of NMF in Skin Hydration. Pract. Dermatology July, 21–34.

Leavens, W., Lane, S., Carr, R., Lockie, A., Waterhouse, I., 2002. Derivatization for liquid chromatography/electrospray mass spectrometry: synthesis of tris(trimethoxyphenyl)phosphonium compounds and their derivatives of amine and carboxylic acids. Rapid Commun. Mass Spectrom. 16, 433–441.

Lee, K., Drescher, D., 1978. Fluorometric amino-acid analysis with o-phthaldialdehyde

(OPA). Int. J. Biochem. 9, 457–467.

Levin, J., Friedlander, S., Del Rosso, J., 2013. Atopic dermatitis and the stratum corneum: part 1: the role of filaggrin in the stratum corneum barrier and atopic skin. J. Clin. Aesthet. Dermatol. 6, 16–22.

Lian, G., Chen, L., Han, L., 2008. An evaluation of mathematical models for predicting skin permeability. J. Pharm. Sci. 97, 584–598.

Loden, M., Andersson, A.-C., Andersson, C., Frodin, T., Oman, H., Lindberg, M., 2001. Instrumental and dermatologist evaluation of the effect of glycerine and urea on dry skin in atopic dermatitis. Ski. Res. Technol. 7, 209–213.

López, O., Cócera, M., Wertz, P.W., López-Iglesias, C., de la Maza, A., 2007. New arrangement of proteins and lipids in the stratum corneum cornified envelope. Biochim. Biophys. Acta - Biomembr. 1768, 521–529.

Lowes, M., Bowcock, A., Krueger, J., 2007. Pathogenesis and therapy of psoriasis. Nature 445, 866–873.

Madison, K., 2003. Barrier Function of the Skin: "La Raison d'Être" of the Epidermis. J. Invest. Dermatol. 121, 231–241.

Marks, R., Nicholls, S., King, C.S., 1981. Studies on isolated corneocytes. Int. J. Cosmet. Sci. 3, 251–259.

Marquez-Lago, T., Allen, D., Thewalt, J., 2010. A novel approach to modelling water transport and drug diffusion through the stratum corneum. Theor. Biol. Med. Model. 7, 33.

Masson-Bessière, C., Sebbag, M., Girbal-Neuhauser, E., Nogueira, L., Vincent, C., Senshu, T., Serre, G., 2001. The major synovial targets of the rheumatoid arthritis-specific antifilaggrin autoantibodies are deiminated forms of the α- and β-chains of fibrin. J. Immunol. 166, 4177–4184.

McAleer, M., Jakasa, I., Raj, N., O'Donnell, C., Lane, M., Rawlings, A.V., Voegeli, R., McLean, W., Kezic, S., Irvine, A., 2018. Early-life regional and temporal variation in filaggrin-derived natural moisturizing factor, filaggrin-processing enzyme activity, corneocyte phenotypes and plasmin activity: implications for atopic dermatitis. Br. J. Dermatol. 179, 431–441.

McCarley, K.D., Bunge, A.L., 2001. Pharmacokinetic models of dermal absorption. J. Pharm. Sci. 90, 1699–719.

McGrath, J., Eady, R., Pope, F., 2008. Anatomy and Organization of Human Skin, in: Tony,

B., Stephen, B., Neil, C., Christopher, G. (Eds.), Rook's Textbook of Dermatology. Blackwell Publishing, Inc., Malden, Massachusetts, USA, pp. 45–128.

Meckfessel, M., Brandt, S., 2014. The structure, function, and importance of ceramides in skin and their use as therapeutic agents in skin-care products. J. Am. Acad. Dermatol. 71, 177–184.

Menon, G., 2002. New insights into skin structure : scratching the surface 54, S3–S17.

Menter, A., Gottlieb, A., Feldman, S., Van Voorhees, A., Leonardi, C., Gordon, K., Lebwohl, M., Koo, J., Elmets, C., Korman, N., Beutner, K., Bhushan, R., 2008. Guidelines of care for the management of psoriasis and psoriatic arthritis: Section 1. Overview of psoriasis and guidelines of care for the treatment of psoriasis with biologics. J. Am. Acad. Dermatol. 58, 826–850.

Michaels, A., Chandrasekaran, S., Shaw, J., 1975. Drug permeation through human skin: Theory andinvitro experimental measurement. AIChE J. 21, 985–996.

Michel, S., Schmidt, R., Shroot, B., Reichert, U., 1988. Morphological and biochemical characterization of the cornified envelopes from human epidermal keratinocytes of different origin. J. Invest. Dermatol. 91, 11-15.

Mitragotri, S., 2003. Modeling skin permeability to hydrophilic and hydrophobic solutes based on four permeation pathways. J. Control. Release 86, 69–92.

Mizutani, Y., Mitsutake, S., Tsuji, K., Kihara, A., Igarashi, Y., 2009. Ceramide biosynthesis in keratinocyte and its role in skin function. Biochimie 91, 784–790.

Mojumdar, E., Pham, Q., Topgaard, D., Sparr, E., 2017. Skin hydration: interplay between molecular dynamics, structure and water uptake in the stratum corneum. Sci. Rep. 7, 1–13.

Mollee, T., Bracken, A., 2007. A Model of Solute Transport through Stratum Corneum Using Solute Capture and Release. Bull. Math. Biol. 69, 1887–1907.

Moser, K., Kriwet, K., Naik, A., Kalia, Y.N., Guy, R.H., 2001. Passive skin penetration enhancement and its quantification in vitro. Eur. J. Pharm. Biopharm. 52, 103–112.

Naegel, A., Heisig, M., Wittum, G., 2013. Detailed modeling of skin penetration—An overview. Adv. Drug Deliv. Rev. 65, 191–207.

Nagy, K., Takáts, Z., Pollreisz, F., Szabó, T., Vékey, K., 2003. Direct tandem mass spectrometric analysis of amino acids in dried blood spots without chemical derivatization for neonatal screening. Rapid Commun. Mass Spectrom. 17, 983–990.

Nenoff, P., Donaubauer, K., T, A., UFl., H., 2004. Topically applied arginine hydrochloride.

Effect on urea content of stratum corneum and skin hydration in atopic eczema and skin aging. Hautarzt 55, 58–64.

Neubert, R., 1978. Zur Bewertung des Permeations- und Resorptionsverhaltens von Arzneistoffen durch Modellmethoden. Martin Luther University, Halle-Wittenberg.

Neubert, R., Fürst, W., 1989. In vitro-Untersuchungen des Arzneistofftransportes. — Methoden, Möglichkeiten, Mechanismen —. Pharm. Unserer Zeit 18, 112–122.

Ng, K., Lau, W., 2015. Skin Deep: The Basics of Human Skin Structure and Drug Penetration, in: Dragicevic, N., Maibach, H. (Eds.), Percutaneous Penetration Enhancers Chemical Methods in Penetration Enhancement. Springer Berlin Heidelberg, Berlin, Heidelberg, pp. 3–11.

Nishimura, H., Ikehara, O., Naito, T., Higuchu, C., Sanaka, T., 2009. Evaluation of taurine as in osmotic agent for peritoneal dialysis solution. Perit. Dial. Int. 29, 204–216.

Nitsche, J., 1999. Cellular Microtransport Processes: Intercellular, Intracellular, and Aggregate Behavior. Annu. Rev. Biomed. Eng. 1, 463–503.

Nitsche, J.M., Frederick Frasch, H., 2011. Dynamics of diffusion with reversible binding in microscopically heterogeneous membranes: General theory and applications to dermal penetration. Chem. Eng. Sci. 66, 2019–2041.

Norlén, L., 2001. Skin Barrier Structure and Function: The Single Gel Phase Model. J. Invest. Dermatol. 117, 830–836.

Norlén, L., Forslind, B., Nicander, I., Rozell, B., Ollmar, S., 1999. Inter- and Intra-Individual Differences in Human Stratum Corneum Lipid Content Related to Physical Parameters of Skin Barrier Function In Vivo. J. Invest. Dermatol. 112, 72–77.

O'Regan, G., Sandilands, A., McLean, W., Irvine, A., 2008. Filaggrin in atopic dermatitis. J. Allergy Clin. Immunol. 122, 689–693.

Odetti, P., Pesce, C., Traverso, N., Menini, S., Maineri, E., Cosso, L., Valentini, S., Patriarca, S., Cottalasso, D., Marinari, U., Pronzato, M., 2003. Comparative Trial of N-Acetyl-Cysteine, Taurine, and Oxerutin on Skin and Kidney Damage in Long-Term Experimental Diabetes. Diabetes 52, 499–505.

Pan Ba, M., Heinecke, G., Bernardo, S., Tsui, C., Levitt, J., 2013. Urea: a comprehensive review of the clinical literature. Dermatol. Online J. 19, 20392.

Pande, S., Merker, H., Bohl, K., Reichelt, M., Schuster, S., de Figueiredo, L., Kaleta, C., Kost, C., 2014. Fitness and stability of obligate cross-feeding interactions that emerge upon gene loss in bacteria. ISME J. 8, 953–962.

Patel, D., Kumar, V., Kesharwani, R., Mazumdar, B., 2015. Lipid nanoparticle a novel carrier for cosmetics and topical preparation: a review. Inven. Rapid Cosmeceuticals 2015, 1–6.

Peju, G., Rajat, H., 1906. Note sur le polymorphisme des bactéries sans l'urée. Compt. rend. Soc. biol. 61, 477.

Persson, J., Nasholm, T., 2001. A GC-MS method for determination of amino acid uptake by plants. Physiol. Plant. 113, 352–358.

Piérard, G., Goffin, V., Hermanns-le, T., Piérard-franchimont, C., 2000. Corneocyte desquamation (Review). Int. J. Mol. Med. 6, 217–221.

Piraud, M., Vianey-Saban, C., Bourdin, C., Acquaviva-Bourdain, C., Boyer, S., Elfakir, C., Bouchu, D., 2005. A new reversed-phase liquid chromatographic/tandem mass spectrometric method for analysis of underivatised amino acids: evaluation for the diagnosis and the management of inherited disorders of amino acid metabolism. Rapid Commun. Mass Spectrom. 19, 3287–3297.

Piraud, M., Vianey-Saban, C., Petritis, K., Elfakir, C., Steghens, J.-P., Morla, A., Bouchu, D., 2003. ESI-MS/MS analysis of underivatised amino acids: a new tool for the diagnosis of inherited disorders of amino acid metabolism. Fragmentation study of 79 molecules of biological interest in positive and negative ionisation mode. Rapid Commun. Mass Spectrom. 17, 1297–1311.

Ponec, M., Weerheim, A., Lankhorst, P., Wertz, P., 2003. New Acylceramide in Native and Reconstructed Epidermis. J. Invest. Dermatol. 120, 581–588.

Potts, R., Guy, R., 1992. Predicting Skin Permeability. Pharm. Res. 9, 663–669.

Prausnitz, M.R., Mitragotri, S., Langer, R., 2004. Current status and future potential of transdermal drug delivery. Nat. Rev. Drug Discov. 3, 115–124.

Proksch, E., Brandner, J., Jensen, J.-M., 2008. The skin: an indispensable barrier. Exp. Dermatol. 17, 1063–1072.

Rawlings, A.V., 2014. Molecular basis for stratum corneum maturation and moisturization. Br. J. Dermatol. 171, 19–28.

Rawlings, A.V., Harding, C., 2004. Moisturization and skin barrier function. Dermatol. Ther. 17, 43–48.

Rawlings, A.V., Scott, I.R., Harding, C.R., Bowser, P., 1994. Stratum Corneum Moisturization at the Molecular Level. J. Invest. Dermatol. 103, 731–740.

Rawlings, A.V., Scott, I.R., Harding, C.R., Bowser, P.A., 1994. Stratum corneum

moisturization at the molecular level. J. Invest. Dermatol. 103, 731–740.

Rawlings, A.V, Voegeli, R., 2013. Stratum corneum proteases and dry skin conditions. Cell Tissue Res. 351, 217-235.

Richter, T., Müller, J., Schwarz, U., Wepf, R., Wiesendanger, R., 2001. Investigation of the swelling of human skin cells in liquid media by tapping mode scanning force microscopy. Appl. Phys. A Mater. Sci. Process. 72, 125–128.

Richter, T., Peuckert, C., Sattler, M., Koenig, K., Riemann, I., Hintze, U., Wittern, K.-P., Wiesendanger, R., Wepf, R., 2004. Dead but highly dynamic--the stratum corneum is divided into three hydration zones. Skin Pharmacol. Physiol. 17, 246–57.

Rigas, P., 2013. Post-column labeling techniques in amino acid analysis by liquid chromatography. Anal. Bioanal. Chem. 405, 7957–7992.

Rim, J., Pinsky, P., van Osdol, W., 2009. Multiscale Modeling Framework of Transdermal Drug Delivery. Ann. Biomed. Eng. 37, 1217–1229.

Rippke, F., Schreiner, V., Doering, T., Maibach, H.I., 2004. Stratum Corneum pH in Atopic Dermatitis. Am. J. Clin. Dermatol. 5, 217–223.

Rippke, F., Schreiner, V., Schwanitz, H., 1999. The acidic milieu of the horny layer/new findings on physiology and pathophysiology of the skin ph-value. Dermatosen Beruf und Umwelt 47, 230–245.

Robinson, M., Visscher, M., Laruffa, A., Wickett, R., 2010. Natural moisturizing factors (NMF) in the stratum corneum (SC). I. Effects of lipid extraction and soaking. J. Cosmet. Sci. 61, 13–22.

Rutherfurd, S., Gilani, G., 2009. Amino acid analysis, Current Protocols in Protein Science.

Schade, H., Marchionini, A., 1928. Der Säuremantel der Haut (nac Gaskettenmessung). Klin Wschr 7, 12–14.

Schmid-Wendtner, M., Korting, H., 2006. The pH of the skin surface and its impact on the barrier function. Skin Pharmacol. Physiol. 19, 296–302.

Schölermann, A., Banké-Bochita, J., Bohnsack, K., Rippke, F., Herrmann, W., 1998. Efficacy and safety of Eucerin 10 % Urea Lotion in the treatment of symptoms of aged skin. J. Dermatolog. Treat. 9, 175–179.

Scott, I., Harding, C., 1981. Studies on the synthesis and degradation of a high molecular weight, histidine-rich phosphoprotein from mammalian epidermis. Biochim. Biophys. Acta - Protein Struct. 669, 65–78.

Scott, I.R., Harding, C.R., Barrett, J.G., 1982. Histidine-rich protein of the keratohyalin

granules: Source of the free amino acids, urocanic acid and pyrrolidone carboxylic acid in the stratum corneum. Biochim. Biophys. Acta - Gen. Subj. 719, 110–117.

Seguchi, T., Chang-Yi, C., Kusuda, S., Takahashi, M., Aisu, K., Tezuka, T., 1996. Decreased expression of filaggrin in atopic skin. Arch. Dermatol. Res. 288, 442–446.

Seidenari, S., Giusti, G., 1995. Objective assessment of the skin of children affected by atopic dermatitis: a study of pH, capacitance and TEWL in eczematous and clinically uninvolved skin. Acta Derm. Venereol. 75, 429–33.

Seif, S., Hansen, S., 2012. Measuring the stratum corneum reservoir: desorption kinetics from keratin. J. Pharm. Sci. 101, 3718–28.

Serre, G., Mils, V., Haftek, M., Vincent, C., Croute, F., Réano, A., Ouhayoun, J.-P., Bettinger, S., Soleihavoup, J.-P., 1991. Identification of Late Differentiation Antigens of Human Cornified Epithelia, Expressed in Re-Organized Desmosomes and Bound to Cross-Linked Envelope. J. Invest. Dermatol. 97, 1061–1072.

Shimbo, K., Oonuki, T., Yahashi, A., Hirayama, K., Miyano, H., 2009a. Precolumn derivatization reagents for high-speed analysis of amines and amino acids in biological fluid using liquid chromatography/electrospray ionization tandem mass spectrometry. Rapid Commun. Mass Spectrom. 23, 1483–1492.

Shimbo, K., Yahashi, A., Hirayama, K., Nakazawa, M., Miyano, H., 2009b. Multifunctional and Highly Sensitive Precolumn Reagents for Amino Acids in Liquid Chromatography/Tandem Mass Spectrometry. Anal. Chem. 81, 5172–5179.

Simon, M., Jonca, N., Guerrin, M., Haftek, M., Bernard, D., Cile Caubet, C., Rn Egelrud, T., Schmidt, R., Serre, G., 2001. Refined Characterization of Corneodesmosin Proteolysis during Terminal Differentiation of Human Epidermis and Its Relationship to Desquamation. J. Biol. Chem. 276, 20292-20299.

Simpson, E., 2010. Atopic dermatitis: a review of topical treatment options. Curr. Med. Res. Opin. 26, 633–640.

Smeden, J., Janssens, M., Gooris, G., Bouwstra, J., 2013. The important role of stratum corneum lipids for the cutaneous barrier function. BBA - Mol. Cell Biol. Lipids 1841, 295-313.

Sonoda, J., Natto, S., Takada, S., Miyauchi, Y., 2012. Noninvasive In Vivo Measurement of Natural Moisturizing Factor Content in Stratum Corneum of Human Skin by Attenuated Total Reflection Infrared Spectroscopy. Appl. Spectrosc. 66, 26-32.

Spier, H., Pascher, G., 1955. Die wasserlslichen Bestandteile der peripheren Hornschicht

(Hautoberflche). Quantitative Analysen. Arch. Dermatol. Syph. 199, 411–427.

Spurr, A., 1969. A low-viscosity epoxy resin embedding medium for electron microscopy. J. Ultrastruct. Res. 26, 31–43.

Sugawara, T., Kikuchi, K., Tagami, H., Aiba, S., Sakai, S., 2012. Decreased lactate and potassium levels in natural moisturizing factor from the stratum corneum of mild atopic dermatitis patients are involved with the reduced hydration state. J. Dermatol. Sci. 66, 154–159.

Sylvestre, J.-P., Bouissou, C.C., Guy, R.H., Delgado-Charro, M.B., 2010. Extraction and quantification of amino acids in human stratum corneum in vivo. Br. J. Dermatol. 163, 458–465.

Sznitowska, M., Janicki, S., Williams, A., 1998. Intracellular or Intercellular Localization of the Polar Pathway of Penetration Across Stratum Corneum. J. Pharm. Sci. 87, 1109–1114.

T'Kindt, R., Jorge, L., Dumont, E., Couturon, P., David, F., Sandra, P., Sandra, K., 2012. Profiling and Characterizing Skin Ceramides Using Reversed-Phase Liquid Chromatography–Quadrupole Time-of-Flight Mass Spectrometry. Anal. Chem. 84, 403–411.

Takahashi, H., Tsuji, H., Minami-Hori, M., Miyauchi, Y., Iizuka, H., 2014. Defective barrier function accompanied by structural changes of psoriatic stratum corneum. J. Dermatol. 41, 144–148.

Takahashi, M., Tezuka, T., 2004. The content of free amino acids in the stratum corneum is increased in senile xerosis. Arch. Dermatol. Res. 295, 448–452.

Takenouchi, M., Suzuki, H., Tagami, H., 1986. Hydration Characteristics of Pathologic Stratum Corneum--Evaluation of Bound Water. J. Invest. Dermatol. 87, 574–576.

Thyssen, J., Kezic, S., 2014. Causes of epidermal filaggrin reduction and their role in the pathogenesis of atopic dermatitis. J. Allergy Clin. Immunol. 134, 792–799.

Tojo, K., 1987. Random brick model for drug transport across stratum corneum. J. Pharm. Sci. 76, 889–891.

Tollefson, M., Bruckner, A., 2014. Atopic dermatitis: skin-directed management., Pediatrics. American Academy of Pediatrics 134, 1735-1744.

Trianse, S., 1974. The search for the ideal moisturizer. Cosmet. Perfum. 57.

Urry, D., 2004. The change in Gibbs free energy for hydrophobic association: Derivation and evaluation by means of inverse temperature transitions. Chem. Phys. Lett. 399,

177–183.

Verdier-Sévrain, S., Bonté, F., 2007. Skin hydration: A review on its molecular mechanisms. J. Cosmet. Dermatol. 6, 75–82.

Visscher, M., Utturkar, R., Pickens, W., LaRuffa, A., Robinson, M., Wickett, R., Narendran, V., Hoath, S., 2011. Neonatal Skin Maturation-Vernix Caseosa and Free Amino Acids. Pediatr. Dermatol. 28, 122–132.

Visscher, M.O., Tolia, G.T., Wickett, R.R., Hoath, S.B., 2003. Effect of soaking and natural moisturizing factor on stratum corneum water-handling properties, j. Cosmet. Sci.

Wang, T., Kasting, G., Nitsche, J., 2006. A multiphase microscopic diffusion model for stratum corneum permeability. I. Formulation, solution, and illustrative results for representative compounds. J. Pharm. Sci. 95, 620–648.

Warner, R., Stone, K., Boissy, Y., 2003. Hydration Disrupts Human Stratum Corneum Ultrastructure. J. Invest. Dermatol. 120, 275–284.

Watanabe, M., 1991. Functional Analyses of the Superficial Stratum Corneum in Atopic Xerosis. Arch. Dermatol. 127, 1689.

White-Chu, E., Reddy, M., 2011. Dry skin in the elderly: Complexities of a common problem. Clin. Dermatol. 29, 37–42.

Wilkerson, V., 1934. Chemistry of Human epidermis. J. Biol. Chem. 107, 477–480.

Williams, A., Barry, B., 2004. Penetration enhancers. Adv. Drug Deliv. Rev. 56, 603–618.

Wilschut, A., ten Berge, W., Robinson, P., McKone, T., 1995. Estimating skin permeation. The validation of five mathematical skin permeation models. Chemosphere 30, 1275–1296.

Wilson, W., 1906. Pleomorphism, as exhibited by bacteria grown on media containing urea. J. Pathol. Bacteriol. 11, 394–404.

Wolfersberger, M., Tabachnick, J., Finkelstein, B., Levin, M., 1973. L-Pyrrolidone carboxylic acid content in mammalian epidermis and other tissues. J. Invest. Dermatol. 60, 278–281.

Wolter, S., Price, H.N., 2014. Atopic Dermatitis. Pediatr. Clin. North Am. 61, 241-260.

Wu, G., 2013. Functional amino acids in nutrition and health. Amino Acids 45, 407–411.

Wu, G., 2009. Amino acids: metabolism, functions, and nutrition. Amino Acids 37, 1–17.

Wysocki, A., 1999. Skin anatomy, physiology, and pathophysiology. Nurs. Clin. North Am. 34, 777–97.

Xiao, P., Imhof, R., 2012. Two dimensional finite element modelling for dynamic water

diffusion through stratum corneum. Int. J. Pharm. 435, 88–92.

Yotsuyanagi, T., Huguchi, W., 1972. A two phase series model for the transport of steroids across the fully hydrated stratum corneum. J. Pharm. Pharmacol. 24, 934–941.

Yu, B., Kim, K., So, P., Blankschtein, D., Langer, R., 2003. Evaluation of Fluorescent Probe Surface Intensities as an Indicator of Transdermal Permeant Distributions Using Wide-Area Two-Photon Fluorescence Microscopy. J. Pharm. Sci. 92, 2354–2365.

Zeeuwen, P., 2004. Epidermal differentiation: The role of proteases and their inhibitors. Eur. J. Cell Biol. 83, 761–773.

Appendices

A. FAA/urea analysis

A1. MS parameters of MRM transitions for the AAs including taurine quantified using LC-ESI-MS/MS.

Following is the table with MRM parameters of all the AAs used in the study and analysis using LC-ESI MS/MS.

Table A1. MS parameters for MRM-transitions

Amino acid	MRM transitions	Declustering potential (DP), V	Entrance potential (EP), V	Cell entrance potential (CEP), V	Collision potential (CE), V	Cell exit potential (CEX), V	Retention time (min)
Ala	310→88	-15	-8	-24	-14	0	4.3
	310→114	-15	-8	-24	-16	0	
Cys	342→146	-30	-10	-25	-14	-2	3.6
	342→120	-30	-10	-25	-12	-2	
Asp	354→158	-25	-5	-26	-16	0	3.1
	354→132	-25	-5	-26	-16	0	

Glu	368→128	-20	-5	-26	-28	0	3.2
	368→146	-20	-5	-26	-16	0	
Phe	386→164	-15	-9	-27	-16	-2	6.9
	386→190	-15	-9	-27	-18	-2	
Gly	296→74	-10	-9	-23	-14	0	3.6
	286→100	-15	-8	-23	-16	0	
His-1	376→154	-30	-7	-27	-26	0	1.2
	376→180	-25	-8	-27	-28	-2	
His-2	598→154	-30	-7	-36	-26	0	8.0
	598→180	-25	-8	-36	-28	-2	
Ile	352→130	-15	-8	-26	-12	0	6.8
	352→156	-15	-8	-26	-14	0	
Lys	589→145	-30	-5	-36	-26	0	8.0
	589→171	-25	-6	-36	-28	0	
Leu	352→130	-15	-8	-26	-12	0	6.9
	352→156	-15	-8	-26	-14	0	
Met	370→174	-15	-9	-26	-16	-2	5.7
	370→148	-15	-9	-26	-12	-2	
Met-oxide	386→190	-15	-9	-27	-16	-2	2.5
	386→164	-15	-9	-27	-12	0	
Asn	353→113	-20	-8	-26	-22	0	2.4
	353→131	-20	-7	-26	-14	0	
Pro	336→114	-10	-8	-25	-24	0	4.9
	336→158	-10	-9	-25	-6	0	
Gln	367→171	-20	-6	-26	-14	-2	2.4
	367→145	-15	-8	-26	-14	-2	
Arg	395→173	-30	-7	-28	-14	0	1.4

	395→199	-30	-7	-28	-18	-2	
Ser	326→130	-15	-8	-25	-14	0	2.8
	326→104	-15	-8	-25	-12	0	
Thr	340→100	-15	-8	-25	-28	0	3.4
	340→118	-20	-6	-25	-12	0	
Val	338→116	-15	-9	-25	-12	0	5.8
	338→142	-15	-9	-25	-18	0	
Trp	425→203	-15	-8	-29	-16	-2	6.6
	425→229	-15	-8	-29	-18	-2	
Tyr-1	402→180	-30	-9	-28	-12	-2	4.6
	402→206	-30	-9	-28	-18	-2	
Tyr-2	624→180	-30	-9	-37	-12	-2	8.2
	624→206	-30	-9	-37	-18	-2	
Norvaline	338→116	-15	-8	-25	-12	0	6.0
	338→142	-15	-8	-25	-18	0	
Citrulline	396→200	-20	-7	-28	-16	-2	2.5
	396→157	-20	-7	-28	-28	0	
Ornithine	575→131	-20	-10	-35	-24	0	8.0
	375→157	-20	-10	-35	-24	-2	
Taurine	346→124	-35	-5	-20	-28	0	2.2
	346→80	-35	-5	-20	-82	0	

Quantifier and qualifier transitions are indicated in bold and italics, respectively.

A2. LC chromatograms of FAAs of the corneocytes isolated from the skin samples obtained from pedicure left over.

Chromatogram of FAAs analysis after pre-column derivatization with FMOC-Cl in group in the corneocytes isolated from skin sample obtained after pedicure treatment

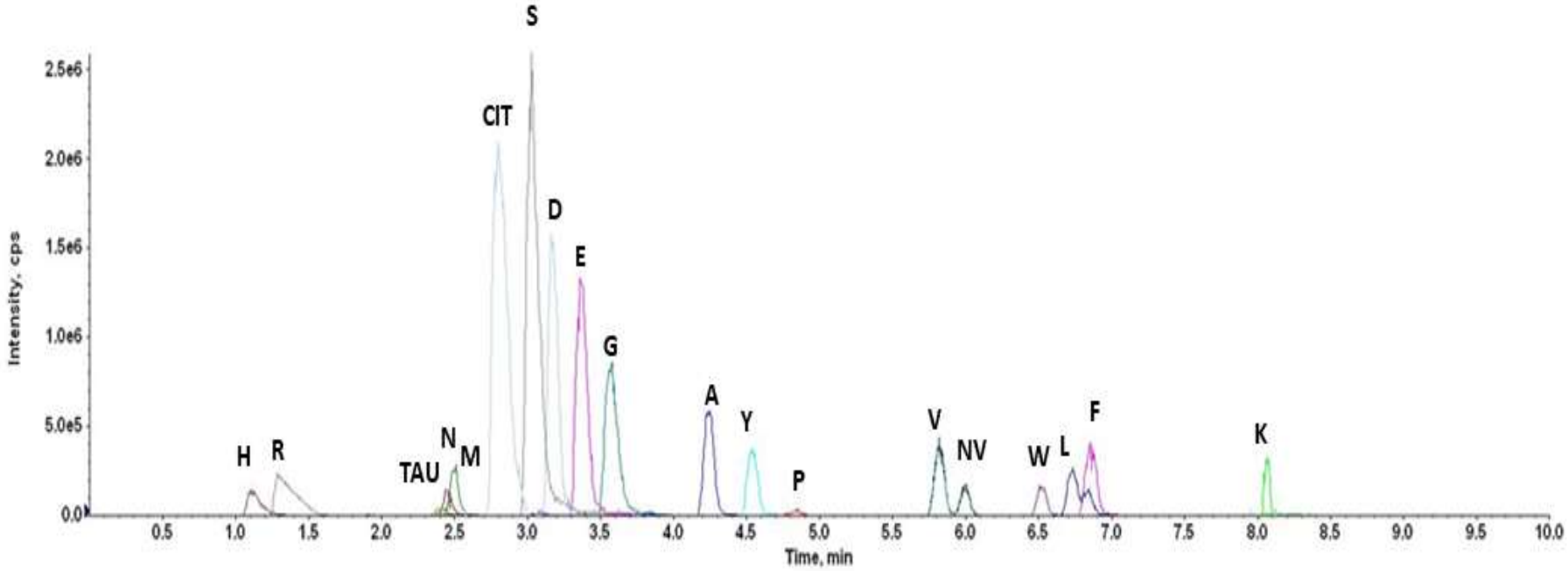

A3. Chromatogram of FAAs analysis after pre-column derivatization with FMOC-Cl in each group. A) healthy young (HY) B) healthy old (HO) C) atopic dermatitis (AD) and D) psoriasis (PS)

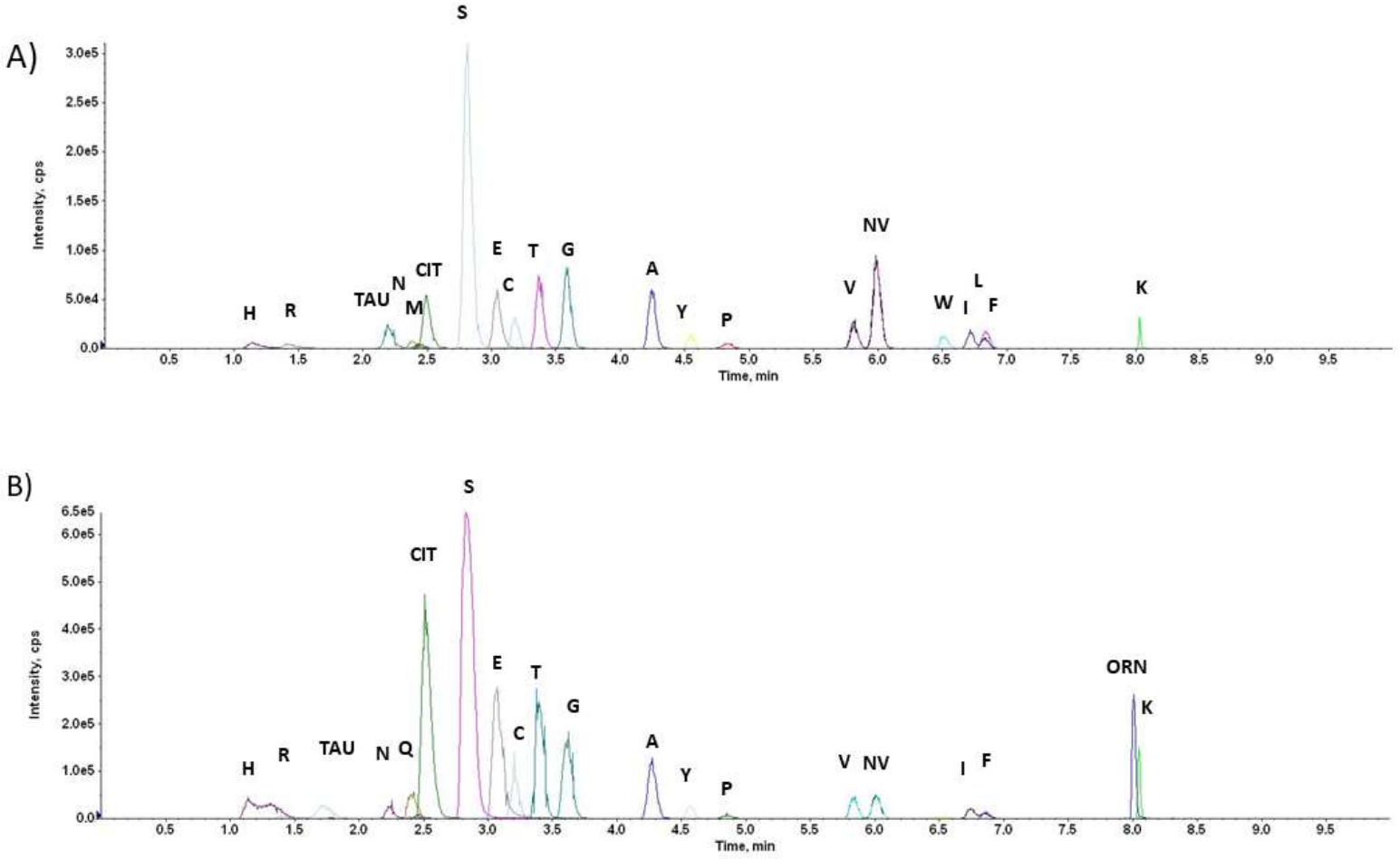

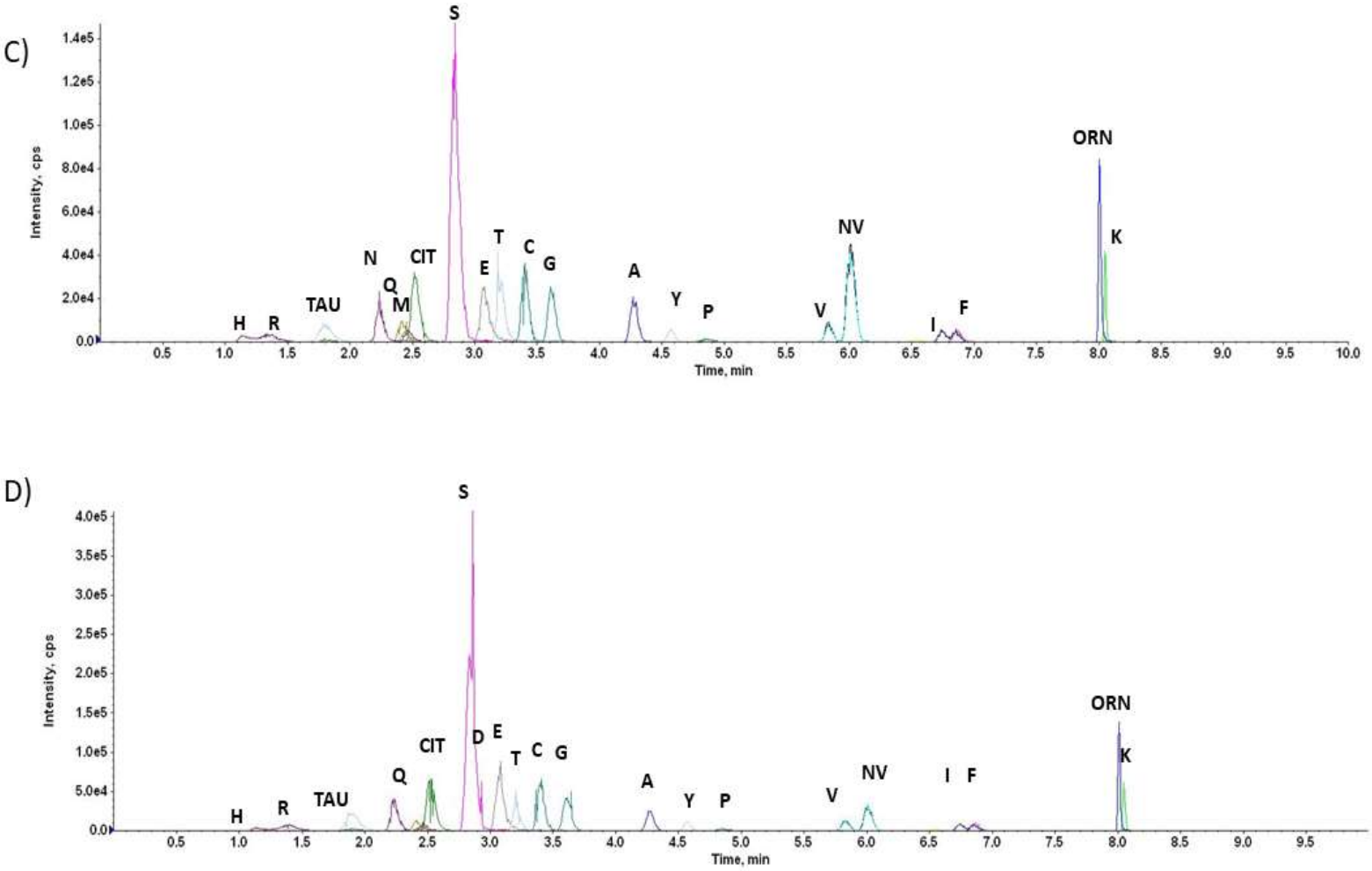
C)
Intensity, cps
Time, min
S
T
C
G
E
N
CIT
Q
M
TAU
H
R
A
Y
P
V
NV
I
F
ORN
K
D)
Intensity, cps
Time, min
S
D
E
T
C
G
CIT
Q
TAU
H
R
A
Y
P
V
NV
I
F
ORN
K

Table A1. Concentration of each FAAs/urea in the corneocytes isolated from skin sample taken after tape stripping from right and left forearm of HY group

Right forearm			Left forearm			Right forearm			Left forearm		
Concentration (nmol)/mg of the corneocytes											
AA	Avg.	±SD	AA	Avg.	±SD	AA	Avg.	±SD	AA	Avg.	±SD
Aln	0.8293	± 0.2447	Aln	0.9586	± 0.5600	Lys	0.2337	±0.1240	Lys	0.2824	± 0.1996
Asn	0.0236	± 0.0114	Asn	0.0364	± 0.0470	Met	0.0013	± 0.0006	Met	0.0010	± 0.0004
Asp	0.8034	± 0.3208	Asp	0.9825	± 0.3816	Phe	0.0298	± 0.0114	Phe	0.0395	± 0.0132
Arg	0.0428	± 0.0274	Arg	0.0564	± 0.0207	Pro	0.0245	± 0.0092	Pro	0.0270	± 0.0156
Cit	5.7776	± 2.7690	Cit	6.7450	± 4.5054	Ser	0.2308	± 0.0554	Ser	0.3043	± 0.1282
Cys	0.0146	± 0.0057	Cys	0.0192	± 0.0095	Thr	0.0789	± 0.0277	Thr	0.0691	± 0.0215
Gln	0.0379	± 0.0098	Gln	0.0445	± 0.0020	Trp	0.0133	± 0.0035	Trp	0.0129	± 0.0042
Glu	0.0030	± 0.0008	Glu	0.0029	± 0.0011	Tyr	0.0088	± 0.0030	Tyr	0.0079	± 0.0044
Gly	0.3600	± 0.0928	Gly	0.4060	± 0.0985	Val	0.0464	± 0.0178	Val	0.0513	± 0.0200
His	0.0515	± 0.0472	His	0.0601	± 0.0403	Tau	0.0032	± 0.0012	Tau	0.0037	± 0.0021
Ile	0.0343	± 0.0139	Ile	0.0280	± 0.0089	orn	0.2814	± 0.1429	orn	0.3050	± 0.2202
Leu	0.0484	± 0.0206	Leu	0.0522	± 0.0350	Urea	2.3578	± 1.2976	Urea	2.8552	± 1.7931

Table A2. Concentration of each FAAs/urea in the corneocytes isolated from skin sample taken after tape stripping from right and left forearm of of HO group

Right forearm			Left forearm			Right forearm			Left forearm		
Concentration (nmol)/mg											
AA	Avg.	± SD	AA	Avg.	± SD	AA	Avg.	± SD	AA	Avg.	±SD
Aln	5.443	±3.508	Aln	5.271	± 2.867	Lys	2.235	± 1.420	Lys	2.519	± 1.206
Asn	1.011	± 0.503	Asn	1.034	± 0.440	Met	0.273	± 0.140	Met	0.252	± 0.144
Asp	2.873	± 1.932	Asp	2.517	± 0.998	Phe	0.587	± 0.339	Phe	0.571	± 0.293
Arg	0.065	± 0.037	Arg	0.060	± 0.036	Pro	1.211	± 0.624	Pro	0.984	± 0.526
Cit	10.495	± 6.640	Cit	9.932	± 6.918	Ser	9.364	± 3.858	Ser	9.532	± 5.868
Cys	0.182	± 0.133	Cys	0.189	± 0.084	Thr	3.646	± 1.913	Thr	3.531	± 1.989
Gln	0.080	± 0.049	Gln	0.086	± 0.061	Trp	0.260	± 0.172	Trp	0.246	± 0.150
Glu	0.681	± 0.346	Glu	0.690	± 0.109	Tyr	1.271	± 0.584	Tyr	0.905	± 0.591
Gly	9.346	± 5.362	Gly	9.426	± 4.566	Val	1.137	± 0.639	Val	1.208	± 0.599
His	0.349	± 0.233	His	0.356	± 0.222	Tau	0.067	± 0.050	Tau	0.072	± 0.053
Ile	0.632	± 0.335	Ile	0.599	± 0.277	orn	2.321	± 1.274	orn	1.991	± 1.193
Leu	0.793	± 0.435	Leu	0.839	± 0.392	Urea	13.717	± 7.026	Urea	13.041	± 8.213

Table A3. Concentration of each FAAs/urea in the corneocytes isolated from skin sample taken after tape stripping from right and left forearm of of atopic dermatitis (AD) group

Right forearm			Left forearm			Right forearm			Left forearm		
Concentration (nmol)/mg of the corneocytes											
AA	Avg.	± SD	AA	Avg.	± SD	AA	Avg.	± SD	AA	Avg.	± SD
Aln	1.7041	± 1.0566	Aln	1.6842	± 0.8988	Lys	0.5798	± 0.2263	Lys	0.5743	± 0.4564
Asn	0.0977	± 0.0366	Asn	0.0969	± 0.0533	Met	0.1355	± 0.0546	Met	0.1247	± 0.0792
Asp	1.9041	± 1.3971	Asp	1.7437	± 1.1830	Phe	0.1402	± 0.1261	Phe	0.1180	± 0.0566
Arg	0.0488	± 0.0272	Arg	0.0329	± 0.0183	Pro	0.1344	± 0.0804	Pro	0.1030	± 0.0515
Cit	5.2832	± 4.0300	Cit	5.1154	± 3.3722	Ser	1.4654	± 1.1024	Ser	0.9688	± 0.7477
Cys	0.0302	± 0.0164	Cys	0.0258	± 0.0169	Thr	0.3883	± 0.2200	Thr	0.3232	± 0.1987
Gln	0.1217	± 0.0636	Gln	0.1423	± 0.0596	Trp	0.0405	± 0.0133	Trp	0.0493	± 0.0278
Glu	0.0260	± 0.0217	Glu	0.0216	± 0.0120	Tyr	0.1521	± 0.1341	Tyr	0.1329	± 0.0353
Gly	1.3640	± 0.6254	Gly	1.2975	± 0.6378	Val	0.1491	± 0.0884	Val	0.1194	± 0.0605
His	0.0398	± 0.0215	His	0.0410	± 0.0266	Tau	0.0223	± 0.0180	Tau	0.0244	± 0.0091
Ile	0.1137	± 0.0811	Ile	0.0975	± 0.0676	orn	0.5834	± 0.2322	orn	0.5065	± 0.3608
Leu	0.4321	± 0.2313	Leu	0.3937	± 0.2684	Urea	12.804	± 7.767	Urea	11.6702	± 7.0073

Table A4. Concentration of each FAAs/urea in the corneocytes isolated from skin sample taken after tape stripping from right and left forearm of of psoriasis (PS) group

Right forearm			Left forearm			Right forearm			Left forearm		
Concentration (nmol)/mg of the corneocytes											
AA	Avg.	± SD	AA	Avg.	± SD	AA	Avg.	± SD	AA	Avg.	± SD
Aln	1.995	± 0.851	Aln	2.333	± 1.169	Lys	0.665	± 0.307	Lys	0.707	± 0.353
Asn	0.290	± 0.152	Asn	0.312	± 0.198	Met	0.143	± 0.142	Met	0.150	± 0.057
Asp	2.208	± 1.539	Asp	1.871	± 1.181	Phe	0.228	± 0.205	Phe	0.171	± 0.094
Arg	0.098	± 0.037	Arg	0.093	± 0.054	Pro	0.263	± 0.171	Pro	0.252	± 0.156
Cit	4.620	± 3.711	Cit	5.073	± 3.434	Ser	2.707	± 1.591	Ser	3.154	± 2.065
Cys	0.540	± 0.427	Cys	0.520	± 0.245	Thr	0.655	± 0.362	Thr	0.588	± 0.327
Gln	0.228	± 0.204	Gln	0.264	± 0.125	Trp	0.093	± 0.025	Trp	0.090	± 0.022
Glu	0.228	± 0.204	Glu	0.265	± 0.146	Tyr	0.083	± 0.067	Tyr	0.086	± 0.066
Gly	2.300	± 0.832	Gly	2.800	± 1.816	Val	0.311	± 0.158	Val	0.326	± 0.142
His	0.049	± 0.034	His	0.051	± 0.026	Tau	0.024	± 0.015	Tau	0.025	± 0.013
Ile	0.217	± 0.132	Ile	0.192	± 0.062	orn	0.857	± 0.389	orn	0.918	± 0.619
Leu	0.339	± 0.288	Leu	0.382	± 0.297	Urea	8.296	± 3.622	Urea	8.852	± 0.420

Table A6. Differences ($p < 0.01$) for FAAs/urea composition between groups

The group showed significantly higher amount of given FAAs/urea	
HY vs HO	
HO	Asn, Glu, Gly, Ileu, Leu, Met, Pro, Phe,Ser, Thr, Trp, Val, Tau, Urea
HY vs AD	
AD	Asn, Gln, Glu, Gly, Leu, Met, Pro, Ser, Thr, Trp, Val, Tau
HY vs PS	
PS	Asn, Glu, Gly, Ileu, Leu, Met, Phe, Pro, Ser, Thr, Trp, Tyr, Val, Tau

Healthy young (HY), healthy old (HO), atopic dermatitis (AD), psoriasis (PS).

B. Analysis of taurine and urea in diffusion profile

B1. Chromatogram of taurine analysis after pre-column derivatization with FMOC-Cl in diffusion profile of taurine using LC-ESI-MS/MS-MRM

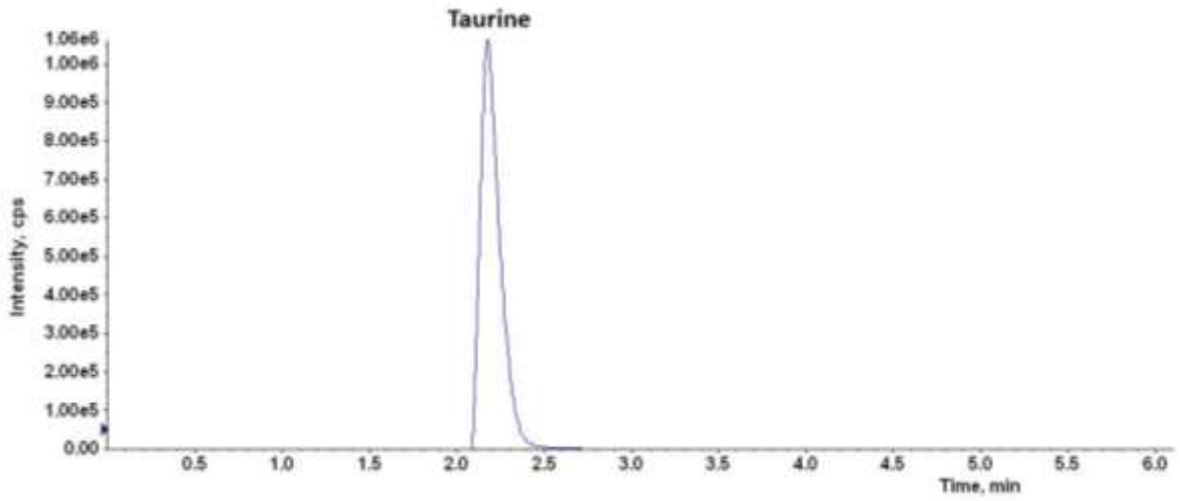

Figure B1. Chromatogram of taurine after LC.

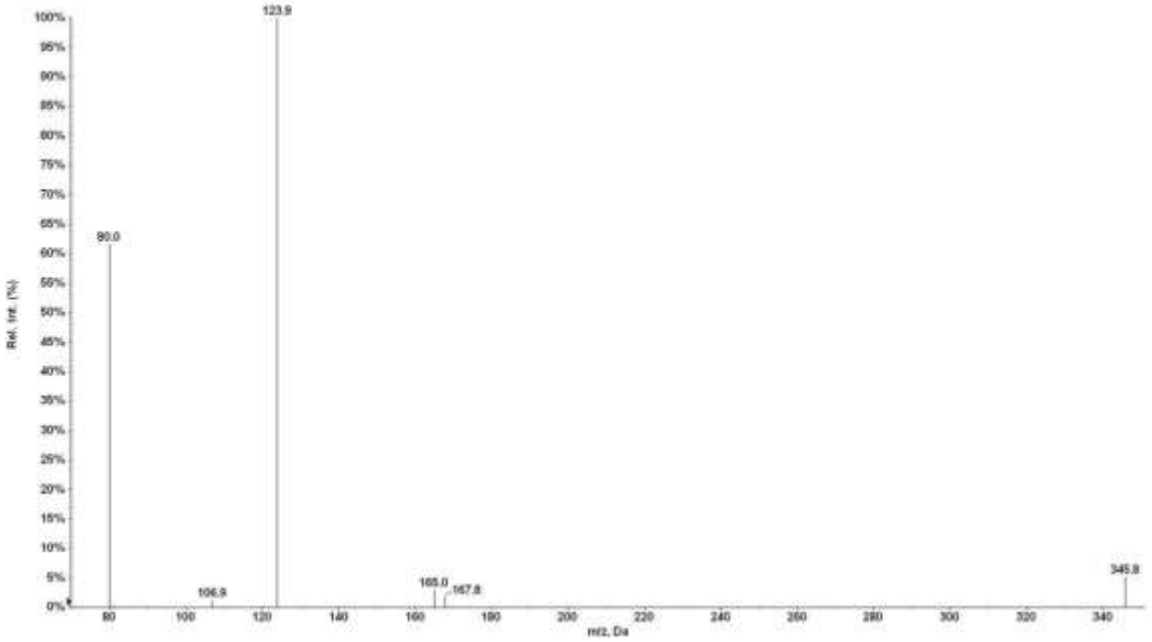

Figure B1.1. MS/MS spectra of taurine.

B2. Chromatogram of urea obtained with HPLC analysis in diffusion proofile of urea

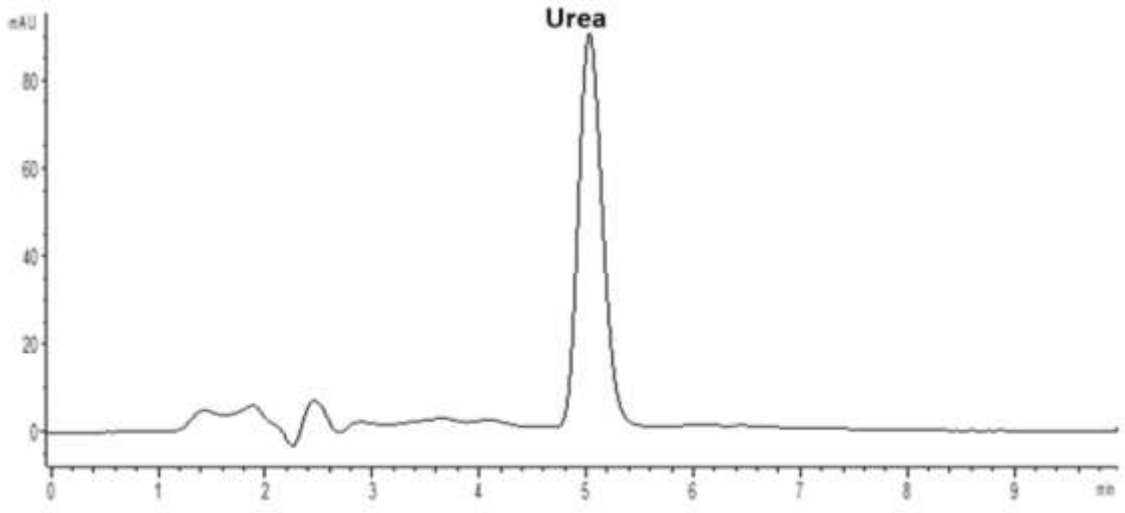

Figure B2. Chromatogram of urea analysis using HPLC in diffusion profile of urea.

Acknowledgments

Firstly, I will like to pay my deepest gratitude and appreciation to my supervisor Prof. Dr. Dr. H. H. Reinhard Neubert for all your supports and scientific guidance. I appreciate your willingness to accept my request to join your research group and all the things you have done to me. I am also very thankful to Prof. Dr. Johannes Wohlrab, for your kind support in the conduct of study in hospital and all other scientific guidance and advices.

I am deeply grateful to Dr. Jörg Ziegler, Leibniz Institute of Plant Biochemistry, for your advices on key scientific aspects of my work, especially your scientific support in the analytical part of the work and allowing me use LC-MS. I would like to acknowledge Frank Syrowatka, Interdisciplinary Center for Material Science, and Dr. Gerd Hause, Biocentrum, MLU, for taking microscopic images of the isolated corneocytes.

I am thankful for the scientific guidance of Dr. Yahya Mrestani. I would like to offer my special thanks to Mrs. Manuela Woigk, Mrs. Anke Nies, Pascal Rudwig, Mrs. Kerstin Schwarz, Mrs. Birgit Orte and Andrea Stennett for excellent technical assistance.

I am very grateful to my all the friends and fußflege studio manager, Neustadt, Halle for always willing to provide me the samples for my preliminary studies. I greatly acknowledge the financial support provided by the HEC Pakistan and German Academic Exchange Service (DAAD).

I thank Anne Ripperger and Dr. Thomas Schmitt for your help in translating the English version of the 'Summary' into German version.

I would like to extend my appreciations to all the members of the former 'AG Neubert' and 'AG Dailey' for making my stay enjoyable. Special thanks to Efrem Nigusso, Ranju Chutia, Prodyut Mondal, Khaled Alkassem and Angela Cristina Mora Huertas, Abid Riaz Ahmed.

Finally, I am very grateful to my family and my friends for their emotional and moral supports and understanding.

Publications

Research papers

1. Hina Hussain, Jörg Ziegler, Gerd Hause, Johannes Wohlrab, Reinhard H.H. Neubert. Quantification of free amino acids and urea in isolated corneocytes of healthy, aged and diseased skin, Skin Pharmacol Physiol 2019;32:94–100 DOI: 10.1159/000495992.

2. Hina Hussain, Jörg Ziegler, Yahya Mrestani, Reinhard H.H. Studies of the corneocytary pathway across the Stratum corneum. Part I: Diffusion of amino acids into the isolated corneocytes (accepted)

Book Chapter

1. Jörg Ziegler., **Hina Hussain.**, Reinhard H.H. Neubert., Steffen Abel**.** Sensitive and selective amino acid profiling of minute tissue amounts by HPLC/electrospray negative tandem mass spectrometry using 9-fluorenylmethoxycarbonly (Fmoc-Cl) derivatization. (Waiting for publishing).

Posters

1. **Hina Hussain**., Jörg Ziegler., Yahya Mrestani., Reinhard H.H. Neubert. In-vitro permeation model of taurine: A comparative permeation behaviour with and without the corneocytes. 16/10/2017-18/10/2017. Presented in 9th international conference of dermatology/psoriasis, psoriatic arthritis and skin diseases, NY, USA.

Curriculum vitae

Hina Hussain, MPhil (Pharmaceutics)

Date of birth: 06-09-1984
Place of birth: Lahore, Pakistan
Nationality: Pakistan
Education

10/2014– To-date	Ph.D student in the group of Prof. Dr. Dr. Reinhard H. H. Neubert, Institute of Pharmacy (Pharmaceutical Technology and Biopharmacy), Martin-Luther University Halle-Wittenberg
02/2012	MPhil (Pharmaceutics), Institute of pharmaceutical technology, University of Veterinary and Animal Sciences, Lahore. Pakistan
05/2008	Pharm.D Institute of pharmacy, Lahore College for Women University, Lahore, Pakistan

Work experience

10/2014 – To-date	PhD scholar at the Institute of Pharmacy, Martin-Luther University Halle-Wittenberg
02/2013 – 05/2014	Lecturer, Lahore pharmacy college, Lahore Medical and Dental College, Lahore, Pakistan.
10/2009 – 01/2013	Teaching Assistant, Institute of pharmaceutical sciences, University of Veterinary and Animal Sciences, Lahore, Pakistan.
08/2010 – 08/2011	Pharmacist clinical trials, bioequivalence study center, University of Veterinary and Animal Sciences, Lahore, Lahore, Pakistan
03/2009 – 08/2009	Clinical resident pharmacist, Children hospital and institute of child health, Lahore, Pakistan

Selbstständigkeitserklärung

Hiermit erkläre ich, dass ich die Ergebnisse der vorliegenden Dissertationsarbeit

`Diffusion pathway across stratum corneum via the corneocytes and quantification of free amino acids and urea in the isolated corneocytes´

am Institut für Pharmazie der Martin-Luther Universität Halle-Wittenberg unter Anleitung von Herrn Prof. Dr. Dr. Reinhard Neubert selbstständig erarbeitet bzw. im Rahmen der angegebenen Kooperationen erhalten habe. Die Dissertation habe ich ohne fremde Hilfe angefertigt und dazu keine anderen als die von mir angegebenen Quellen und Hilfsmittel benutzt. Die den verwendeten Werken wörtlich oder inhaltlich entnommenen Stellen sind als solche kenntlich gemacht.

Ferner erkläre ich, dass ich mich erstmals um die Erlangung eines Doktorgrades bewerbe und die vorliegende Dissertationsschrift keiner anderen in- oder ausländischen Fakultät vorgelegt habe.

Hina Hussain _____